Heinrich Heine
Universität Düsseldorf

Investigating the pro-myelinating activity of a corticosteroid in a cuprizone-dependent chronic demyelination model

Inaugural dissertation

For the attainment of the title of doctor of philosophy in natural sciences by the Faculty of Mathematics and Natural Science at the Heinrich Heine University of Düsseldorf

Presented by

Markley Silva Oliveira Junior

From Feira de Santana, Brazil
Date of Birth: 11/09/1992

Düsseldorf, Germany, October 2022

From the laboratory for Neuroregeneration, Department of Neurology, University Clinic Düsseldorf, Medical Faculty, Heinrich Heine University.

Published by permission of The Faculty of Mathematics and Natural Science at Heinrich Heine University, Düsseldorf

Supervisor Prof. Dr. Patrick Küry

Co-supervisor Prof. Dr. Christine Rose

Date of the oral examination: 10/18/2022

Acknowledgments

I decided to become a scientist around age seven. At that time, I already knew that being a scientist was something to be achieved, no matter what. Excited to learn more about this profession, I read several books and comics about scientists. Later, I noticed I was addicted to learning about anything besides Maths and Physics. Then I discovered that this is what science is about: LEARNING and LEARNING again. Facing a PhD process is harsh. Today I admire pretty much all PhDs folks around the world. What a journey! Now I have learned that the doctoral program also allows you to better understand yourself, and this is hard. Facing your demons in struggling situations is so scary, and the process of being a doctor puts you in this place several times. That was so difficult and overwhelming, an odyssey for sure. In fact, what I have learned is that I am still naive, but with a little more experience. This part of my life will forever be remembered as the most challenging time I have ever experienced. Far from my home country Brazil, far from my roots and the smell of joy that Brazil spontaneously exhales in each corner. Yet, having my wife Mariana here by my side, always supporting me, what a gift. Thank you, “ursa” this title is also yours, be sure of that. Thank you for trusting in me and for never giving up on us. Spirituality is also a great part of my life, and here I confirmed that those things could walk together, and this mindset is essential to thrive over the challenges of all days, a forever thank you to the" kind helpers of all time". Kaz, I am glad for your contribution, for receiving me as your mentored in my first year of PhD and for introducing me to the Oligo Boss, Prof. Dr Patrick Küry. Patrick, you really inspired me over these years. Thank you for making me a better scientist. I am glad to have the opportunity to be supervised by such a professional and experienced neuroscientist such as yourself. It was a pleasure to work by your side. Thank you for trusting me and inspiring me. Prof. Dr Christine Rose, many thanks for your help through this process. Your contribution to the field of astrocyte biology is remarkable and unique, and it is an honour to have you as my co-supervisor. Jessica S., you really were a breakthrough in my journey over this PhD. Your support, guidance and kindness were tremendously necessary for me to succeed. Thank you for your support, supervision, advice, patience and collaboration. My sincerest greetings and many, many thanks to all from the AG Küry and most especially to Laura (we had a lot of buddy therapies sessions, eh?), Anastasia, Peter, Cagla, Vanessa (parceira), Zippora, Seulki, Iria, Joel, Rainer, Birgit, Julia, Brigida, Frank. Many thanks to you guys for all your support. We hold this title together as a

team, and I am really proud to have had the opportunity to work by your side. Hopefully, we will see each other again, around the world. My dear friends Monique Marylin, Luã Costa, and Ines Kortebi, a forever thank you for all your support in the development of this dissertation and for always being there whenever I need. Last but not least, thank you to my family in Brazil, my parents and my sister. ‘Mãe (mom)’, you have always inspired me. While getting older and now seeing more of life, I get able to understand all struggles you have been through in raising Barbara and me. Thank you, mom, for supporting my academic dreams and for believing in me since day one. Victor, Mario, Daniel and Brenno, my soul friends, you guys were eyes and ears to my struggles and victories. Thank you all/Obrigado a todos vocês!

“*Somewhere, something incredible is waiting to be known*.”

Prof. Dr. **Carl** Edward **Sagan**

List of Reviewers:

1st Reviewer: Prof. Dr. Patrick Küry, Heinrich Heine University

2nd Reviewer: Prof. Dr. Christine Rose, Heinrich Heine University

Statutory declaration I hereby affirm in lieu of an oath that the submitted dissertation was prepared by me independently and without unauthorized help.

Düsseldorf, the 10/18/2022

(Signature: Markley Silva Oliveira Junior)

List of abbreviations

BBB- Blood brain barrier

Bcas1- Breast carcinoma-amplified sequence 1

BDNF- Brain-derived neurotrophic factor

BMP- Bone morphogenetic receptor 1

C3- Complement factor 3

C3d- Complement factor 3d

CC1- Adenomatous polyposis coli clone CC1

CNPase- 2',3'-Cyclic-nucleotide 3'-phosphodiesterase

CNS- Central nervous system

CNTF- Ciliary neurotrophic factor

CPZ- Cuprizone

CXCR3- Chemokine receptor 3

d-SVZ- dorsal subventricular zone

E12, -18- Embryogenesis stage

EAE- Experimental autoimmune encephalomyelitis

EGF- Epidermal growth factor

EGFR- Epidermal growth factor receptor

FDA- Food and Drug Administration

GDNF- Glial cell line-derived neurotrophic factor

Gfap/GFAP- Glial fibrillary acid protein

GFP- Green fluorescent protein

Glast- Glast-astrocyte cell surface antigen-1

GPx- Glutathione peroxidase

GS- Glutamine synthase

GSTπ- Glutathione S-transferase Pi

GW- Gestational week

Hopx- Homeodomain-only protein X

Igf1- Insulin-like growth factor one

IL-1β, -6, -17, -18- Interleukin

INF-γ- Interferon-gamma

iNOS- Inducible nitric oxide synthase

Lcn2- Lipocalin 2

LIF- Leukaemia inhibitory factor

LPC- Lysophosphatidylcholin

MAFG- MAFG-heterodimers

MAT2α- Methionine adenosyltransferase 2 alfa

MBP- Myelin basic protein

MHCII- Major histocompatibility complex 2

MMPs- Mettalopeptidases

MOG- Myelin oligodendrocyte glycoprotein

MS- Multiple Sclerosis

NfκB- Nuclear factor kappa-light-chain-enhancer of activated B cells

NG2- Neural Glial antigen 2

Nrf2- Nuclear factor erythroid 2-related factor 2

NSCs- Neural stem cells

Olig2- Oligodendrocyte Transcription Factor 2

OLs- Oligodendrocytes

OPCs- Oligodendrocyte precursor cells

P2, -6, -7, -11- Postnatal day

Pax6- Paired box homeotic gene-6

PDGFRα- Platelet derived growth factor alpha

PLP- Myelin proteolipid protein

PPMS- Primary progressive Multiple sclerosis

RGs- Radial glia

ROS- Reactive oxygen species-

RRMS- Relapsing-remitting Multiple sclerosis

S100a10- S100 calcium-binding protein A10

Sox9- SRY-box transcription factor 9

SPMS-Secondary progressive Multiple sclerosis

Stat3- Signal transducer and activator of transcription 3

TAPs- transient amplifying progenitors

Timp- Tissue metallopeptidase inhibitors

Timp1- Tissue metallopeptidase inhibitor 1

TNF-α- Tumour necrosis Factor alpha

VZ- Ventricular zone

Table of Contents

List of figures

Summary

Demyelinating diseases such as Multiple sclerosis (MS) result from inflammatory insults and lead to myelin loss and oligodendrocyte (OLs) death. Taking advantage of a cuprizone (CPZ)-dependent chronic demyelination model, we analysed the consequences of this treatment on the white matter damage and the dorsal-subventricular zone (d-SVZ), the key oligodendroglial niche within the subventricular zone (SVZ). Medrysone, a Food and Drug Administration (FDA) approved anti-inflammatory corticosteroid predicted to promote oligodendroglial cell fate decision, was repurposed and evaluated under several methods to validate its predicted mechanisms. Our analyses in cerebellar *ex vivo* slices revealed an enhancement in the number of myelin basic protein positive cells (MBP+) and axonal myelination after medrysone application. Moreover, medrysone drove d-SVZ cell cultures to increased numbers of Neural glial antigen 2- (NG2) and Glial fibrillary acid protein- (Gfap) positive cells. However, no effect on myelination was observed in primary oligodendrocyte precursor cells (OPCs) treated with the corticosteroid. Primary astrocytes prior-stimulated with tumour necrosis factor alpha (TNF-α) rescued their non-neurotoxic fate after medrysone application, confirming an effect of this drug on astroglial cells in a pro-inflammatory environment. *In vivo*, medrysone treatments in chronic demyelinated hGFAP-GFP reporter mice rescued MBP- and myelin proteolipid protein- (PLP) levels and replaced a myriad of mature OLs populations in the corpus callosum. The main finding of this work is the astroglial heterogeneity ignited by medrysone, enhancing a more remarkable number of astrocytes with a pro-remyelination signature [positive for tissue metallopeptidase inhibitor 1 (Timp1), S100 calcium-binding protein A10 (S100a10), Signal transducer and activator of transcription 3 (Stat3)], within the remyelinated areas earlier than saline-treated mice. Indeed, medrysone contributes to remyelination in chronic demyelinated mice and its repair activities are accompanied by beneficial reactive astrogliosis. These findings indicate that medrysone has the potential to treat chronic myelin damage in MS.

Zusammenfassung

Demyelinisierende Erkrankungen wie MS sind die Folge von entzündlichen insulten und führen zum Verlust von Myelin und zum Absterben von OL. Anhand eines von CPZ abhängigen Modells der chronischen Demyelinisierung haben wir die Auswirkungen dieser Behandlung auf die Schädigung der weißen Substanz und der d-SVZ, der wichtigsten oligodendroglialen Nische innerhalb der SVZ, untersucht. Medrysone, ein von der FDA zugelassenes entzündungshemmendes Kortikosteroid, von dem vorhergesagt wird, dass es die Entscheidung über das Schicksal oligodendroglialer Zellen fördert, wurde neu eingesetzt und mit verschiedenen Methoden untersucht, um die vorhergesagten Mechanismen zu validieren. Unsere Analysen in Ex-vivo-Scheiben des Kleinhirns ergaben, dass die Anzahl der MBP+ und die axonale Myelinisierung nach Medrysone-Anwendung zunahmen. Außerdem führte Medrysone in d-SVZ-Zellkulturen zu einer erhöhten Anzahl von NG2 und Gfap positiven Zellen. Bei primären OPCs, die mit dem Kortikosteroid behandelt wurden, wurde jedoch keine Auswirkung auf die Myelinisierung beobachtet. Primäre Astrozyten, die zuvor mit TNF-α stimuliert worden waren, wurden nach der Medrysone-Anwendung wieder nicht-neurotoxisch, was eine Wirkung dieses Medikaments auf Astrogliazellen in einem pro-inflammatorischen Umfeld bestätigt. In vivo retteten Medrysone-Behandlungen in chronisch demyelinisierten hGFAP-GFP-Reportermäusen die MBP- und PLP-Spiegel und ersetzten eine Vielzahl von reifen OLs-Populationen im Corpus callosum. Das wichtigste Ergebnis dieser Arbeit ist die durch Medrysone ausgelöste astrogliale Heterogenität, die zu einer bemerkenswerten Anzahl von Astrozyten mit einer Pro-Remyelinisierungs-Signatur (positiv für Timp1, S100a10, Stat3) innerhalb der remyelinisierten Bereiche führt, und zwar früher als bei salzbehandelten Mäusen. Tatsächlich trägt Medrysone zur Remyelinisierung bei chronisch demyelinisierten Mäusen bei, und seine Reparaturaktivitäten werden von einer positiven reaktiven Astrogliose begleitet. Diese Ergebnisse deuten darauf hin, dass Medrysone das Potenzial hat, chronische Myelinschäden bei MS zu behandeln.

Aims of the study

Aim 1. Identify the protein and gene signature of rodent brain-derived primary cultures treated with medrysone, focusing on myelination, neurotoxicity and neuroprotective features.

Aim 2. Determine the dynamics of remyelination on chronic-demyelinated mice treated or not treated with medrysone.

Aim 3. Determine the spatial distribution of subpopulations of astroglial and oligodendroglial cells on the corpus callosum and d-SVZ throughout the de- and remyelination phase.

Introduction

The SVZ harbors neural stem cells (NSCs) throughout life, which contribute to neuronal, oligodendroglial and astroglial cell populations, supporting axon integrity, neuronal communication, and myelination in both homeostasis and inflammation (Nave, 2010; Xing et al., 2014). OLs are the myelinating cells of the central nervous system (CNS) that mainly contribute to neuronal communication (Bradl and Lassmann, 2010; Kuhn et al., 2019), being preferentially generated by the NSCs and OPCs inhabiting the d-SVZ (Menn et al., 2006; Azim et al., 2018). On the other hand, astrocytes are born and develop from the lateral SVZ (Menn et al., 2006; Platel et al., 2008). However, in a stressful environment such as stroke, astrocytes can also be generated at the d-SVZ (Benner et al., 2013; Faiz et al., 2015). This region can be more precisely divided into three micro-niches (i) middle-d-SVZ (the center area of the d-SVZ), (ii) dorsal-horn (where the lateral and dorsal wall create a corner) and dorsal-medial (where the medial and dorsal wall are connected), (see Figure 9; Azim et al., 2017; 2020).

Chronic myelin damage is one of the main features of MS. Its pathophysiology is based on pro-inflammatory mechanisms, OLs apoptosis, myelin destruction, and consequently gliosis (Wu and Alvarez, 2011; You et al., 2020). In addition, once affected, SVZ niches nearby get surrounded by reactive glial cells, and the upgrading inflammation contributes to the depletion of NSCs, thus weakening remyelination (Xing et al., 2014; Liu et al., 2016; Hillis et al., 2016). Nevertheless, studies utilizing CPZ have shown that mature OLs derived of OPCs generated at the SVZ more efficiently than the ones derived of parenchymal OPCs, can better remyelinate axons (Nait-

Oumesmar et al., 2007; Xing et al., 2014; Moraga et al., 2015), highlighting this niche as an endogenous alternative for stimulation of remyelinating cells. Reactive astrogliosis is known to follow demyelination, and these cells commonly surround the SVZ during damage and repair. However, the implication of reactive astrocytes and their heterogeneity throughout the d-SVZ under demyelination is unclear. It is known that the primary trigger for OLs loss is dependent on reactive astrocytes that upregulate apoptosis-related interleukins and complement factors (Baxi et al., 2017; Taraboletti et al., 2017; Pandur et al., 2019). In contrast, remyelination and OPCs/NSCs maturation depend on trophic factors individually released by resident reactive astrocytes (Butti et al., 2019; Lohrberg et al., 2020). These molecules can induce SVZ-OPCs into a myelinating profile (Platel et al., 2012), and regulate the electrical impulses within mature OLs and myelinated axons, thus improving myelination (Ishibashi et al., 2006).

A consensus towards the determination of the function of reactive astrocytes lies in identifying the transcriptomic and proteomic signature, the region of the brain (healed or diseased), and several other factors that, combined, can better define its function (Escartin et al., 2021). Transcriptomic evaluations have shown that astrocytes differ in gene and protein expression profiles during disease models. Depending on their protein and gene expression, reactive astrocytes can be divided into neuroprotective or neurotoxic (Liddelow et al., 2017). Some phenotypes even express neurotoxic and neuroprotective molecules concomitantly, configuring a hybrid phenotype that seems to contribute to brain regeneration (Das et al., 2020; Hasel et al., 2021). Therefore differing from the obsolete consensus of A1 and A2 as the only subtypes existing (Escartin et al., 2021). During demyelination, neurotoxic astrocytes regularly express complement factor three (C3) and are observed in MS (Liddelow et al., 2017) and experimental autoimmune encephalomyelitis (EAE) active lesions (Tassoni et al., 2019), while neuroprotective astrocytes commonly express Stat3 and/or S100a10 both known to be involved in tissue repair (Monteiro de Castro et al., 2015; Herrmann et al., 2008; Das et al., 2020). A group of molecules expressed and released by neuroprotective astrocytes are the tissue metallopeptidase inhibitors (Timp), specifically Timp1. This molecule is known to induce a myelinating profile in NSCs (Samper-Agrelo et al., 2020) and rescues white matter-myelination via OPCs and

early-stage OLs maturation (Moore et al., 2011; Houben et al., 2020; Hasel et al., 2021).

Extensive myelin deterioration is connected to chronic OLs loss which comprise a cycle of insufficient remyelination and extended-inflammatory insult (Ludwin, 2006; Wang et al., 2019). Identification of drugs, which promote cell repair and reduce inflammation and, at the same time, impede disease progression, is an outstanding biomedical challenge (da-Cunha et al., 2020; Manousi and Küry, 2021). Medrysone, an FDA-approved anti-inflammatory corticosteroid, has been predicted to enhance oligodendrogenesis and myelination fate on lateral SVZ-NSCs (Azim et al., 2017). The corticosteroid was also reported to promote myelination of immortalized OLs (Oli-neuM; Porcu et al., 2015). Those findings strengthen our hypothesis of medrysone as a remyelination-drug. Hence, in order to characterize such theory, we investigated the impact of medrysone on developmental myelination, OPCs differentiation, astrocyte heterogeneity, and differentiation of d-SVZ mixed cell cultures. Furthermore, *in vivo* experiments aimed to investigate the capacity of medrysone to promote remyelination and reactive astrogliosis at the d-SVZ and corpus callosum in hGFAP-GFP reporter mice exposed to chronic demyelination.

1. Chapter 1: Multiple sclerosis

1.1 Epidemiology and basic etiology of Multiple sclerosis

Roughly 2.8 million people suffer from MS worldwide, with the United States (US), Canada and Europe showing the most significant prevalence of cases of 1 in every 300 people. Yearly, MS costs 28 billion dollars in the US alone (ICERS, 2017). At least 30,000 people under 18 years of age have been diagnosed with MS. This disease is more prevalent in females between 25-35 years old, a key disadvantage for countries such as Germany that struggle with low rates of births and a high percentage of retirement. Every five minutes, a new case of MS is diagnosed in Europe. Germany has a prevalence of 303 cases per 100,000 people, having one of the world's higher numbers of MS patients (MSIF, 2020). This fact is alarming in a governmental and financial manner. Most newly MS diagnosed people are young and still building a family and career. Due to MS complications, they stop contributing to social development earlier than expected for their age group (ICERS, 2017). Great talents of music and science have perished under the aggravation of MS. The British cellist Jacqueline Mary du Pré died aged 42, 14 years after being diagnosed (Daliot, 1999). Another great personality was Alberto Santos Dumont, a Brazilian aeronaut scientist and inventor who contributed to the early ages of aircraft technology in Europe. Santos Dumont “early-retired" and stopped his contributions to the scientific community due to MS complications only 12 years after his diagnosis (Frazão, 2021).

Worsening throughout ageing, those affected by MS bear a chronic disease and exhibit symptoms such as memory loss, blindness, kidney failure, muscular dystrophy and brain atrophy. Demyelination is the milieu within these symptoms and is the key cause of MS aggravation (Lassmann, 2019). Myelin is a lipid structure that insulates axons, enabling faster electrical communication between neurons throughout their connecting cables, the axons (Stadelmann et al., 2018). The most common feature behind demyelination is the neurotoxic glial reactivity (Sofroniew and Vinter, 2010; Sofroniew, 2020). This activated stage of astrocytes and microglia induces a pro-inflammatory cascade of molecules, improving the migration of immune periphery cells such as lymphocytes (Baaklini et al., 2019; Lassmann, 2019). These cells, once reaching the CNS, can communicate with microglia by a system called major histocompatibility complex 2 (MHCII), which recognizes MBP as a foreign pattern,

therefore enlarging pro-inflammatory cascades within the tissue, worsening myelin destruction, moreover also targeting OLs the myelin-maker of the brain (Hiremath et al., 2008; Chastain et al., 2011).

In fact, remyelination can still occur throughout demyelination. However, it is not enough to surpass the side effects of myelin loss (Chari et al., 2007). The lack of growth factors and oxidative stress commonly found in this inflamed environment hinders new myelin formation, enlarging damage and extending chronification (Carlström et al., 2020; Cayre et al., 2021). Over time, the demyelinated tissue undergoes scarification. This particular situation is organized by astrocytes and aims to decrease brain tissue destruction, creating an inert region that commonly appears as circular white areas in magnetic resonance imaging (MRI; Baaklini et al., 2019; Brune et al., 2020). Details of chronic MS pathophysiology and reactive glial cells within will be better explained in the upcoming chapters.

There is no cure for MS, and the current treatments do not impair the disease's progress but rather treat symptoms and reduce the inflammatory process (Lassmann, 2019). Therefore, drug-repurposing approaches can support finding new therapies, especially for the still unmet clinical necessity for promoting endogenous repair activities (Manousi and Küry, 2021).

1.2 Myelin loss and chronification within MS

According to Lublin and colleagues (2014) and Lassmann (2019), MS can be divided into three subtypes, which differ in the interval of demyelination episodes, scar spreading and severity. These three subtypes are (i) Relapsing-remitting MS (RRMS), the most common subtype, which is characterized by a Relapsing phase where the demyelination occurs more frequently, with a medium lesion spreading and higher infiltration of leucocytes. This process is followed by a remitting phase characterized by either active (with worsening of symptoms) or inactive lesion spreading (not showing worsening of symptoms). (ii) Secondary progressive MS (SPMS) is the worsening clinical condition of an RRMS patient, basically defined by an accumulation of disability symptoms, such as urinary incontinence and muscular dysfunction, and relapsing phases still occur. However, the lesion spreading is more severe, outnumbering the RRMS plaques output. (iii) Primary progressive MS (PPMS) is more

severe if taking into account the advancement of symptoms. PPMS patients showed more lesions in the spinal cord than in the brain, with their plaques presenting fewer leucocytes and other pro-inflammatory brain cells than RRMS or SPMS patients, making it more difficult to diagnose and treat.

The pathology of MS has its basis in spatial and temporal myelin disruption followed by astroglial scar generation. The myelin, once destroyed by microglia, stimulates cytotoxic lymphocytes that cross the blood-brain-barrier (BBB), instantly creating an autoimmune environment, inducing astrocytes and microglia along with the infiltrated immune periphery cells to target myelinated axons and OLs. This induction is followed by a loss of OLs, injury in nerve fibres and neuronal death (Baecher-Allan et al., 2018). Despite the patient's age, chronification has been the key matter of concern in MS. Young and elderly humans with a current stage of MS have differences in remyelinating potential, where the latter lack in remyelinated regions in the brain (Compston and Coles, 2008; Goldschmidt et al., 2009). Nonetheless, both age groups exhibit impaired remyelination in the chronic stages of the disease (Neumann et al., 2019).

Myelin repair via endogenous NSCs modulation has been reported as the key aim of drug-repurposing strategies, more specifically aiming for OLs regeneration and subsequent remyelination (Azim et al., 2017; Küry et al., 2018; Manousi and Küry, 2021). The SVZ harbours NSCs in the mammalian brain throughout ageing. These cells have an inherent potential to differentiate into astrocytes, OLs and neurons (Doetsch et al., 1999; Menn et al., 2006; Platel et al., 2012). NSCs are also a great target for anti-inflammatory drugs that can enhance their potential to differentiate into OLs to establish remyelination in the chronic demyelinated brain (Akkermann et al., 2016; Azim et al., 2020; Manousi and Küry, 2021). Supporting a biomedical translation of such strategies, human chronic-MS post-mortem brains were found to exhibit proliferation of SVZ-NSCs, suggesting that prolonged exposure to repetitive insults does not impede NSCs activation. (Nait-Oumesmar et al., 2007). However, even when MS patients show NSCs proliferation potential, they exhibit a decrease in the production of myelin oligodendrocyte glycoprotein (MOG; Tepavčević et al., 2011) and inadequate maturation of OPCs (Kuhlmann et al., 2008; Gruchot et al., 2019). A few number of OPCs can still differentiate. Although, a large number is obstructed in a pre-myelinating stage, not reaching mature stages (Chang et al., 2002). Mature-OLs that

survive demyelination enter a paucity stage and do not contribute to axonal myelination (Bacmeister et al., 2020; Orthmann-Murphy et al., 2020). These features together explain the lack of efficient remyelination observed in chronic MS patients, highlighting the need of new approaches to foster these intrinsic repair mechanisms.

In fact, as described above, demyelination is the key mechanism of concern in MS and one of the key brain cell subtypes to be involved in this process is the glial cells. From now on, we will focus on their characteristics during development, homeostasis, and disease, more particularly MS and pre-clinical models of demyelination.

2. Chapter 2: Glial cells, subventricular zone and myelination

2.1 Basic definition of glial cells

The brain is composed of neuronal cells and glial cells (see Figure 1). The latter comprise 50%-88% of the CNS tissue (von Barthheld et al., 2016; Jakel et al., 2017; Salas et al., 2020). Deprived of protruding axons, glial cells are unable to generate action potentials along their elongated cytoplasm (Azevedo et al., 2009; von Barthheld et al., 2016). Glial cells do not communicate via neurotransmitters. However, they utilize several other mechanical and chemical components to support neuronal communication, blood flow, metabolic and energy support within the brain (Vasile et al., 2017). According to Jakel and Dimou (2017), glial cells can be divided into three subtypes: (i) Microglia, the immune first responder of the brain which regulates synapse pruning and supports neuronal metabolism by debris digestion. (ii) OLs, the myelin maker in the brain. Myelin is a proteolipid structure that composes the whole cell body of mature OLs and is used by this cell to wrap around axons permitting faster electrical communication between neurons. (iii) Astrocytes are the neuronal life support, they regulate the metabolism of cholesterol, glucose and insulin, generate hormones and support axonal growth over development. Astrocytes and oligodendrocytes are the key cells to be discussed in this dissertation and details on astrogenesis and oligodendrogenesis will be dicussed further.

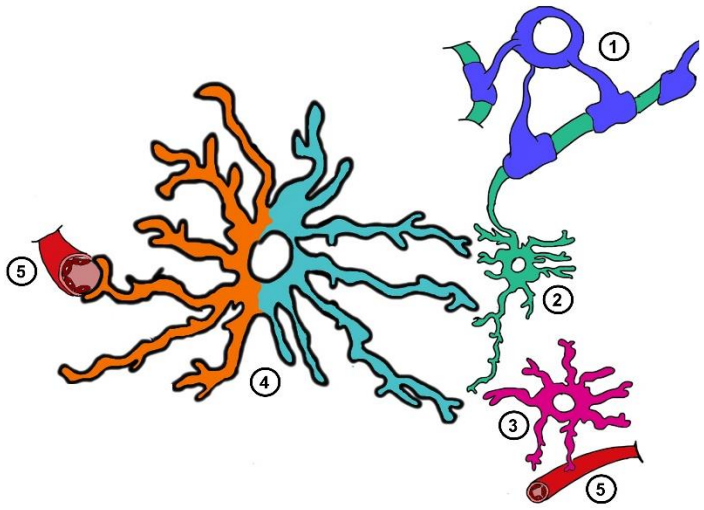

Figure 1 Brain cells. Brain cells can be divided into four categories (1) OLs, (2) neurons, (3) microglia and (4) astrocytes. Both astrocytes and microglia communicate with blood vessels (5).

2.2 Subventricular zone and neural stem cells subtypes within

The SVZ harbours glial progenitors throughout development into senescence. NSCs that populate this region give birth to neurons, OLs, astrocytes and their subtypes.

Thus, understanding the contribution of this neurogenic niche is indispensable to advancing endogenous strategies of cell replacement in health and disease. During the first stages of the mouse embryogenesis stage (E), the neuroepithelial cells give birth to the first neurons that will populate the cortex. At this level, this phenomenon occurs between E9-E11, and only two epitheliums are existent, the marginal zone and the neuroepithelium (Kriegstein and Alvarez-Buylla, 2009).

After E15, the radial glia (RGs) cells develop. These cells are the precursor of all cells during embryonic brain development. The RGs are located at the edge of the ventricles in the ventricular zone (VZ) area. A portion of the RGs that did not fix their protuberances on the VZ will differentiate into intermediate neurogenic progenitor cells. VZ-RGs that did not differentiate into neuronal precursors will expand their cytoplasm, elongating their end feet towards the cortical borders (basement membrane, marginal zone and cortical plate). These elongations are used by newborn neurons to "climb" towards their site of destiny in the brain (Platel and Bordey, 2016). Towards the end of the embryonic period, RGs that remained at the VZ start to retract their end-feet elongations, differentiate into astrocytes and OLs and migrate throughout the brain. Another portion of RGs that stay at the SVZ after birth then differentiate in NSCs, presenting a well-known bipolar morphology (Fuentealba et al., 2015; Platel et al., 2019). In the postnatal and adult CNS, the spatial heterogeneity within the SVZ is more stable. Cell subtypes will differ in gene signature and SVZ-wall origin. For example, the dorsal-SVZ will give birth to neurons and OLs, while the ventral wall provides GABAergic neurons (Rakic and Zecevic, 2003; Fiorelli et al., 2015; Azim et al., 2012, Azim et al., 2016; Kriegstein and Alvarez-Buylla, 2009; Platel and Bordey, 2016). In the adult mouse brain, the SVZ cells are subdivided into four subtypes: (i) type E/ependimall cells. (ii) type-A cells/neuroblasts, these NSCs reach the olfactory bulb and cortex, through the rostral migratory stream, and then differentiate to mature neurons. (iii) type B/SVZ-astrocytes can generate different progenitors and intermediate maturation of type A and Type C cells at the SVZ. (iv) type C is the transient amplifying progenitors (TAPs). These cells present an active migrating characteristic and develop into OLs and astrocytes (Garcia-Verdugo et al., 1998; Doetsch et al., 1999; Platel and Bordey, 2016).

2.3 SVZ-oligodendrogenesis and oligodendrocytes maturation

OLs are the last cell type to develop in the brain and comprise 20% of the mature cells in the adult mice CNS (Valerio-Gomes et al., 2018). Oligodendrogenesis begins in human and non-human primate brains at the 10th gestational week (GW). The first wave of pre-myelinating OLs (MBP+) is detected at the 18th GW in humans and on the E18 in mice (Yakovlev and Lecourse, 1967; Jakovcevski et al., 2009). Most of the OLs presented in the adult brain are derived from the SVZ during embryogenesis (Rakic and Zecevic, 2003; Kessaris et al., 2006), and the replacement of OLs after birth is held by SVZ-derived OPCs that migrate and develop into myelinating OLs in the grey and white matter (see Figure 2; Nait-oumesmar et al., 1999; Pluchino et al., 2003; Bond et al., 2015; Bergles and Richardson, 2016).

Within the SVZ, NSCs and OPCs differentiation into OLs are dependent of key TFs. Downregulation of Dlx1/2 (neurogenic key factors) and overexpression of oligodendrocyte transcription factor two (Olig2) naturally stimulate TAPs (Pcna+/Ki67+/Emx2+/Olig2+) to differentiate into OPCs (see Figure 2). In fact, 50% of OPCs in the adult brain are generated at the end of the embryonic stage. This system is regulated by Mash1/Ascl1, which stimulates platelet derived growth factor alpha (PDGFRα) and Olig2 expression in OPCs. The latter, when mature, declines in PDGFRα expression while enhancing MBP expression and sustaining Olig2. This process also regulates the differentiation of NG2-glia into OLs in the parenchyma (Petryniak et al., 2007; Parras et al., 2007; Nakatani et al., 2013). Fate-mapping investigations showed that Olig2 expression is mandatory for OPCs maturation in adult mice. OPCs that reach the white matter will develop into myelinating OLs, while those who reach the grey matter develop into NG2-glia (Dimou et al., 2008).

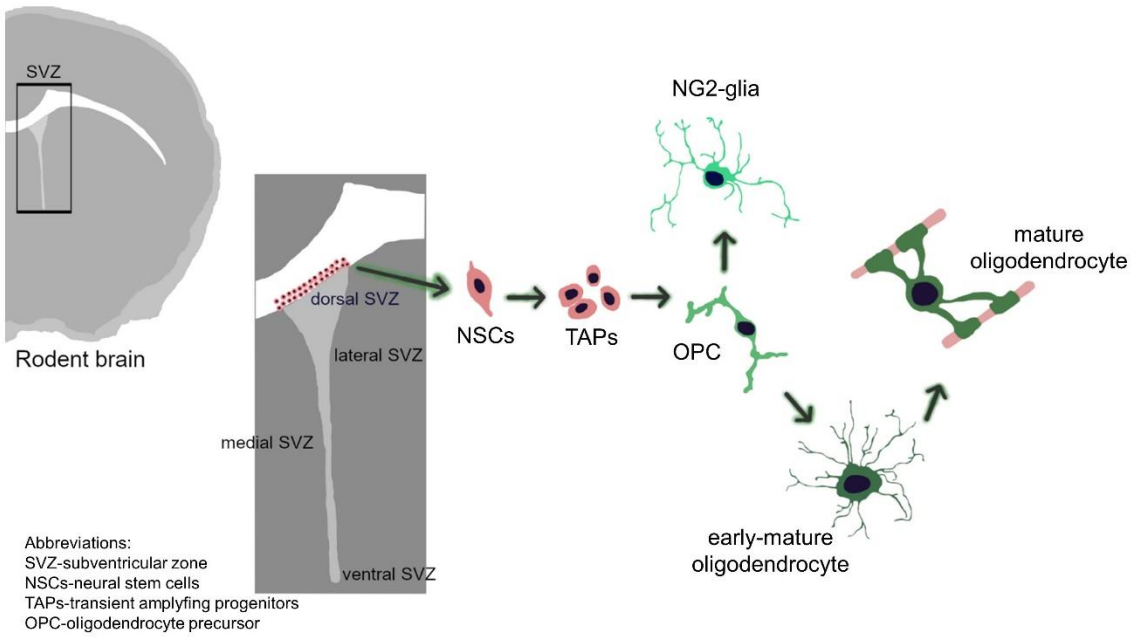

Figure 2 SVZ-Oligodendrogenesis. The d-SVZ is a niche for oligodendrogenesis. NSCs will generate TAPs that develop early on into OPCs and NG2-glia. These cells will later develop into an immature stage with no myelination processes. Once the myelin sheath is established, these cells become mature.

A gradual decline in Olig2 is commonly observed between postnatal day 7 (P7) and P91 when parenchyma OPCs start to mature (Rash et al., 2019). d-SVZ NSCs that are double-positive for paired box homeotic gene-6 (Pax6) and homeodomain-only protein X (Hopx) are more likely to progressively become OPCs in the postnatal and young primates' corpus callosum. The key gene regulating this development throughout embryonic and adult SVZ-oligodendrogenesis is also Mash1 (Petryniak et al., 2007; Parras et al., 2007; Nakatani et al., 2013; Bergles and, Richardson, 2016).

Epidermal growth factor (EGF) and epidermal growth factor receptor (EGFR) guide the expansion of TAPs and activated NSCs into an oligodendrogenic phenotype in human and rodent embryogenesis (Filipovic and Zecevic, 2008; Jakovcevski et al., 2009; Gonzalez-Perez and Alvarez-Buylla, 2011). In mouse tissue, fate-mapping approaches revealed that activated NSCs (EGFR+) will exclusively generate Olig2+ and PDGFRα+ cells in the rodent SVZ. The same study found that activated NSCs in the adult mice came from d-SVZ and arose from Gfap+ TAPs. These cells later in development reached the septum and corpus callosum as mature OLs (Ortega et al., 2013.2). Single-cell analysis with SVZ-derived NSCs revealed that most SVZ-NSCs

express an astrocytic fate. However, the proximity of the d-SVZ with the corpus callosum creates an epigenetic environment that directs these NSCs into an oligodendroglial fate (Azim et al., 2012; 2017; Vancamp et al., 2019; Mizrak et al., 2019).

Recently both galectin-3 (Al-Dalahmah et al., 2019) and fibrinogen (Pous et al., 2020) were identified as the major factors for dorsal- and lateral-SVZ oligodendrogenesis in both adult rodents and young humans. Both TFs upregulate the bone morphogenetic receptor one (BMP-1) which stimulates the development of SVZ-NSCs into astrocytic or oligodendroglial fate.

2.4 Mature oligodendrocytes: markers, subtypes and functions in brain myelination

Throughout development, OPCs lose expression of Gfap to become mature OLs. OPCs and NG2-glia, if still expressing Gfap, are considered immature, mostly due to their conserved potential to become an astrocyte (Tripathi et al., 2010; Alghamdi and Fern, 2015; Juarez et al., 2016). However, if these cells lose Gfap expression and maintain Pdgfrα, NG2 (oligodendroglial progenitors cell-structure markers), Sry-box transcription factor 10 (Sox10) and Olig2 expression (canonical oligodendroglial lineage nuclei-markers), they can then be considered mature (Kang et al., 2010; Juarez et al., 2016). These mature OPCs and NG2-glia now develop into myelinating cells and, by entering an early-mature stage, start to express molecules such as 2',3'-Cyclic-nucleotide 3'-phosphodiesterase (CNPase), and glutathione S-transferase Pi (GSTπ), which both enable OLs to start wrapping axons and growing their end feet (El-Waly et al., 2014; Juarez et al., 2016). However, these cells are only able to remyelinate when undergoing morphology maturation. This mature phase is commonly identified by the expression of adenomatous polyposis coli clone CC1 (CC1), MBP and PLP. These proteins are usually expressed when the myelin sheath is completely formed (Juarez et al., 2016; Gruchot et al., 2019). High expressions of Olig2 and Sox10 were also identified after the early-mature OLs started to spread their branches and wrap their end feet around axons, initiating the myelination process (Emery, 2013; Hornig et al., 2013; Zhang et al., 2022). Once the myelination is finished, these now mature myelinating OLs will sustain the expression of PLP, MBP, CC1, Olig2 and Sox10 (Juarez et al., 2016). The active myelination phase was recently

identified in OLs when breast carcinoma-amplified sequence 1 (Bcas1) is expressed (Fard et al., 2017). Previously identified in breast carcinoma, ablation of this protein in the brain prevents myelination and was found to be expressed in OLs when actively myelinating in both development and disease (Ishimoto et al., 2017; Fard et al., 2017; Li et al., 2022). See Figure 3 below for more details on OLs development and related cell markers.

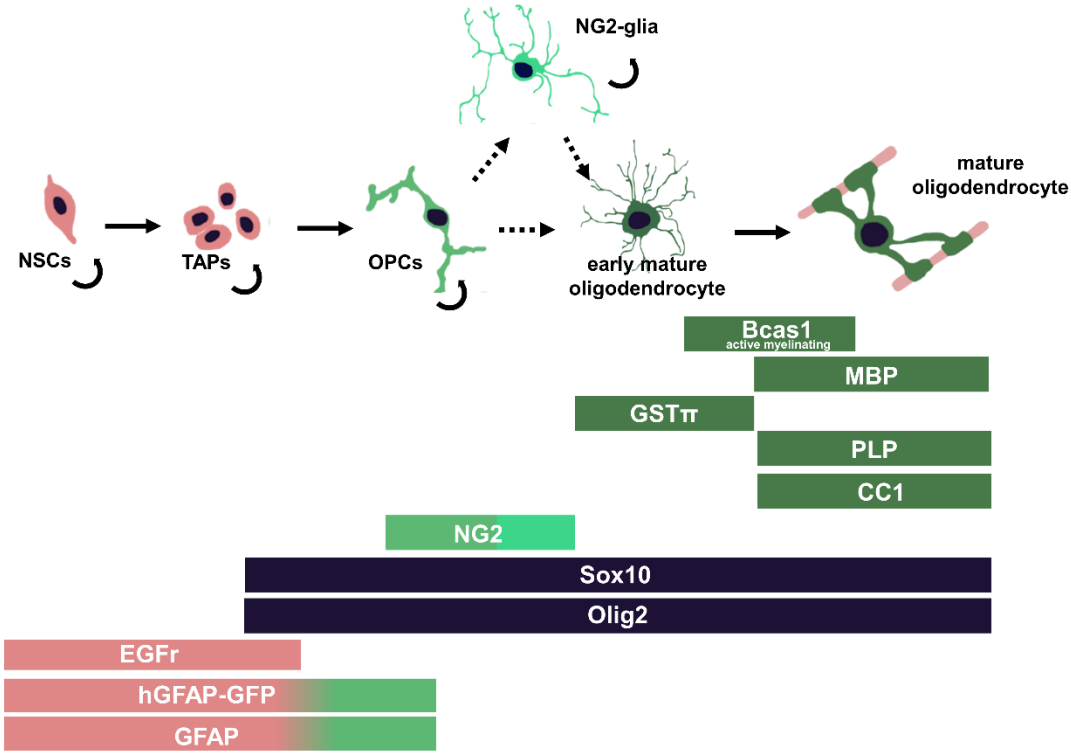

Figure 3. Oligodendrocyte development and related markers. The figure shows the canonical oligodendrocyte development in the mammal brain and the stages and related markers within the maturation of NSCs into a mature oligodendrocyte. TAPs that are positive for EGFR, Sox10/Olig2 exhibit an oligodendroglial fate and will mature into an OPC or NG2-glia, expressing Gfap and NG2 when in an immature stage. These cells lose expression of Gfap and enter an early mature stage by expressing GSTπ. Bcas1 indicates that these cells are in the early-myelinating active process and, once mature, express MBP, PLP and CC1. The expression of Sox10 and Olig2 is nuclei related and identifies the oligodendroglial lineage cells in all stages during and after early differentiation (TAPs stage).

3. Chapter 3: Astroglial heterogeneity, reactive astrogliosis and its contribution to myelination

3.1 Astrogliogenesis

Similar to OLs, astrocytes are generated in the SVZ during GW 18 in humans and between E12-18 in mice. Early after birth, murine astrocytes divide and expand throughout the brain, reaching a mature morphology at P21 (Yuasa, 2001; Menn et al., 2006; Moreno-Garcia and Molnar, 2015; Tabata, 2015). SVZ-resident type b cells are the key progenitors of astrocytes in adult mice. These NSCs differ in quiescent or activated and present two subtypes (i) B1 (“Bushy” morphology expressing Gfap, Nestin, CD133, EGFR), (ii) B2 (bipolar morphology; expressing Gfap, Nestin, negative for CD133 and Egfr), (Platel and Bordey, 2016).

Once mature, astrocytes (earlier type-b cells) lose expression of EGFR, sustain expression of Gfap (Platel and Bordey, 2016) and enlarge their branches. Mature astrocyte branches show increased morphology complexity and enhanced expression of S100β and glutamate system-related proteins such as Glast-astrocyte cell surface antigen-1 (Glast), Glutamine synthase (GS) and Glut-1 (Sofroniew and Vinters, 2010; Schiweck et al., 2018). Astrocytes are endowed with a large capability to change their transcriptomic and proteomic phenotype. In the event the brain is affected by injury or disease, astrocytes become reactive, expressing and releasing neurotoxic molecules [C3d, lipocalin 2 (Lcn2), inducible nitric oxide synthase (iNOS)] and neuroprotective molecules [Stat3, Timp1, S100a10 (Liddelow et al., 2017; Clarke et al., 2018; Escartin et al., 2021)]. Astrocyte plasticity in injury, disease and ageing is defined as reactive astrogliosis (Escartin et al., 2021) and will be further explained in the following section. See figure 4 below for more details on astroglial development and related protein expression.

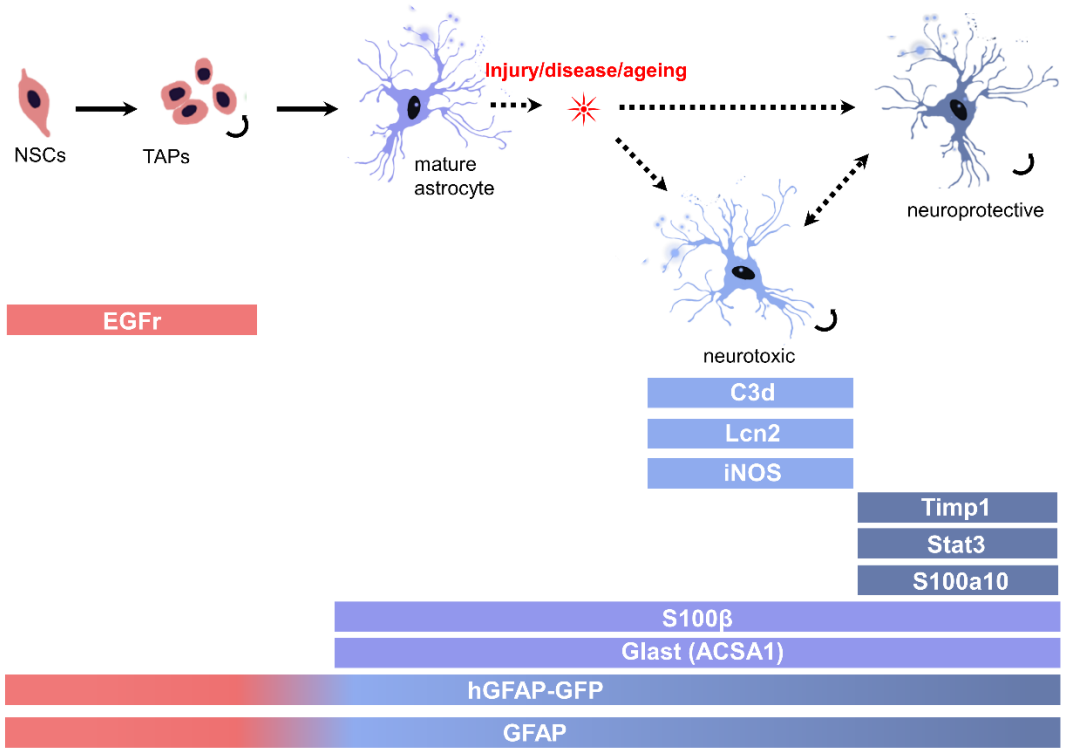

Figure 4. Astrocyte development and related markers. The figure shows the canonical astrocyte development in the mammal brain, the stages and related markers within the maturation of NSCs into a mature astrocyte, and the markers that identify a reactive astrocyte in a neurotoxic or neuroprotective state. Mature astrocytes are developed from NSCs and TAPs positive for EGFR, and Gfap. Once mature, astrocytes lose expression of EGFR and express S100β, Glast (ACSA1). Following injury, disease or ageing, mature astrocytes acquire a reactive state defined by their contribution to tissue damage or recovery. C3d, Lcn2 and iNOS identify neurotoxic reactive astrocytes, while Timp1, Stat3 and S100a10 identify neuroprotective reactive astrocytes.

3.2 Astrocyte subtypes and functions within the mammalian brain

The first characterization of astroglial morphology and possible function was performed by Santiago Ramon y Cajal (1909), defining these cells in accordance with their morphology and complexity. Astrocytes comprise over 20%-40% of all glial cells in human CNS, found as radial glia during embryogenesis, and as protoplasmic or fibrous astrocytes in the adult grey and white matter respectively (Sofroniew and Vinters, 2010). However, there are many other subtypes that are more specialized: the velate astrocytes (in the cerebellum), pituicytes (neurohypophysis), surface-associated astrocytes (Perivascular, marginal and Gomori), radial astrocytes that comprise Bergmann glia (cerebellum), RGs, NSCs (SVZ and hippocampus), tanycytes (hypothalamus) and, Muller glia (retina). Despite the subtypes previously described, humans exhibit three particular subtypes: interlaminar astrocytes, polarized

astrocytes, and varicose projection astrocytes (Vasile et al., 2017). These astrocyte subtypes described above were primarily distinguished by morphological differences and tissue localization (Sofroniew and Vinters, 2010). Nowadays, more accurate strategies such as gene transcriptomics and cell-tracing are able to better identify astrocyte heterogeneity. Additionally, such new strategies have shown that fibrous and protoplasmic astrocytes are derived from a different cell line in the mammalian brain (García-Marqués and López-Mascaraque, 2013). Hence, identifying astrocytes based on their intrinsic heterogeneity within a species throughout development, in different brain regions, and according to their transcriptomic and proteomic signatures is key to identifying their activity in health and disease (Matias et al., 2019; Yang and Jackson, 2019; Escartin et al., 2021).

Astrocytes are responsible for several mechanisms in the brain: providing metabolic support to neurons (Sofroniew and Vinters, 2010), regulating the electric communication within axons via the internodes gap junction, and controlling memory formation and maintenance by either engulfing or promoting synapse formation and maturation (Orthmann-Murphy et al., 2008; Chung et al., 2015; Dutta et al., 2018) to name a few. Astrocytes utilize the thrombin-dependent proteolysis system to regulate attachment in nodes of Ranvier. Once activated in astrocytes, this system reduces the metabolic support within the nodes, decreasing velocity and spike-time electric conduction of axons (Dutta et al., 2018). This system is, among others, the key process to modulating memory plasticity in mice and is dependent on astrocytes (Lee and Chung, 2019). Astrocytes guard the BBB, preserving the brain from pathogens that might affect the body (Sofroniew et al., 2020). Working as the satellite cell of the BBB, they perform two key activities: (i) communicate through their laminin cytoskeleton with the integrin-α2 receptors in pericytes sustaining the integrity of the tight junctions (Tao et al., 2014); (ii) identify activated leukocytes that are surrounding meninges mitigating their migration into the CNS and preventing neuroinflammation (Sofroniew, 2020; Sanmarco et al., 2021).

Still on that topic, the mechanisms which foresee neuroinflammation is unclear, yet, this process does precede neurodegenerative diseases (Guzman-Martinez et al., 2019). Following inflammation, the microglia and astrocyte become reactive and are inclined to deactivate any malfunctioning cells within the CNS (Hui-Ming and Jau-

Shyong, 2008; Guzman-Martinez et al., 2019). In astrocytes, this process is named reactive astrogliosis, and its purpose is unclear (Sofroniew, 2020; Escartin et al., 2021). This stage of glial stress is necessary for both damage and recovery, whether to promote homeostasis or neuroinflammation. However, increased neuroinflammation is the cause of several neurodegenerative diseases such as MS and and the demyelination that ensues (Brambilla, 2019; Sofroniew, 2020).

3.3 What does reactive astrogliosis stands for?

Astrocytes that undergo reactive astrogliosis in response to damage change their morphological, transcriptomic, metabolic and proteomic characteristics. Depending on the disease and region of the brain, astrogliosis can be either proliferative or non-proliferative. Transcriptomic evaluations showed that these astrocytes are divided into subpopulations that differ in their genetic and proteomic signatures, responding either to mitigate or stimulate recovery (Sofroniew, 2020; Escartin et al., 2021; Hasel et al., 2021).

This umbrella of subtypes and activities developed by astrocytes over damage and repair was under a dense cloud of poorly and imprecise characterization. Aware of this dilemma, Escartin and colleagues (2021) published a consensus statement established by 81 authors from 22 scientific institutes, consisting of the ideal approach for characterization of astrocyte heterogeneity and reactive astrogliosis in animal models and human tissue. In this publication, the authors emphasize that to precisely identify the heterogeneity within these cells, key variables of investigations such as healed or diseased tissue, genome or proteome signature, morphological complexity, sex, and species must be investigated. This type of resolution is crucial to improving the understanding of reactivity in astrocytes. Supporting this fact is that Gfap-high expression was erroneously utilized for many decades as a unique identification for astrocyte neurotoxicity (Sofroniew et al., 2020). Reactive astrogliosis was also interpreted as an unchangeable pro-degenerative response and that the ablation of this mechanism could be beneficial over time (Jakel and Dimou, 2017). However, recent studies such as the one performed by Lohrberg and colleagues (2020) have found that a lack of astrocytes diminishes the chances of OPCs maturation, hence, impairing remyelination. Other studies have shown that Gfap-high expression is no

longer a neurotoxicity indicator, and it is also correlated to neuronal repair and tissue recomposition (Xu et al., 2018; Jurga et al., 2021; Moulson et al., 2021).

In recent years, several authors approached reactive astrogliosis heterogeneity following the guidelines indicated in this consensus (Escartin et al., 2021), more precisely determining the involvement of these cells throughout disease development. Fundamental attributes that can define astrocytes as detrimental or not for remyelination will be discussed in the next topic.

3.4 Mechanisms of gliosis and death of oligodendrocytes within the demyelinated SVZ and corpus callosum

The subtypes of MS present three distinct patterns within the active lesion, and these patterns are used to define how the injury is affected. Pattern I in active lesions is related to extensive white matter demyelination (60%-80% of the region is demyelinated) and low oligodendrocyte death (Dutta et al., 2011; Lassmann et al., 2012). Another two patterns characterize the spectrum of cell loss. Pattern II characterizes a defective function of OLs (low demyelination and presence of OLs in degradation), while pattern III identifies a lack of OLs and extensive myelin loss. Both patterns II and III present an enhancement of chemokine receptor 3 (CXCR3), glutamate, nitric oxide, perforin, interferon-gamma (INF-γ) and activated T-cells in the blood and cerebral spinal fluid (Minagar and Alexander, 2003; Mijikovic and Spasojevic, 2013). The death of OLs in MS and EAE is also related to necroptosis, a mechanism regulated by RIPK1 and RIPK3 that phosphorylate MLKL, inducing oligomerization at the OLs plasma membrane. Both RIPK1 and -3 are the antagonists of caspase-8, which activate the release of TNF-α and activate microglia and astrocytes via the MEK/ERK pathway system. This mechanism once activated induces ribosomal impairment and upregulation of pro-inflammatory interleukins via activation of the nuclear factor kappa-light-chain-enhancer of activated B cells (NFκB) pathway (Caprariello et al., 2012; Jha et al., 2010). In addition, this system enhances the release of pro-inflammatory molecules that induce the accumulation of oligomers within the OLs, impairing mitochondrial metabolism, hence, mitigating remyelination in the corpus callosum (Campbell et al., 2014; Ofengeim et al., 2015; Sadeghian et al., 2016; Zelic et al., 2021). During the peak of inflammation in EAE, a gradual decrease in migration of type-A, -B and -C cells from the SVZ is observed. The proliferation of

newly generated neuroblasts (PSA-NCAM+) is still occurring. However, these cells are incapable of clustering and migrating, thus affecting the regeneration of the neuronal population (Pluchino et al., 2008).

Activation of NFκb induce copper impairment, ferroptosis and oxidative stress which leads to upregulation of the complement pathway, and production of metallopeptidases (MMPs). This process directs the OLs loss observed in EAE (Hu et al., 2013; Zarruk et al., 2015), CPZ (Pandur et al., 2019) and MS (Pluchino et al., 2008; Oveland et al., 2021; Siotto et al., 2019; Jing et al., 2021). The NFκB system more specifically upregulates apoptosis-related molecules such as caspase-1, -3, microtubule-associated proteins 1A/1B light chain 3A (LC3), FADD-like apoptosis regulator (cFLIP), interleukins (IL-1β, -6, -17, -18), and, Act1 (Tanner et al., 2015; Mckenzie et al., 2017). Release of such pro-inflammatory factors, sustain a cycle of glial reactivity (Wang et al., 2018) that maintain a cytotoxic environment which limits the OPCs expansion (Kirby et al., 2019). In fact, EAE is adequate to investigate acute stages of demyelination and cell-mediated organ-specific mechanisms (Constantinescu et al., 2011; Oveland et al., 2021). On the other hand, CPZ is more suitable for understanding chronic demyelination and spontaneous remyelination mechanisms (Vega-Riquer et al., 2019; Orthmann-Murphy et al., 2020). In this case, more suitable for the aims of this work.

CPZ induces demyelination through week-pulse-stages episodes, initiating its damage process from the second week of feeding with a primary myelin lesion. However, there is no significant microgliosis or astrogliosis (Gudi et al., 2014; An et al., 2020). The acute stage comprises global demyelination, an increase in reactive astrogliosis and microgliosis, insufficient remyelination, OLs loss and leucocytes activation. Those features can be observed after 5-7 weeks of feeding (Hibbits et al., 2012; Kaddatz et al., 2021). Chronic myelin lesion is observed after 9-34 weeks of feeding (Vega-Riquer et al., 2019; Nomura et al., 2019; Zhan et al., 2020; Gingele et al., 2020), and similarly to chronification in MS, is based on a consistent pro-inflammatory environment that impairs migration of progenitors and maturation of SVZ-NSCs into myelinating OLs, combined to an extensive loss of mature OLs (Butovsky et al., 2006; Pluchino et al., 2008). Insufficient remyelination after CPZ feeding was correlated to survival myelinating OLs. Those cells erroneously remyelinate the neuronal soma, keeping

axons denuded and diminishing the electrical activity within the brain (Bacmeister et al., 2020). New myelinating OLs are more likely to perform effective axonal remyelination, remyelinating 2/3 of the denuded axons in CPZ-fed mice and overcoming the “defected OLs” inefficiency (Orthmann-Murphy et al., 2020). In fact, during the CPZ diet (acute and chronic demyelination), the d-SVZ-derived OPCs still maturate into mature OLs. However, they cannot remyelinate axons efficiently (Brousse et al., 2015). This insufficiency is led by glial-dependent production of prostaglandins, caspase-3, and FAS-ligand, which mitigate the maturation of OPCs in the demyelinated lesion (Hesse et al., 2010; Palumbo et al., 2011). It is known that reactive astrocytes can regulate the fundamental origin of demyelination and loss of OLs in MS and CPZ-models by stimulating mitochondrial impairment, cholesterol abduction, copper deficiency and other mechanisms involved in apoptosis and neuroinflammation (Filippi et al., 2019; Bernaus et al., 2020). In this manner, declining inflammation and stimulating a pro-remyelinating state in astrocytes could foster the spontaneous remyelination found in CPZ, and RRMS or SPMS patients during the recovery/remitting stage, respectively (Piraino et al., 2005; Chari, 2007).

Gene levels of Gfap and SRY-box transcription factor 9 (Sox9) were upregulated in the chronic demyelinated brain between 6 and 9 weeks of CPZ feeding (Hibbits et al., 2012). During this stage, microglia and astrocytes enhance, migrate (Gingele et al., 2020) and accumulate near the deteriorated myelin, promoting de/remyelination (see Figure 5; An et al., 2020). Interestingly upregulation of Gfap in the white matter is sustained for six weeks after cessation of CPZ-feeding, highlighting a pro-remyelination feature of astrocytes in CPZ (Hibbits et al., 2012). In fact, astrocytes are key to regulating brain metabolism (Matias et al., 2019), and metabolic impairment is the main cause of OLs death in CPZ. Neurotoxic reactive astrocytes enhance the production of Lcn2 and reactive oxygen species (ROS), dysregulating the glutathione peroxidase (GPx), copper and iron machinery of OLs (Gudi et al., 2014; Baxi et al., 2017; Stidworthy et al., 2006; Al-Nimer et al., 2016; Itoh et al., 2018; Pandur et al., 2019). Neurotoxic reactive astrocytes downregulate growth factors and neurotrophins [brain-derived neurotrophic factor (BDNF), insulin-like growth factor one (Igf1), ciliary neurotrophic factor (CNTF)], combined with overexpression of complement molecules (C3 and C5a) and chemokines (CX3CRI), increasing loss of nodes and lipid metabolic

impairment within the myelin sheath (Praet et al., 2014; Lampron et al., 2015; Taraboletti et al., 2017).

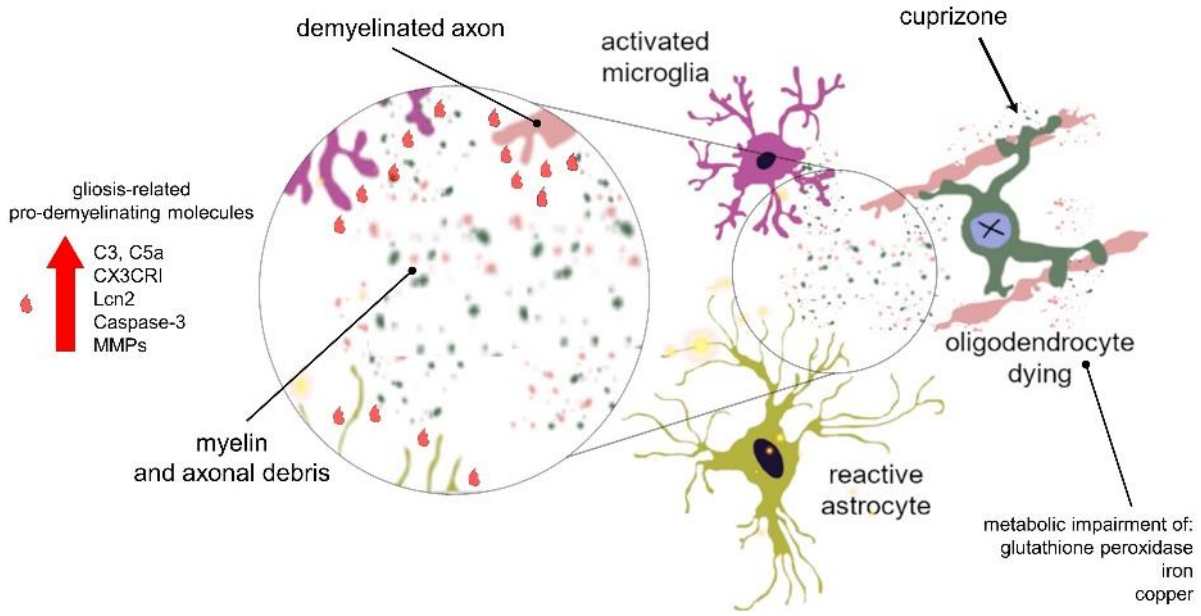

Figure 5. Key immunological features and gliosis within the demyelinated brain in cuprizone treated mice. The figure comprises the key features of the demyelinated brain of CPZ-fed mice. CPZ induces a metabolic impairment in OLs that die due to iron and copper metabolism complications and failure in the GPx system. The release of debris activates both microglia and astrocyte, increasing the production, expression and release of pro-inflammatory and pro-demyelination molecules such as C3, C5a, CX3CRI, Lcn2, Caspase-3 and MMPs.

Oveland and colleagues (2021) observed that two key pathways activated in CPZ and EAE could be translated to MS: the legumain and C1q complement systems. The latter and its cofactors are certainly the most versatile mechanism in the brain (Rus et al., 2009). Produced locally in the CNS, C1q can induce synapse pruning via microglial activation (Vukojicic et al., 2019), induce tissue damage by a cycle of reactivation of astrocytes in traumatic brain injury (Hammad et al., 2018) and enhance the severity of EAE in mice (Jégou et al., 2007; Hu et al., 2013). However, the complement pathway and its cofactor C5b9 can prevent OLs loss in EAE (Tegla et al., 2009; Tatomir et al., 2017). Hence, ablation of the complement pathway may not be the ideal strategy to avoid demyelination (Schartz and Tenner, 2020; Xin and Chan, 2020).

The complement system is divided into three different cascades: (i) enzymatic, (ii) lectin pathway and (iii) classical pathway. The classical pathway were classified as non-essential to the subset of demyelination in EAE (Boos et al., 2005). Nonetheless, the complement system is still a key interlink between MS, CPZ and EAE-based

models, hence crucial for biomedical translation (Dyer et al., 2005; Tassoni et al., 2019; Oveland et al., 2021; Morgan et al., 2021). C1q is the first co-factor produced in all three cascades and can bind to any structure recognized or not by antibodies (IgM or IgG). Even in the absence of pathogenic specific antibodies, C1q can bind to the surface of pathogens, initiating an inflammatory cascade (Almitairi et al., 2018). In disease, not only microglia and astrocytes can express complement components but also OLs, neurons and other cells within the brain (Carpanini et al., 2019). The key C1q producers in the brain are microglia (Fonseca et al., 2017; Dalakas et al., 2020). These cells can easily target myelin structures by using C1q and C3, initiating a cascade of inflammation and inducing OLs apoptosis (Michailidou et al., 2017). Microglia-derived C1q activate astrocytes that, once exposed to C1q, start to overexpress C3. These same microglial cells recognize their own created complement factors by C3a- and C5a receptors, creating a cycle of reactivation and release of C1q that sustains the inflammation, promoting more myelin disruption (Chen et al., 2020; Schartz and Tenner, 2020; Xin and Chan, 2020).

Chronification in MS was observed to enhance astrocyte production of C3 (Bhargava et al., 2021). Once expressing C3, astrocytes cease the metabolic support to neurons (Goetzl et al., 2018) and OLs (Itoh et al., 2017; Tassoni et al., 2019). Hence, it seems like C3 positive astrocytes are more likely to be neurotoxic than neuro-supportive (Dalakas et al., 2020). C3 is divided into several other co-factors within the complement pathway, and the cofactor d (C3d) was found to be expressed in reactive astrocytes within active lesions in MS (Liddelow et al., 2017) and EAE (Tassoni et al., 2019). C3d can bind to the myelin in OLs and exacerbate EAE output (Jégou et al., 2007). Currently, C3d is considered the key marker for neurotoxic astrocytes in demyelination (Escartin et al., 2021; Wan et al., 2022).

Tassoni and colleagues categorized the complement pathway as the key activated mechanism in astrocytes during optic nerve and spinal cord demyelination during EAE. The same authors and others next confirmed that along with C3, Lcn2, earlier reported as a pan-reactive identifier (Zamanian et al., 2012; Liddelow et al., 2017), is also key for demyelination (Nam et al., 2014; Wan et al., 2022). Lcn2 is known for its detrimental activities upon myelin disruption (Qiang et al., 2020). Its mechanism of action is by controlling iNOS expression in glial cells, therefore enhancing oxidative stress (Zhao

et al., 2020; Al-Nimer et al., 2016). In fact, ablation of Lcn2 in EAE reduced demyelination by diminishing MMPs production (Nam et al., 2014), highlighting this molecule as a key target for remyelination purposes. Discoveries on pro-remyelination molecules dependent on astrocytes to be released or produced are still in their initial unveiling (Rawji et al., 2020). In the next chapter, pro-remyelination mechanisms in astrocytes will be described in correlation with the key molecules that these cells express.

4. Chapter 4: The heterogeneity within reactive astrogliosis in remyelination

4.1 Stat3

Stat3 is one of the first key molecules expressed by reactive astrocytes (Liddelow et al., 2017). Stat3 activation induces CNTF and leukaemia inhibitory factor (LIF) production, promoting remyelination in the lysophosphatidylcholin (LPC)-dependent demyelination (Steelman et al., 2016). Knockout of astrocytic-Stat3 deprives Schwann cells and OLs of their myelinogenic features in the LPC-demyelinated CNS (Monteiro de Castro et al., 2015). Herrmann and colleagues (2008) observed that Stat3 ablation prevents astrogliosis. However, blocking Stat3 enhanced lesion spreading and demyelination. The same authors also found that Stat3 re-expression in astrocytes is mandatory for scar formation and cicatrisation in the demyelinated CNS.

4.2 Mafg and Nrf2

Oxidative stress is one of the key features behind OLs loss in MS (Lassmann and van Horssen, 2016; Carlström et al., 2020). The GPx system is crucial for the mechanism of maturation of OPCs and the survival of OLs during demyelination (French et al., 2009; Hughes and Stockton et al., 2021). This mechanism is regulated by reactive astrocytes, the key regulators of GPx within the demyelinated brain (Chen et al., 2019). The astrocytic production of GPx4, a cofactor of the GPx system, prevents ROS overproduction and ferroptosis in EAE, preventing cell loss (Hu et al., 2019). The GPx system is crucial for DNA-methylation, antioxidant activity and metabolic transition in mammals. The nuclear factor erythroid 2-related factor 2- (Nrf2) and MAFG-heterodimers (MAFG) are among the key components to control GPx activation during stress, whether promoting cytoprotection (Nrf2) or cytotoxicity (MAFG), (Hirotsu et al., 2012). Nrf2 was recently found as the key marker for astrocytes underlying a non-neurotoxic activity in MS and EAE (Wheeler et al., 2020). MAFG upregulation is strongly correlated to the overproduction of pro-apoptosis molecules (Hirotsu et al., 2012; Wang et al., 2021), and Wheeler and colleagues (2020) have shown that ablation of MAFG in astrocytes prevents EAE clinical output and direct astrocytes into a pro-remyelination status by activation of the GPx system via an Nrf2-dependent process. MAFG over-binding the Nrf2 receptors in astrocytes, blocking the activation of the GPx system. This mechanism is dependent on methionine adenosyltransferase

2 alfa (MAT2α) which controls DNA methylation within the nuclei, preventing Nrf2 production that leads to aberrant MAFG expression. The authors conclude that the GPx system's reactivation in astrocytes depends on the GPx-Nrf2 target genes (Gstm1, Gstp1, Gstp2 and Prdx6). These genes, when activated, improve ROS catabolism in astrocytes, depriving oxidative stress and minimizing demyelination.

4.3 S100a10

S100a10 is intrinsically expressed in reactive astrocytes in the hippocampus of healthy, aged mice (Clarke et al., 2018). This molecule was firstly reported by Zamanian and colleagues (2012) that by sequencing pro-inflammatory astrocytes in an *in vivo* model of neuroinflammation (LPS) and stroke (MCAO), found this molecule to be correlated with a neuroprotective phenotype in both models. Later, Liddelow and colleagues (2017) confirmed that in the presence of microglia-derived C1q, IL-1α and TNF-α (key molecules for neurotoxic fate), astrocytes lack S100a10 expression both *in vivo* and *in vitro*. S100a10 was then categorized as the key molecule to be expressed in astrocytes with an anti-inflammatory gene signature in the inflamed mouse brain (Hasel et al., 2021). However, S100a10 is not co-expressed with C3d in reactive astrocytes within the demyelinated MS-brain (Liddelow et al., 2017). Demyelinated mice are deficient in S100a10+ astrocytes in the spinal cord (Haindl et al., 2019) and hippocampus (Hou et al., 2020). However, both studies observed that astrocytes throughout demyelination will preferentially express C3d. Both Haindl and colleagues (2019) and Hou and colleagues (2020) identify that astrocytes within the remyelinated tissue are C3d negative and upregulate S100a10. Of note, investigations on the co- or interdependent expression of C3d and S100a10 were not investigated in chronic myelin damage.

4.4 Timp1 the specific pro-remyelination marker for astrocytes

MMPs play a central role in the degradation of extracellular matrix protein components and are pivotal for producing damage-associated molecular patterns (DAMPs) during inflammation and myelin damage in MS (Hernandez-Pedro et al., 2016; Jing et al., 2021). Production of MMPs is activated after ROS production and expands tissue damage (Yong, 2005; Mirshafiey et al., 2014). Commonly overexpressed in the cerebral spinal fluid of MS patients, MMPs are important biomarkers to identify active

lesions (remitted phase) in all three types of this disease (Aldinucci et al., 2018; Mohammadhosayni et al., 2020). The main role of MMPs in the literature is controversial. The MMP9 subtype was found to be crucial for NG2 glia to mature and differentiate (Larsen et al., 2003). Another study identified that MMP9 ablation slows EAE progression in mice (Onwuha-Ekpete et al., 2016).

The medical consensus about MMPs' contribution to MS converges to pro-demyelinating (Rempe et al., 2016). The MMP subtypes 2, 3, 7, 9 and 12 were found to be secreted by neurons, reactive microglia and astrocytes during damage, facilitating BBB leakage, hence, allowing migration of cytotoxic leukocytes (Song et al., 2015; Safaeinejad et al., 2018; Castellazi et al., 2018). The latter become the key producer of MMPs in the active lesion in MS, more specifically monocytes and T-helper 17 lymphocytes that enhance chemotaxis of T-helper 1 lymphocytes through the release of IL-17 and INF-γ. T-helper 1 lymphocytes will migrate into the site of damage upregulating myelin phagocytosis and improving migration of natural killer cells and other monocytes subtypes into the CNS (Mirshafiey et al., 2014; Song et al., 2015). Depletion of MMPs seems to contribute to remyelination in EAE (Rempe et al., 2016; Onwuha-Ekpete et al., 2016). However, the extended absence of MMPs signalling contributes to remyelination failure in MS (Gorter and Baron, 2020). Therefore removal of MMPs mitigates effective remyelination. In fact, endogenous deactivators of MMPs do exist. The "Timps" (1, 2, 3, and 4) are the most prominent ones and inactivate MMPs by bindings their catalytic site (Parks et al., 2004). Waubant and colleagues (1999) observed in the serum of RRMS-patients that an enhancement of MMP9 is followed by downregulation of Timp1 in MS patients undergoing demyelinating lesions. Highlighting that demyelination is dependent on Timp1 downregulation, and its lack can promote MS chronification (Lee et al., 1999; Trentini et al., 2015).

Timp1 was found to be expressed by astrocytes in elder mice and was recently categorized as a pan reactive marker for normal ageing reactive astrocytes (Clarke et al., 2018). Interestingly, reactive astrocytes at the corpus callosum and a-CC of LPS treated mice upregulate this molecule. These cells, particularly when upregulating Timp1, are more likely to present an anti-inflammatory gene signature and contribute to repair (Hasel et al., 2021). Timp1 is a pleiotropic protein. Additionally, induce MMPs

inactivation also improves cell survival, reduces pro-inflammatory cytokines (TNF-α, Fas/FasL), and modulates astrocytes into a non-inflammatory profile *in vitro* (Ogier et al., 2005). Crocker and colleagues (2006) showed that ablation of Timp1 in adult mice impairs spontaneous remyelination during EAE. The same group observed that Timp1 knockout affects the number of Gfap+ cells in the P7 mice white matter and that OPCs treated with the conditional medium of Timp1-knockout astrocytes cannot express mature OLs markers (A2B5 and O1; Moore et al., 2011). Houben and colleagues (2020) were also able to confirm that astrocyte-derived Timp1 drove OPCs to mature into OLs, and ablation of this molecule in astrocytes impaired spontaneous myelin regeneration in chronic-demyelinated mice (CPZ-fed). Moreover, Timp1 were strongly upregulated after the CPZ diet and were found to be expressed in astrocytes in MS-active lesions. This evidence highlights the importance of Timp1 expression in astrocytes and the role of these cells in fostering remyelination.

5. Chapter 5: Drug repurposing, medrysone and myelination

5.1 Drug repurposing

Brain repair approaches and drug-repurposing strategies are an alternative for myelin repair and oligodendrocyte replacement in MS (Küry et al., 2018; Manousi and Küry, 2021). There is no cure for MS. Current treatments improve patient lifespan by diminishing inflammation and lesion spreading but fail to improve chronification, thus revealing an unmet necessity to find new treatments for MS. (Wei et al., 2021). Fifteen years on average is how long it takes for a drug to be identified, optimized, developed and registered for human use (Hughes et al., 2011). Aggravating this situation, 7 in 10 drugs under clinical trials for MS do not receive approval from regulatory organizations (Gehr et al., 2019; Melamed and Lee, 2020). In the meantime, a patient bearing RRMS has a life expectancy after diagnosis of 15 to 35 years (Lunde et al., 2017). On the other hand, drug repurposing followed by official regulamentation takes on average 6 years, depending on the stage of development and registration within inspection agencies. Repurposing diminishes downtime, enabling a larger 2 to 6 fold chance of identifying a new effective drug (Pushpakom et al., 2018; Küry et al., 2018). In this case, a stronger and faster strategy to identify new drug treatments for MS and other diseases.

5.2 Medrysone and myelination

Notably, anti-inflammatory corticosteroids are among the key prescribed drugs for MS-patients in acute relapse episodes, the disease-stage when most of the immune mediated attacks is happening in the brain and spinal cord. (Elovaara et al., 1998; Lassmann, 2019; Gresle et al., 2020). No interruption of this process enhances the risk of sequeleae and by using corticosteroids the decrease on diapedesis of leucocytes into the CNS (Naray-Fejes-Toth et al., 1988; Williams, 2018) as well as reduction of integrin and selectins such as VLA-4 and LFA-1 in CSF and brain tissue of MS patients (Elovaara et al., 1998), diminish brain tissue damage. Resztak and colleagues (2022;pre-print), shown that dexamethasone regulate RNA levels of ARL6IP4; a gene related to reactivity and recruitment of Natural killer and CD8-T cells in MS. Both cells when activated act by releasing cytokines and proteases the will both enhance inflammation and promote tissue degeneration (Lassmann, 2019; Gresle et

al., 2020). In general, corticosteroids are allocated to promote an immunosuppressing response, regulating reactive leucocytes and promoting down regulation of pro-inflammatory factors (Williams, 2018). However don't necessarily contribute to remyelination in acute stages of demyelination (Not upregulating or regenerating MBP levels). This is confirmed in two publications (Chari et al., 2006 and 2007; Clarner et al., 2011) where prednisone was observed to do not contribute to remyelination and OLs replacement in CPZ-dependent acute demyelination.

Medrysone is a corticosteroid used in ophthalmology against allergic conjunctivitis, episcleritis and epinephrine sensitivity. Medrysone is recommended to high ocular pressure patients suffering from the diseases previously cited (Spaeth, 1966; Bedrossian and Eriksen, 1969). The literature does not report any exclusive mechanism of action performed by medrysone. In fact, pharmacodynamics reports define the pharmacological activity of medrysone is based on corticosteroids effects (VanWert et al., 2010). This category of synthetic drugs is mostly known for diminishing scar formation, fibrin deposition and phagocytic migration, primarily displayed by the downregulation of prostaglandins and leukotrienes, inhibiting the release of arachidonic acid (Naray-Fejes-Toth et al., 1988; Williams, 2018). Corticosteroids also downregulate NFκB activation, mitigating the Th1 inflammatory response in mammals (Auwardt, et al., 1998; Liberman et al., 2018). Notably, anti-inflammatory corticosteroids were reported to not contribute to remyelination and OLs replacement in CPZ-dependent acute demyelination (Chari et al., 2006 and 2007; Clarner et al., 2011). However, medrysone was not yet investigated in chronic demyelinated mice. Medrysone more exclusively was observed to improve myelinating features in Oli-neuM (immortalized cell lineage/*in vitro*) by enhancing MBP expression at the protein and gene level (Porcu et al., 2015) and was predicted (*in silico*) as a myelinogenic drug by enhancing oligodendroglial fate-related genes in SVZ-NSCs (Azim et al., 2017). Those observations raise the importance of understanding how medrysone improves myelination and its regenerative effects against chronic demyelination, and in this work we repurposed this drug with aims of myelin recover in an animal model of progressive MS.

6. Main results

6.1 Main results part 1- Pro-myelinating properties of medrysone

6.1.1 Medrysone does not induce primary OPC differentiation

Medrysone was shown to increase myelin gene expression in an immortalized OLs cell line [Oli-neuM cells; (Porcu et al., 2015)]. However, medrysone recently was predicted to promote SVZ NSCs to differentiate into the oligodendroglial lineage (Azim et al., 2017). Aiming to investigate the capability of medrysone to promote oligodendrogenesis, rat OPC cultures were prepared and exposed either to DMSO containing control buffer or to 5 µM medrysone for 72 hours. The number of myelin basic protein (MBP) positive cells did not change upon medrysone treatment (Figure 6c). Similarly, gene expression levels for Sox10, Pdgfrα, CNPase and Myrf did not change upon medrysone treatment (Figure 6d).

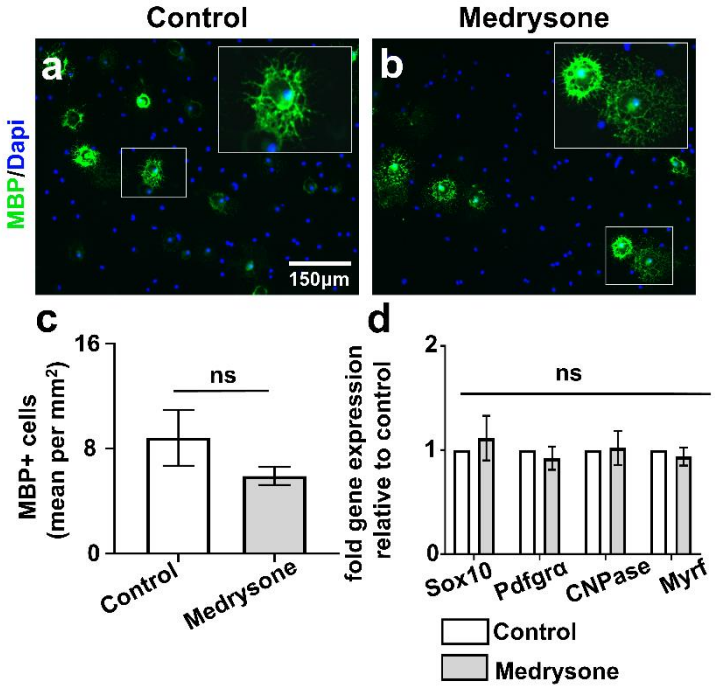

Figure 6. Primary OPC differentiation is not directly affected by medrysone. Primary OPC differentiation is not directly affected by medrysone. (a,b) representative images of primary cultured OPCs treated with DMSO (control) or 5 µM medrysone for 72 hours and stained for MBP. (c) The number of MBP positive cells does not change upon medrysone treatment. (d) Graphical representation of Sox10, Pgdfrα, CNPase and Myrf gene expression levels. Abbreviation: none significant (ns). Bars in (c) correspond to mean cell numbers per mm2 ± standard error of the mean (SEM). Bars in (d) correspond to relative gene expression levels ± standard error of the mean (SEM). Statistical significance was calculated using the two-sided Student´s t-test. Number of experiments n=4. This figure corresponds to the supplemental figure 1 of Oliveira-Junior and colleagues (2022). With permission from the publisher (The Lancet). Experiments not developed by the author.

6.1.2 Medrysone enhanced number of NG2- and Gfap-positive cells in d-SVZ cultured cells.

To understand the impact of medrysone in the differentiation of d-SVZ cells, cell cultures from p11 mice d-SVZ were prepared and treated with DMSO or medrysone at 5 µM. The corticosteoid increased the number of NG2+ cells (Figure 7b, 7c). In additon, the number of Gfap+ cells was also upregulated by the drug (Figure 7e, 7f).

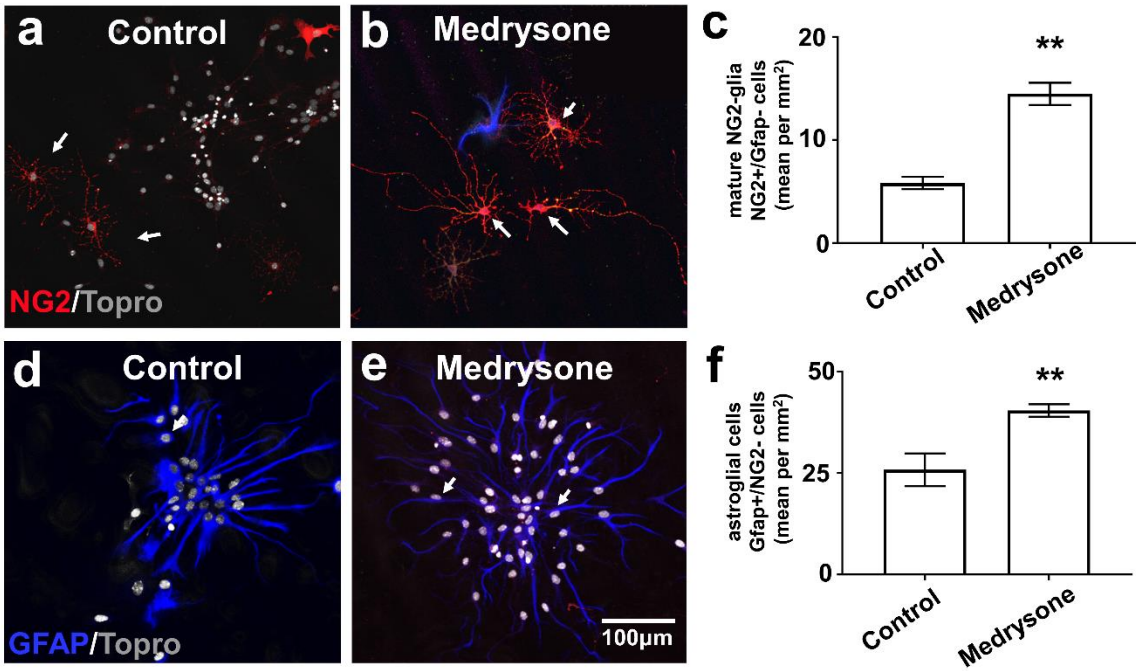

Figure 7. Medrysone enhanced numbers of mature NG2-glia and astroglial cells in d-SVZ cells primary cultures. Representative images of dorsal SVZ cells treated with DMSO or medrysone at 5 µM (a, b, d, e) stained for NG2, Gfap and Topro. Medrysone treatment significantly promoted the differentiation into NG2-glia (c) and astroglial cells (f). Scatter dot plot represents mean ± SEM. White arrows indicate the representative cell. Bars in (c, f) correspond to mean cell numbers per mm2 ± standard error of the mean (SEM). Statistical significance was calculated using the two-sided Student´s t-test. ** represents $p \leq 0.01$. Number of experiments n=4. Data within the figure is unpublished and will be included in a future publication.

6.1.3 Medrysone promotes oligodendrogenesis and myelination in postnatal cerebellar organotypic cultures

Myelinogenesis in OLs and astrocyte formation occur during the early postnatal development phase (Ortega et al., 2013; Rash et al., 2019). Aiming to investigate the capability of medrysone to promote oligodendrogenesis and myelination, cerebellar organotypic slice cultures from P6 rats were prepared and exposed either to DMSO containing control buffer or medrysone (5 µM) for 48 hours. The number of MBP+ cells and neurofilament positive (NF+) axons co-stained for MBP were quantified in the cerebellar superior semil lobe (Figure 8a, green box). Quantification revealed an increased number of MBP+ cells after medrysone application (Figure 8c, 8d). Additionally, the number of myelinated axons significantly increased after medrysone treatment (Figure 8e). Gfap+ cells were quantified in the grey matter and white matter from the cerebellar semil lobe (Figure 8a, red and green box). No impact on the astrocyte population was observed (Figure 8g-8h).

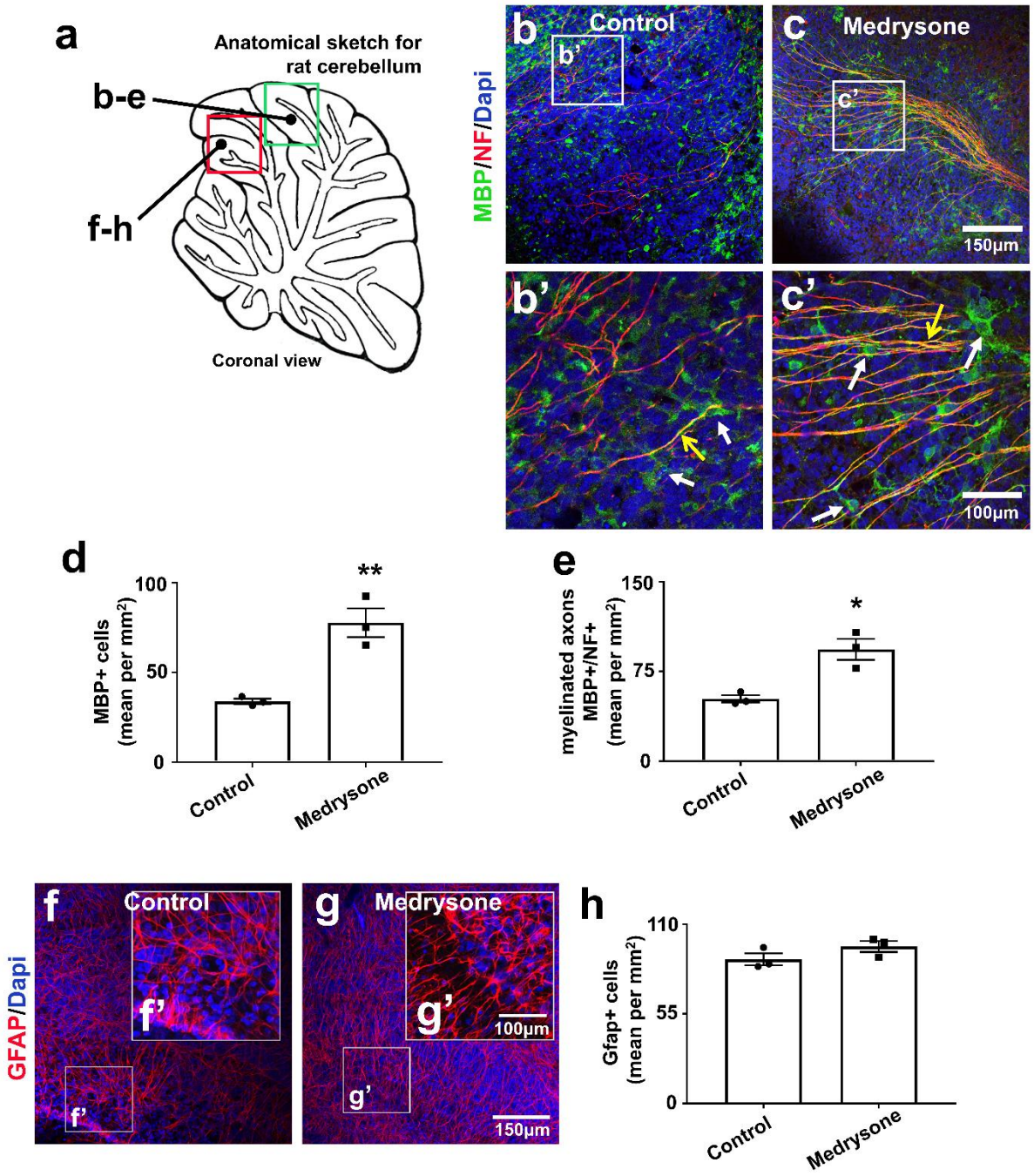

Figure 8 Medrysone promotes oligodendrogenesis and myelination in cerebellum slice cultures. (a) Scheme of rat cerebellum including areas of investigation. Representative images of cerebellar *ex vivo* organotypic cultures treated with DMSO (b, b', f, f') or medrysone at 5 µM (c, c', g, g') stained for MBP, Gfap and Dapi. The amount of MBP positive cells (d) and myelinated axons (e) were significantly increased after medrysone application. No effect on astrocyte formation (Gfap+ cells) were observed after medrysone treatment (g, h). White arrows indicate nuclei of cells, yellow arrows indicate myelinated axons. Bars in (d, e, h) correspond to mean cell numbers per mm2 ± standard error of the mean (SEM). Statistical significance was calculated using the two-sided Student´s t-test. * represents $p \leq 0.05$; ** represents $p \leq 0.01$. Number of experiments n=3. Data within the figure is unpublished and will be included in a future publication.

6.1.4 In vivo demyelination and drug-treatment procedure

To induce demyelination, 24-week-old transgenic hGFAP-GFP reporter mice were exposed to 0.4 % CPZ for nine weeks. During the last five days of CPZ feeding, mice received daily intraperitoneal injections of 5 mg/kg of medrysone- or saline solution. Over the week post cuprizone phase (WPC), mice received normal food for one or three weeks (Figure 1a). Six groups were analysed: (i) non-CPZ fed/control; (ii) 9 weeks CPZ diet/demyelination; (iii) 9 weeks CPZ, plus saline injection and one week of normal food (saline 1 WPC); (iv) 9 weeks CPZ, plus saline injection and three weeks of normal food (saline 3 WPC); (v) 9 weeks CPZ, plus medrysone injection and one week of normal food (medrysone 1 WPC); (vi) 9 weeks CPZ, plus medrysone injection and three weeks of normal food (medrysone 3 WPC). Immunofluorescence analysis was performed using 50 µm rostrocaudal coronal sections (1 rostral section, 1 middle section and 1 caudal section per n; Figure 9b) analyzing the corpus callosum junction (CCJ; Figure 9c' area 1), the corpus callosum adjacent to d-SVZ (a-CC; Figure 9c' area 2) and the d-SVZ (Figure 9c' area 3; divided into three micro-domains: 3.1-medial dorsal-SVZ; 3.2-middle d-SVZ and 3.3-dorsal-horn SVZ). For cell counting, 150 µm were analysed along the z-axis for all anatomic niches (Figure 9c'). For the CCJ an area of interest of 150 µm along the x/y-axis and, for d-SVZ an area of interest of 100 µm along the x/y axis were analysed for cell counts.

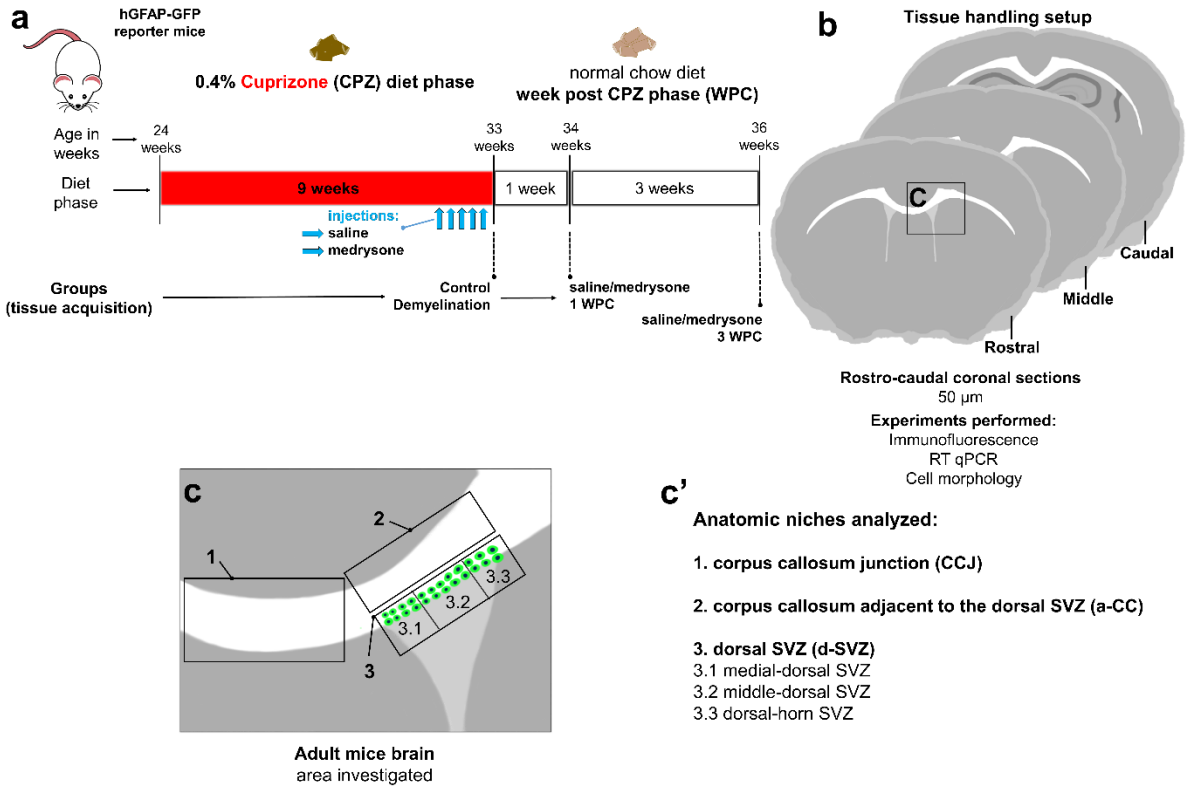

Figure 9. CPZ experimental setup. (a) Timeline of CPZ induced demyelination and of medrysone treatment in adult (24 weeks old) hGFAP-GFP reporter mice. CPZ treatment lasted for 9 weeks, then either medrysone- or saline solutions were applied intraperitoneally starting at five days before the end of the CPZ feeding period. Mice were sacrificed after one or three week's post-CPZ. For additional controls, healthy mice and CPZ fed mice without treatment were sacrificed. (b) Rostrocaudal directed coronal brain slices were collected between 0.745mm to -1.25mm Bregma, and then analysed using immunofluorescence. (c, c') The corpus callosum junction (CCJ), corpus callosum adjacent to the dorsal-SVZ (a-CC) and dorsal-SVZ (divided in micro-domains: 1-medial dorsal SVZ, 2-middle dorsal SVZ, 3-dorsal horn SVZ) were the anatomic niches investigated. This figure is an adapted version to the figure 1 of Oliveira-Junior and colleagues (2022). With permission from the publisher (The Lancet).

6.1.5 Medrysone treatment recovers body weight in chronic demyelinated mice

Bodyweight loss accompanies demyelination in CPZ-feeding (Zhen et al., 2017; Zhan et al., 2020; Toomey et al., 2021). Body mass tracking is fundamental to identifying drug efficacy in rescuing homeostasis (Zhen et al., 2017). Therefore, we measured the final body weight in grams of eight mice per group before humanized euthanasia (Figure 10). Demyelinated mice showed a loss of body weight and saline-treated mice in both time points were unable to recover body mass (Figure 10). Medrysone-treated mice recovered body weight at both time points, with slightly greater weights than control mice (Figure 10b, 10c).

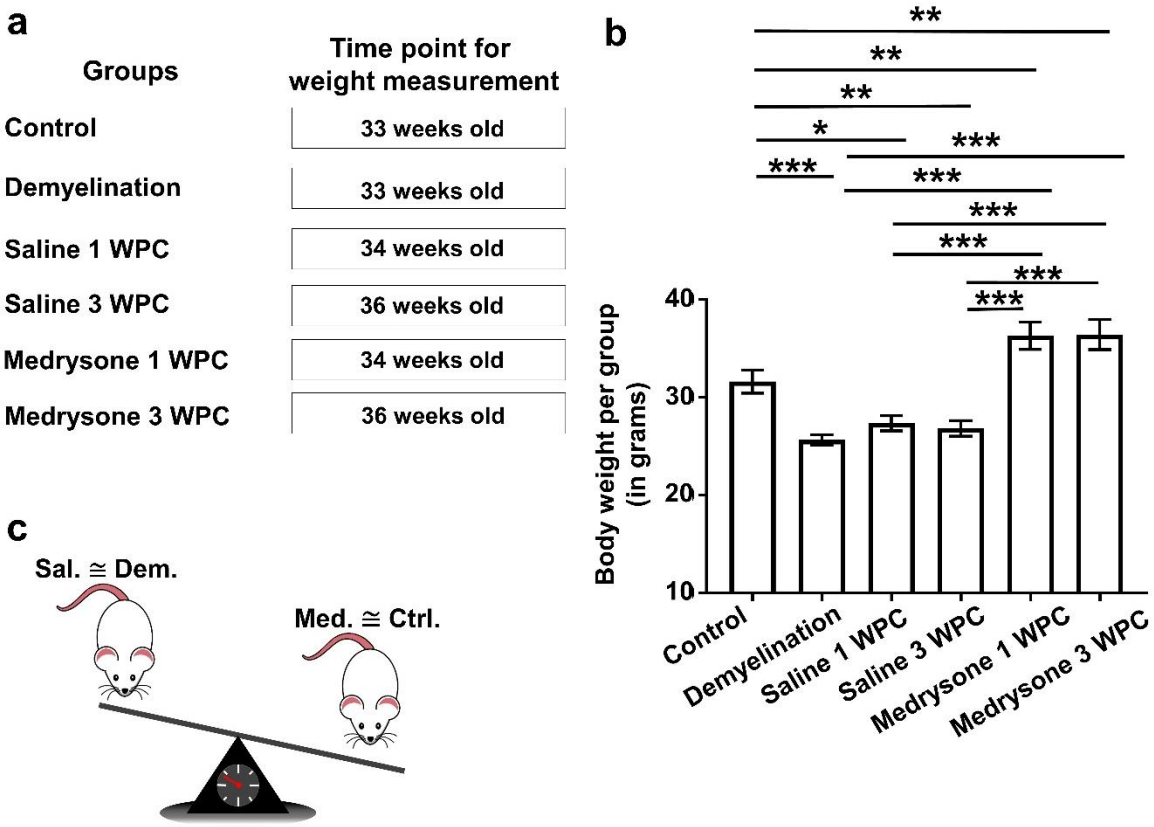

Figure 10. Medrysone treatment rescues body mass weight. (a) Representative organogram showing time points for body weight measurement per group. (b) Quantification of body weight in grams revealed that demyelination induced a decrease in body weight without recovery after saline administration and normal feeding. Medrysone improved weight recovery. (c) Graphical sketch of medrysone efficacy in body weight recovering. Data are shown as mean values ± SEM. Statistical significance was calculated using a two-way ANOVA with multiple comparisons Bonferroni post-test (*p < 0.05, **p < 0.01, and ***p < 0.001). Number of animals n=8. Data within the figure is unpublished and will be included in a future publication.

6.1.6 Remyelination and nodes of Ranvier recovery were improved by medrysone

We aimed to evaluate the potency of medrysone to improve remyelination in chronic demyelinated mice induced by a prolonged CPZ application. Looking at the CCJ (see Figure 9c) we found a diminished MBP expression (Figure 11s) as well as lower numbers of early-stage mature OLs (GSTπ+), mature OLs (Olig2/CC1 double-positive) and of active myelinating OLs after 9 weeks of CPZ diet (Sox10/Bcas1 double-positive cells; Figure 11t,11u,11v; see Figure 11x for OLs maturation stages and representative markers). Adjacent localization of MBP and Caspr was used to identify nodes of Ranvier by their juxtaposition (Figure 11x'). Of note, the number of Caspr+/MBP+ nodes was reduced in response to demyelination (Figure 11w) confirming myelin loss. On the contrary, quantitative analysis revealed that medrysone

significantly promoted the recovery of MBP expression (Figure 11s), early-stage mature OL- (Figure 11t), mature OLs (Figure 11u) and active myelinating OLs (Figure 11v), as well as in nodes of Ranvier (Figure 11w) reaching levels similar to healthy controls at 1 and 3 weeks post CPZ, respectively.

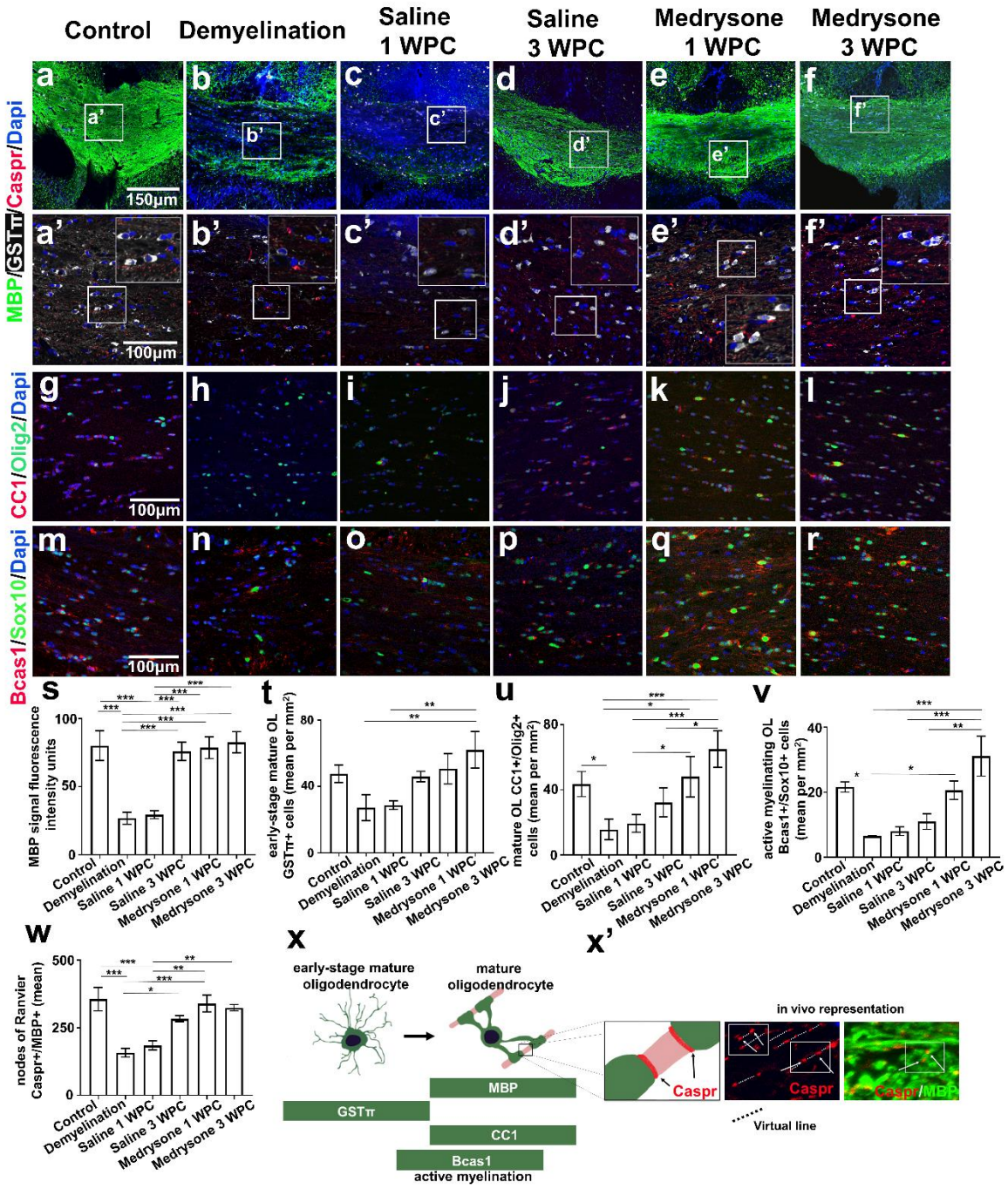

Figure 11. Medrysone promotes oligodendrocyte recovery and remyelination at the CCJ. Representative pictures of the corpus callosum junction (CCJ, Figure 1c) stained for MBP, GSTπ, Caspr (a-d, a'-d') Olig2 and CC1 (g-l), Sox10 and Bcas1 (m-r) protein expression. (s) Quantitative analysis of MBP stained structures revealed a decrease of myelin expression in the demyelination group with saline treatment leading to weak remyelination and medrysone significantly promoting MBP recovery at the

early time point (1 WPC). (t, u, v) Similarly, the numbers of GSTπ positive, Olig2/CC1- and Sox10/Bcas1 double-positive cells recovered upon medrysone application accompanied by improved generation of nodes of Ranvier (w). (x) OLs maturation and representative markers (x') graphical and *in vivo* representation of nodes of Ranvier immunofluorescence (Caspr+/MBP+). Bars in (s) correspond to mean fluorescence intensity ± standard error of the mean (SEM), bars (t, u, v) correspond to mean cell numbers per mm^2 ± standard error of the mean (SEM), bars in (w) correspond to mean number of nodes ± standard error of the mean (SEM). Statistical significance was calculated using a two-way ANOVA with multiple comparison Bonferroni post-test (*$p < 0.05$, **$p < 0.01$, and ***$p < 0.001$). Number of animals per analysis: n=6 (s, t); n=5 (u, v, w). This figure corresponds to the figure 2 of Oliveira-Junior and colleagues (2022). With permission from the publisher (The Lancet).

6.2 Main results part 2- The impact of medrysone in number of astroglial cells in inflammation and demyelination

6.2.1 Demyelination affects hGFAP-GFP cells at the corpus callosum and the d-SVZ

Throughout myelin damage and depending on the inflammatory stage, astrocytes exert either detrimental or beneficial effects on remyelination efficacies (Skripuletz et al., 2013; Schirmer et al., 2021). After CPZ-mediated chronic demyelination, we found that the degree of green fluorescent protein (GFP+) positive cells at the CCJ did not change significantly between groups/pathophysiological stages (Figure 12g). However, when looking at the a-CC, a higher number of GFP+ cells versus all groups was found after demyelination, followed by elevated levels in the medrysone 3 WPC group (Figure 12n) and no difference in the controls. Interestingly, in the d-SVZ, medrysone treated animals at 1 WPC displayed significantly elevated number of transgenic cells which sharply dropped below control levels at 3 WPC (Figure 12o).

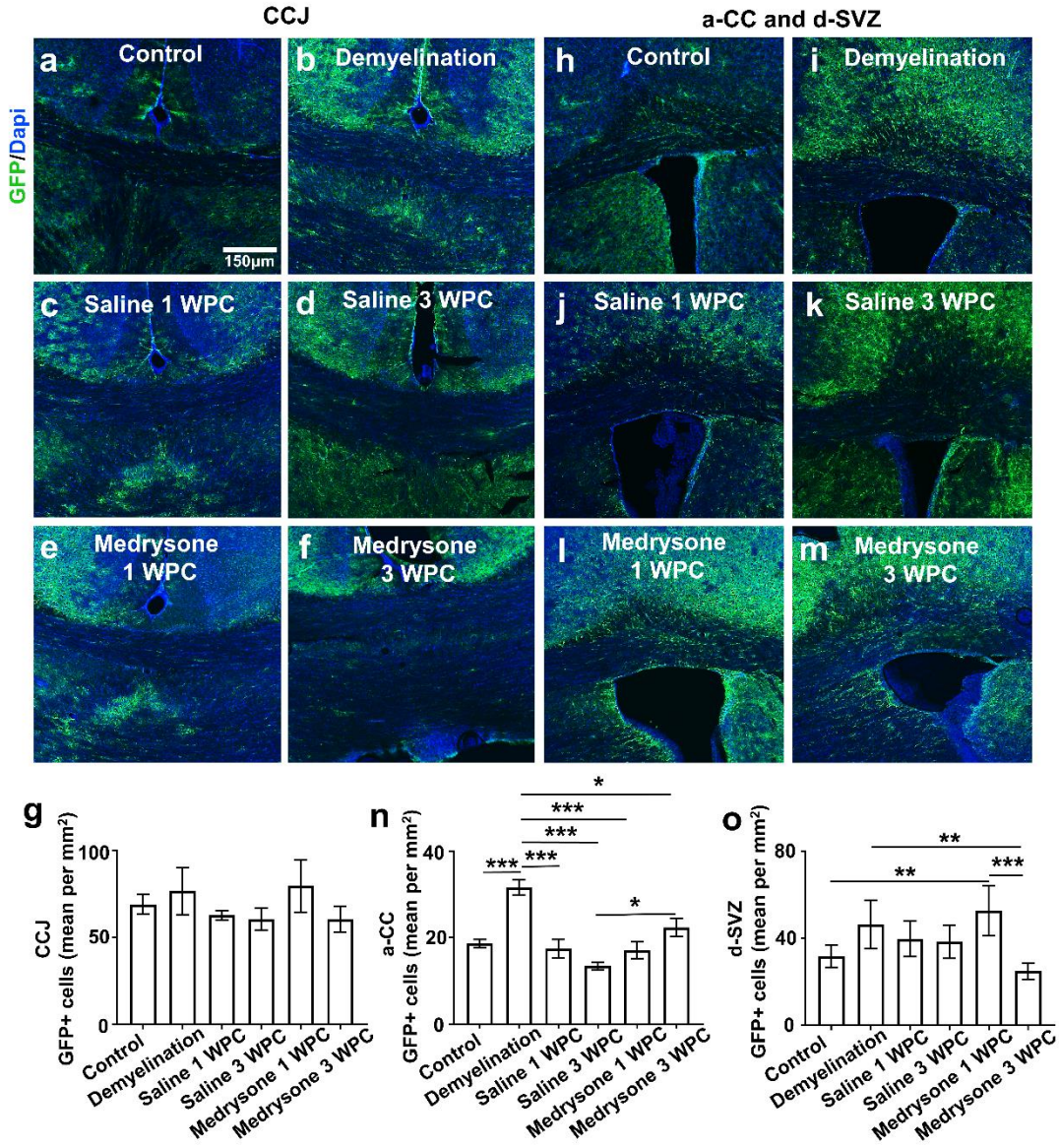

Figure 12. Quantification of hGFAP-GFP positive cells in the corpus callosum and d-SVZ. (a-m) Representative pictures GFP-positive cells at the CCJ, a-CC and the d-SVZ with cell nuclei visualized using Dapi. (g) Quantification of GFP-positive cells revealed similar number of GFP expressing cells in all groups at the corpus callosum junction. (n) In the a-CC demyelination induced the degree of GFP-positive cells (versus control) and a mild induction between medrysone and saline groups was found at 3 WPC. Moreover, in the d-SVZ (o), GFP-positive cells were enriched upon medrysone treatment at 1 WPC (versus control), sharply dropping thereafter (3 WPC). Abbreviation: non-significant (ns). Bars correspond to mean cell numbers per mm2 ± standard error of the mean (SEM). Statistical significance was calculated using Kruskal-Wallis test with Dunn's post-test (g) and two-way ANOVA with multiple comparisons Bonferroni post-test (n; o; *p < 0.05, **p < 0.01, and ***p < 0.001). Number of animals n=6 (g, o), n=7 (n). This figure corresponds to the figure 3 of Oliveira-Junior and colleagues (2022). With permission from the publisher (The Lancet).

6.2.2 Astrocyte dynamics is reflected by elevated Glast-positive cell levels

White matter pathology and OLs loss are also dependent on glutamate excitotoxicity (Li et al., 2016). Aiming to understand Glast expression in mature astrocytes, we performed S100β/Glast co-stainings (Figure 13a), revealing that S100β/Glast double-positive cells enhanced in all groups after CPZ feeding, despite the saline 3 WPC group (Figure 132h). Glast expression per S100β+ cells decreased in all groups over the recovery phase (Figure 13g).

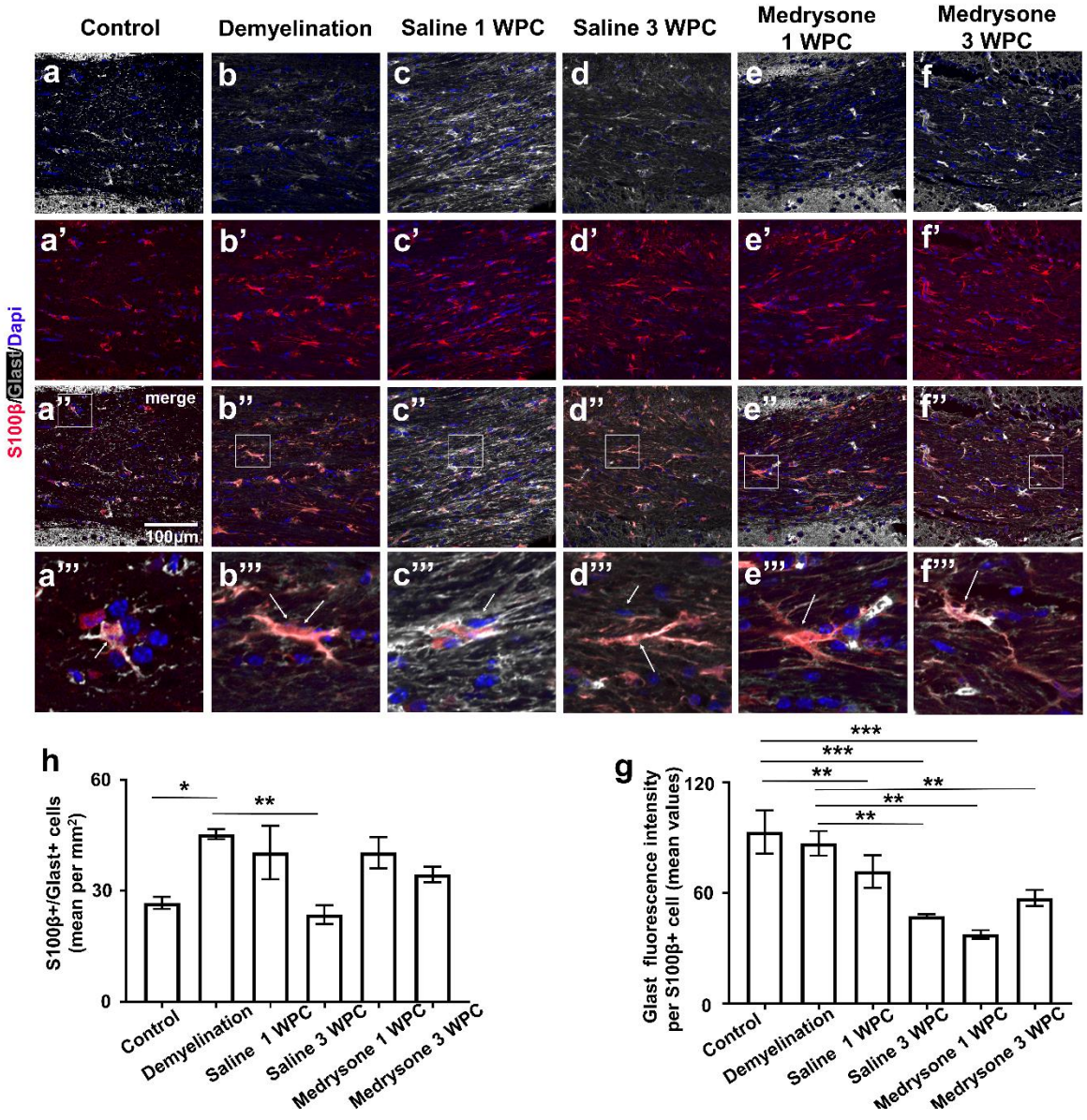

Figure 13. Time-dependent Glast expression in S100β positive astrocytes during CPZ-diet. (a-a'''-f-f''') Representative pictures of the corpus callosum co-stained for S100β and Glast. (h) The number of S100β+/ Glast+ astrocytes enhanced during demyelination, whereas they were less present in the saline 1 WPC group. (g) Glast expression per S100β astrocytes decreases in astrocytes during the

recovery phase. White arrows point to nuclei of representative cells (a'''-f'''). Bars correspond to mean cell numbers per mm2 ± standard error of the mean (SEM). Statistical significance was calculated using a two-way ANOVA with multiple comparisons Bonferroni post-test (*p < 0.05, **p < 0.01, and ***p < 0.001). Number of animals n=3. Data within the figure is unpublished and will be included in a future publication.

6.2.3 Morphological complexity of astrocytes in the de- and remyelinated white matter

Astrocytes change their morphology in both development and disease (Jakel and Dimou, 2017; Schiweck et al., 2018), more specifically to demyelination decrease in their intersections can indicate more toxicity or a decline in interaction within the demyelinated environment (Nash et al., 2010; Allnoch et al., 2019). Investigating the astrocytes in the CCJ, we observed that demyelination decreases the number of branches (Figure 14b, 14g). However, cells in this group showed the largest radius from the center, indicating more complexity in their branches-tree organization (Figure 14i). Saline and medrysone-treated mice showed greater values in the number of branches. However, the radius values were decreased in relation to demyelination (Figure 14i). Branch length was similar between all the groups (Figure 14h).

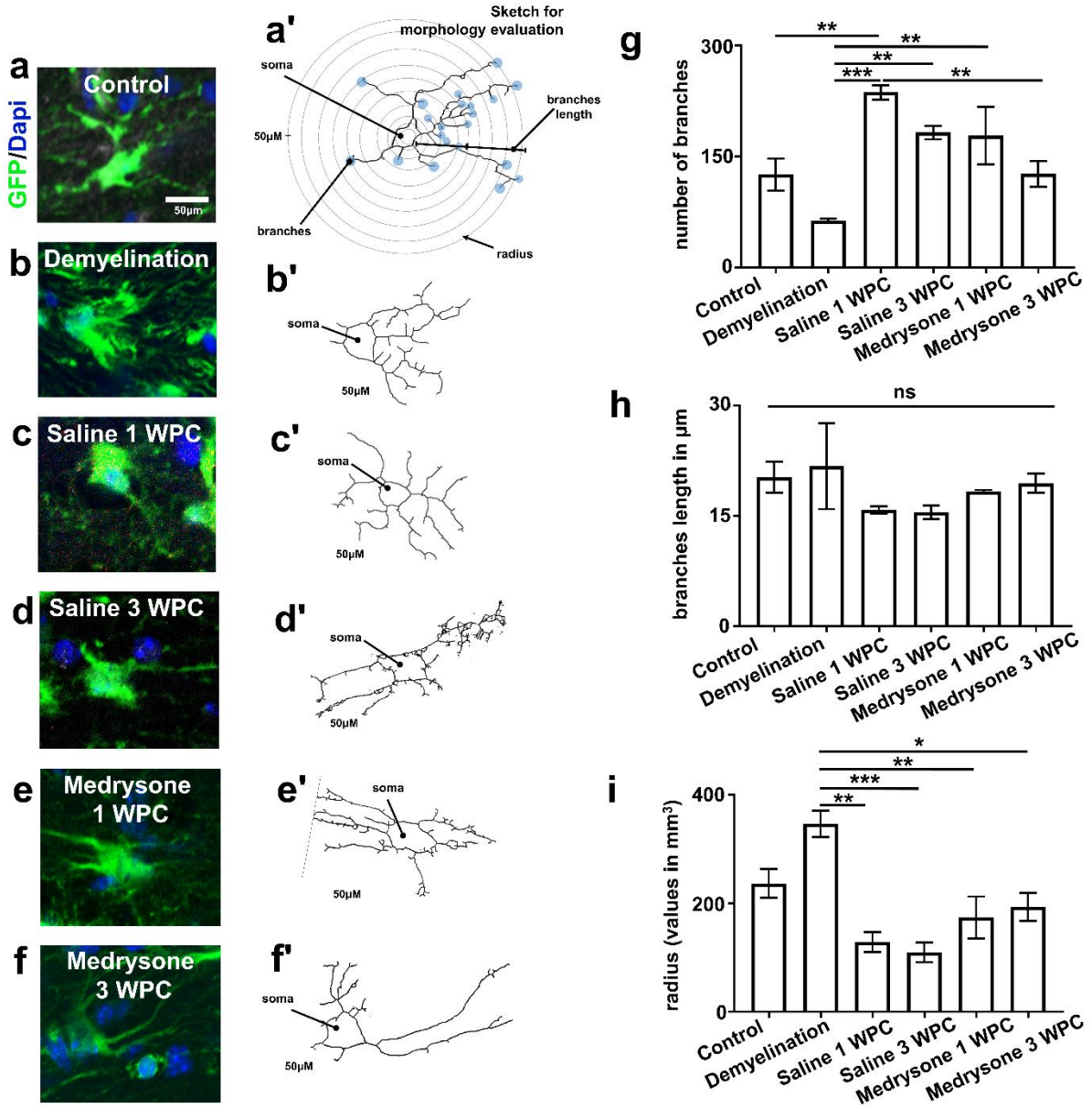

Figure 14. Shift in morphology complexity of astrocytes in the de- and remyelinated corpus callosum. (a-f) Representative photomicrographs of .astrocytes at the CCJ. (a-f) Representative picture of skeletonized morphological data of astrocytes. (a'-f') Graphical sketch for morphology parameters. (g) Quantification of number of branches per cell, shown astrocytes in the recovery phase with more cytoplasm prolongations. (h) Branches length were similar in all groups. (i) mean values for radium from the center shown astrocytes in the demyelination group with more complexity in branches tree organization. Data are shown as mean values ± SEM. Statistical significance was calculated using a two-way ANOVA with multiple comparisons Bonferroni post-test (*p < 0.05, **p < 0.01, and ***p < 0.001). Number of animals n=4. Number of cells analysed (at least 4 per animal). Data within the figure is unpublished and will be included in a future publication.

6.2.4 Medrysone decreases neurotoxic features in cultured primary astrocytes

Aiming to characterize the response of astrocytes after medrysone treatment, astroglial monocultures derived from P0 rats were co-stimulated with TNF-α (which

induces the neurotoxic phenotype) and medrysone (Figure 15a-15d). At 24h after stimulation, there was no significant difference in the number of Gfap+ cells between all groups (Figure 15e). However, TNF-α strongly enhanced the number of A1 (C3d+/Gfap+) cells compared to all other groups (Figure 15f). No neurotoxic astrocytes were detected upon medrysone treatment alone (Figure 15c, 15f). In contrast, medrysone co-treatment with TNF-α reduced the number of A1 astrocytes significantly (Figure 15d, 15f). Gene levels of the neurotoxicity-related genes C3, and IL-6 were upregulated by TNF-α and downregulated by medrysone (Figure 15g)

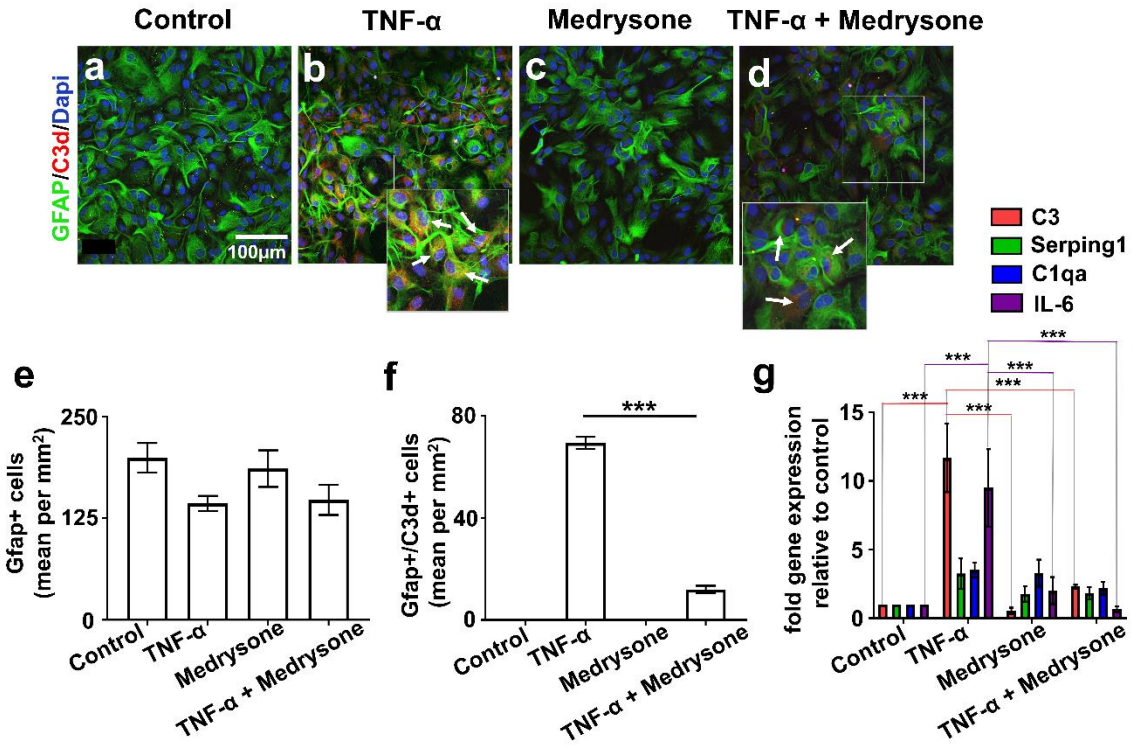

Figure 15. Medrysone counteracts the neurotoxic profile of TNF-α treated astrocytes. Representative images of rat astrocyte monocultures treated with DMSO (control), TNF-α, medrysone and TNFα plus medrysone for 24 hours and stained for Gfap and C3d (a-d). (e) Quantitative analysis of Gfap positive cells revealed no difference between the groups. (f) The number of Gfap+/C3d+ cells increased upon TNF-α stimulation, however, medrysone treatment counteracted the TNF-α effect. (g) Quantitative analysis of fold expression relative to control of the neurotoxicity-related genes C3, Serping1, C1q and IL-6, revealed an increase of C3 and IL-6 gene level by TNF-α and this effect were counteracted by medrysone. Abbreviation: non-significant (ns). White arrows point astrocyte nuclei. Bars in (e, f) correspond to mean cell numbers per mm2 ± standard error of the mean (SEM). Bars in (g) correspond to relative gene expression levels ± standard error of the mean (SEM). Statistical significance was calculated using two-way ANOVA, Bonferroni's multiple comparisons post-test. Data were collected based on experiments n=4 (e, f), n=3 (g). This figure corresponds to the supplemental figure 2 of Oliveira-Junior and colleagues (2022). With permission from the publisher (The Lancet).

6.3 Main results part 3- Heterogeneity of reactive astrocytes within the remyelinated CCJ: medrysone fosters pro-remyelination protein signature in astrocytes

6.3.1 Medrysone fosters hybrid reactive astrocytes in the remyelinated CCJ

Depending on the phenotype, astroglial cells can promote demyelination or remyelination (Miyamoto et al., 2015; Liddelow et al., 2017; Matias et al., 2019). Quantification of transgenic cells expressing C3d and Stat3, revealed that medrysone treatment leads to an increase in C3d+/Stat3+/GFP+ astroglial subpopulation in the CCJ (Figure 16n) and especially in the dorsal horn SVZ (Figure 16h). In contrast, demyelination led to an increased number of C3d+ cells devoid of Stat3 (C3d+/Stat3-/GFP+) which were subsequently reduced or fully depleted in the recovery phase after both saline and medrysone treatment, respectively (Figure 16m). Senescence naturally induces astrocytes to express S100a10 (Clarke et al., 2018). Nonetheless, during disease, S100a10 expression identifies astrocytes within remyelinated lesions in MS as well as upon experimental demyelination (Tassoni et al., 2019). We performed triple staining for C3d, S100a10 and GFP aiming at identifying reactive astrocytes at the CCJ (Figure 16g-16l). C3d+/S100a10-/GFP+ cells were significantly induced by demyelination (Figure 16o, 16h, 16h') with medrysone counteracting this effect leading to decreased numbers of C3d+/S100a10-/GFP+ cells at both investigated time points (Figure 16o). Our findings revealed that C3d+/S100a10+/GFP+ astrocytes (Figure 16p) appear after demyelination and saline or medrysone treatment, but were not detectable in healthy control tissue. Medrysone treatment significantly promoted the C3d+/S100a10+/GFP+ phenotype at 1 WPC which further increased at 3 WPC.

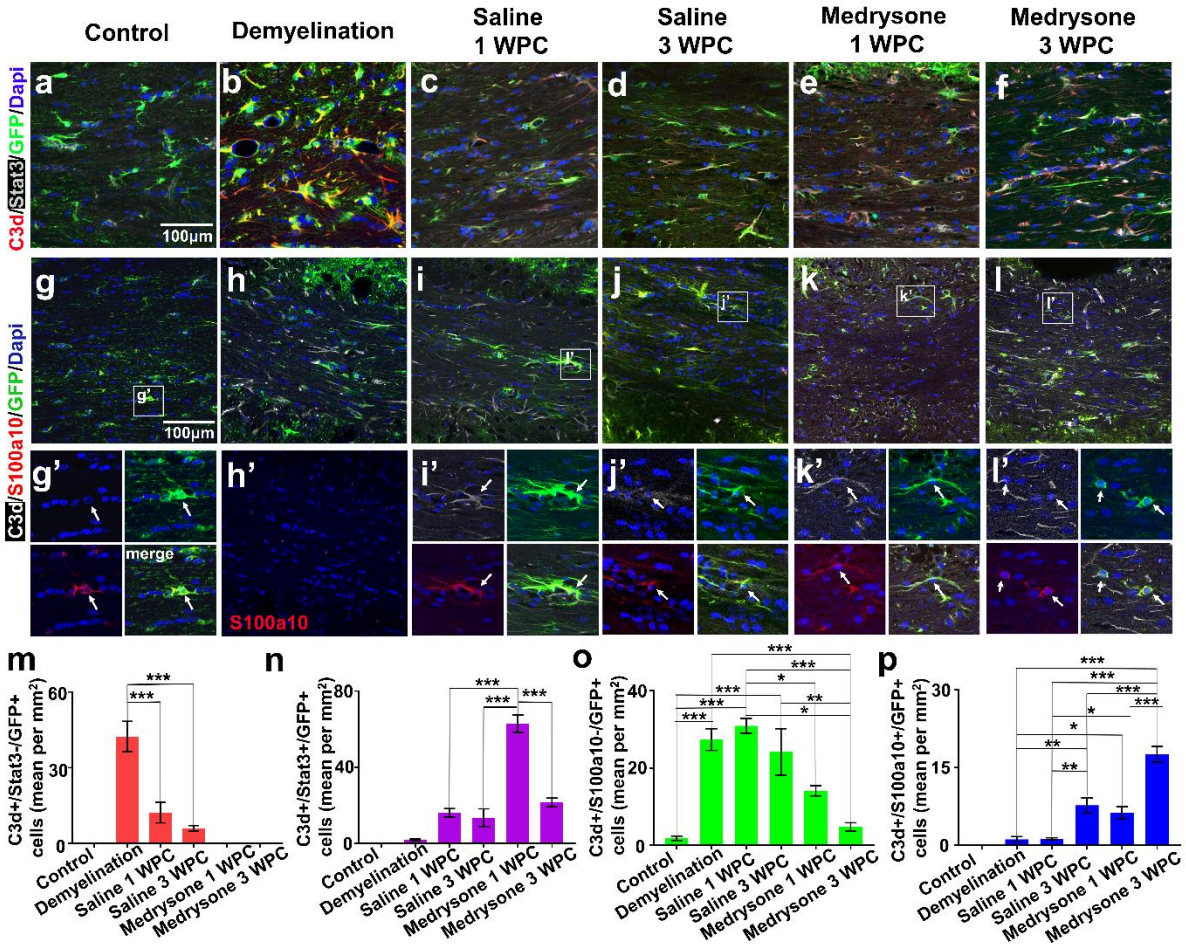

Figure 16. Dynamics of different astroglial subpopulations in the de- and remyelinated corpus callosum. (a-f) Representative pictures of the corpus callosum co-stained for C3d, Stat3 and GFP. (g-l, g'-l') Representative pictures of the corpus callosum co-stained for C3d, S100a10 and GFP. (m) Demyelination enhanced the number of C3d+/Stat3- astrocytes whereas in the recovery phase they were less present. Medrysone treated mice did not exhibit this astroglial phenotype. (n) Medrysone led to a transient increase of C3d+/Stat3+ astrocytes. (o) C3d+/S100a10- astrocytes increased after demyelination independent of the treatment, medrysone more effectively reduced this phenotype in both WPC phases. (p) Quantification of C3d+/S100a10+/GFP+ astrocytes revealed that medrysone promoted this phenotype. White arrows point to nuclei of representative cells (g'-l'). Abbreviations: Lateral ventricle (LV). Bars correspond to mean cell numbers per mm^2 ± standard error of the mean (SEM). Statistical significance was calculated using a two-way ANOVA with multiple comparisons Bonferroni post-test (*$p < 0.05$, **$p < 0.01$, and ***$p < 0.001$). Number of animals n=5 (m-p). This figure corresponds to the figure 4 of Oliveira-Junior and colleagues (2022). With permission from the publisher (The Lancet).

6.4 Main results part 4- Medrysone enhanced type B cells and pro-myelinating astrocytes within the d-SVZ and a-CC over chronic demyelination.

6.4.1 Medrysone anticipate type B cells onset at d-SVZ upon cuprizone-induced chronic demyelination.

Type B cells it is a subpopulation of adult NSCs that in most cases adopt a glial fate, found in both humans (Bond et al., 2015) and mice (Menn et al., 2006; Platel and Bordey, 2016). EGFR expression identifies these cells in the d-SVZ. Co-expression of EGFR and hGFAP-GFP stains activated type-B-cells with an astroglial fate in mice (Pastrana et al., 2009; Platel et al., 2008; Platel and Bordey, 2016). We observed that aside from the demyelinated mice, all other groups expressed cells that were Egfr+/GFP+ at the d-SVZ (Figure 17b, 17b', 17b'', 17g). Medrysone-treated mice appeared to have greater numbers of type B cells at the d-SVZ (Figure 17e', 17e'', 17g). However, no statistical significance was found between the groups.

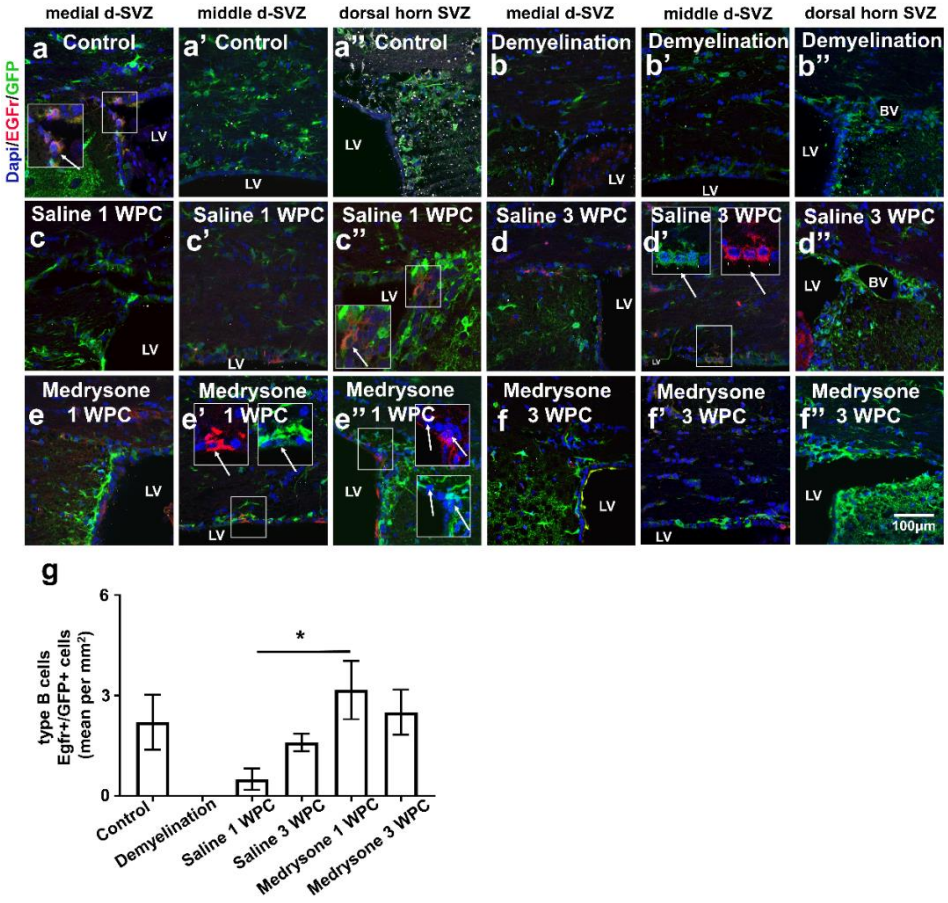

Figure 17. Medrysone rescues type B cells at the d-SVZ of the chronic demyelinated brain. (a, a', a''-f, f', f'') Representative pictures of the d-SVZ and its micro domains (see Figure 1c for anatomic guidance) showing co-localization of Egfr and GFP. (g) Quantification of Egfr+/GFP+ cells revealed their absence in demyelinated animals and their reappearance after demyelination. Abbreviations: non-

significant (ns); lateral ventricle (LV); blood vessel (BV). Bars in (g) correspond to mean cell numbers per mm2 ± standard error of the mean (SEM). Statistical significance was calculated using Kruskal-Wallis test with Dunn's post-test. Data were collected based on animal number n=4. This figure corresponds to the supplemental figure 4 of Oliveira-Junior and colleagues (2022). With permission from the publisher (The Lancet).

6.4.2 Astroglial heterogeneity within the d-SVZ walls

The SVZ is known to contribute to astrocyte generation throughout brain damage (Menn et al., 2006; Benner et al., 2013; Azim et al., 2020). However, the role of the d-SVZ environment and astrogliosis during chronic demyelination is poorly reported. Our results revealed that C3d+/ Stat3+ cells can only be found in the d-SVZ and more exclusively during the early recovery phase (Figure 18c, 18e, 18m) decreasing over the 3 WPC in both saline and medrysone treated groups (Figure 18d, 18f, 18m). In addition, high numbers of C3d+/ Stat3- cells were found in the dorsal horn SVZ throughout demyelination (Figure 18b, 18m), whereas in all other groups except saline treated mice related activated cell populations such as Lcn2+/iNOS+ (DRA) were not identified (see Figure 20o). C3d+/S100a10-/GFP+ and C3d+/S100a10+/GFP+/ hybrid cells were only found at the middle d-SVZ. Hybrid cells were more enhanced by medrysone at 1 WPC phase, decreasing over the 3 WPC stage (Figure 18k, 18l, 18n). Demyelination and saline groups hold a greater number of C3d+/S100a10-/GFP+ cells at middle d-SVZ, both demyelinated and saline-treated mice showed low levels of hybrid cells (Figure 18h, 18i, 18j, 18n). In control mice C3d+/S100a10-/GFP+ and hybrid cells were absent at the middle d-SVZ.

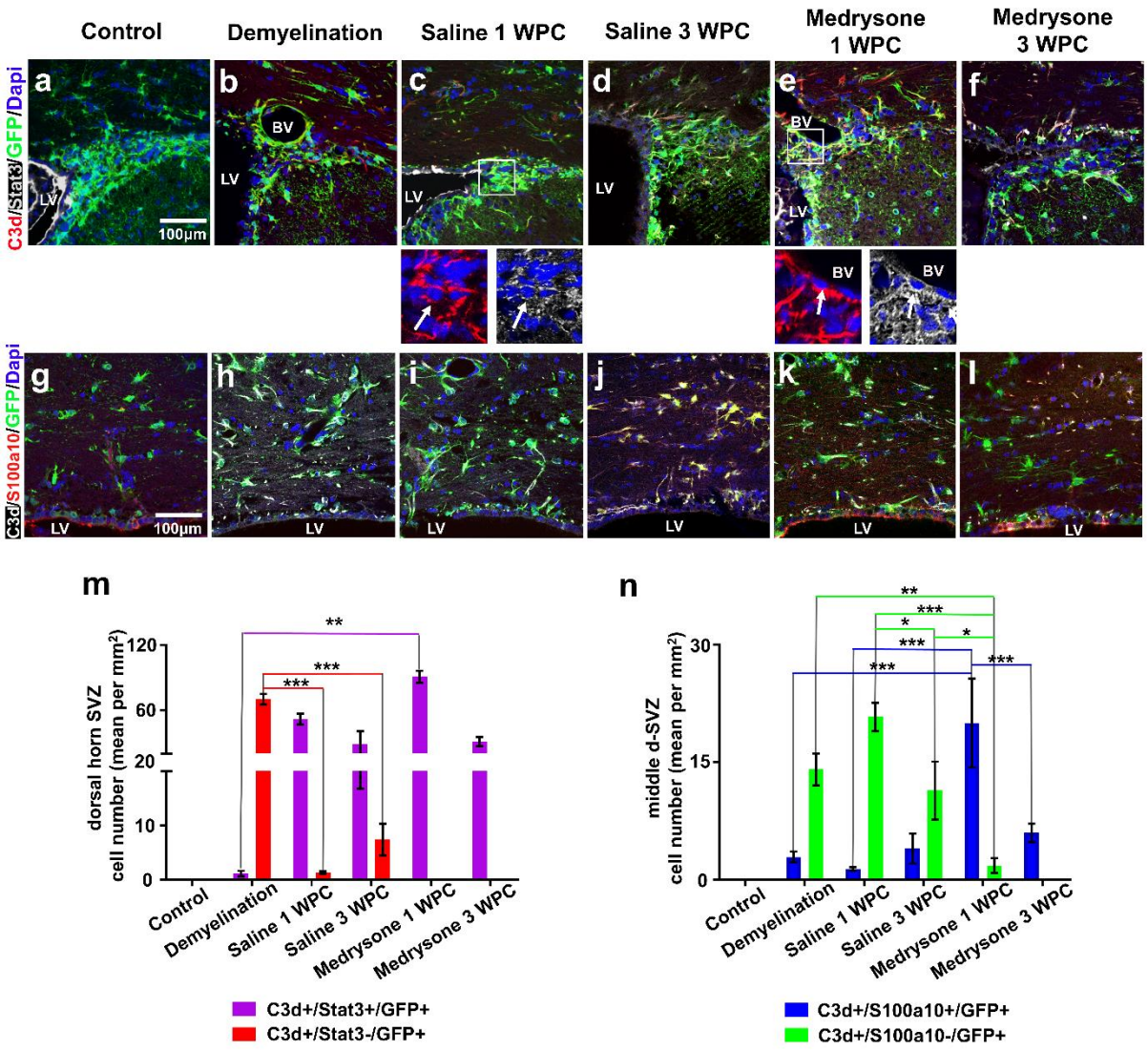

Figure 18. Change in patterns of spatial distribution of reactive astrocytes at middle dorsal and dorsal horn SVZ. (a-f) Representative pictures of dorsal horn SVZ showing co-localization of C3d, Stat3 and GFP. (g-l) Representative photomicrographs of C3d, S100a10, GFP co-localization at middle dorsal SVZ. (m) Quantification of C3d+/Stat3+/GFP+ cells showed that medrysone induced higher levels as compared to saline treated animals improving this phenotype at early phases of recovery. (h) Numbers of C3d+/Stat3-/GFP+ cells increased upon demyelination and decreased during the early recovery phase, and were not found after medrysone treatment. (n) Quantification of C3d+/S100a10+/GFP+/hybrid cells and of C3d+/S100a10-/GFP+ cells. Hybrid cells were detected at higher levels in medrysone 1 WPC mice, whilst C3d+/S100a10-/GFP+ cells were mostly found over demyelination and in saline treated mice. White arrows point to cell nuclei (c'-e'). Abbreviations: Lateral ventricle (LV); Blood vessel (BV). Bars in (m, n) correspond to mean cell numbers per mm2 ± standard error of the mean (SEM). Statistical significance was calculated using Kruskal-Wallis test with Dunn's post-test (m: purple bars) and two-way ANOVA, Bonferroni's multiple comparisons post-test (m: red bars; n: green bars and blue bars). Data were collected based on animal number n=5. This figure corresponds to the supplemental figure 3 of Oliveira-Junior and colleagues (2022). With permission from the publisher (The Lancet).

6.4.3 Mafg and Nrf2 expression is limited to a small number of reactive astrocytes at a-CC

Mafg and Nrf2 are expressed in reactive astrocytes during de- and remyelination (Wheeler et al., 2020; Escartin et al., 2021, Greiner and Kipp, 2021). These markers identify pro-demyelination (Mafg+/Nrf2-) and pro-remyelination (Mafg-/Nrf2+) subtypes within active lesions in both EAE and MS (Wheeler et al., 2020). Our results revealed that Mafg-/ Nrf2+ and Mafg+/Nrf2- cells can only be found at the a-CC and more exclusively in the control and saline 1 WPC group, respectively (Figure 19a, 19c, 19d).

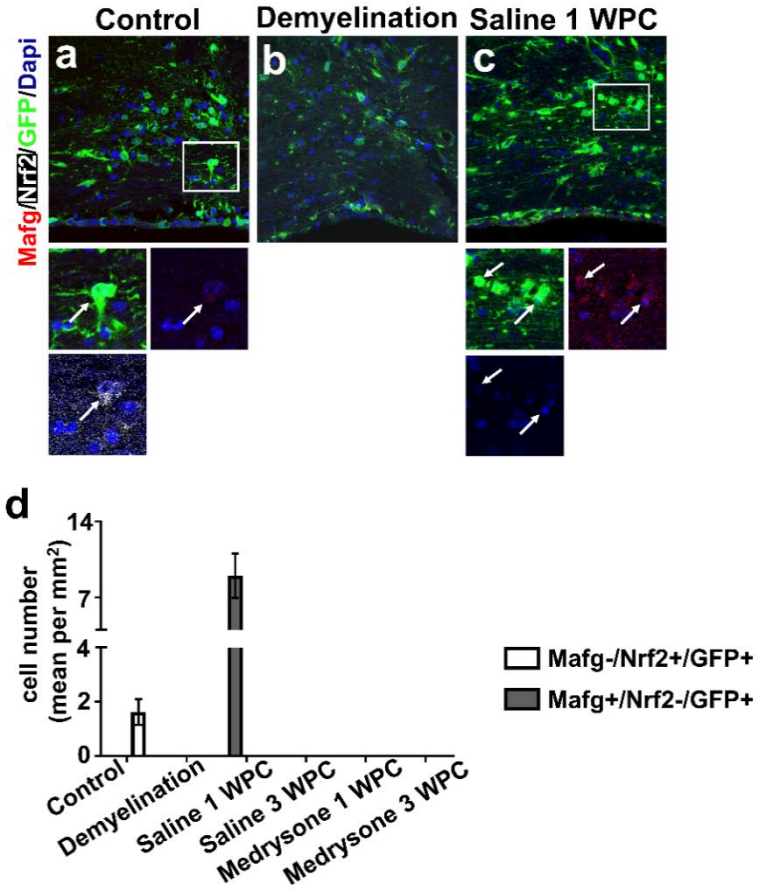

Figure 19. Reactive astrocytes expressing Mafg and Nrf2 are limited to the a-CC of demyelinated mice. (a-c) Representative pictures of a-CC showing immunofluorescence for Mafg, Nrf2 and GFP. (d) Quantification of Mafg-/Nrf2+/GFP+ and Mafg+/Nrf2-/GFP+ cells at a-CC, showed the control group exclusively expressing Mafg-/Nrf2+ astrocytes. Mafg+/Nrf2- astrocytes were only observed at saline 1 WPC group. White arrows point to cell nuclei (a, c). Bars in (d) correspond to mean cell numbers per mm^2 ± standard error of the mean (SEM). Statistical significance was calculated using two-way ANOVA, Bonferroni multiple comparisons post-test. Data were collected based on animal number n=4. This figure corresponds to the supplemental figure 4 of Oliveira-Junior and colleagues (2022). With permission from the publisher (The Lancet).

6.4.4 C3d+/Stat3+ and C3d+/S100a10+ astrocytes were regulated at the a-CC throughout remyelination

As a next step, quantification of C3d/Stat3 double-positive, C3d+/S100a10+/GFP+ and C3d-/S100a10+/GFP+ astrocytes in the a-CC (see Figure 9c, 9c') was conducted. C3d+/Stat3-/GFP+ cell numbers were only induced during demyelination then decreasing in saline 1 WPC and being absent in all other groups (Figure 20m; red bars). C3d+/Stat3+/GFP+ cells were not present in control and demyelinated mice (Figure 20a, 20b, 20m), they were moderately induced in saline treated animals (Figure 20c, 20d, 20m) and strongly induced upon medrysone treatment at both time points (Figure 20e, 20f, 20m; purple bars). C3d+/S100a10-/GFP+ astrocytes were strongly upregulated upon demyelination and at both remyelination time-points in saline treated mice (Figure 20h, 20i, 20j, 20n; green bars). However, a robust reduction of this phenotype was observed in medrysone treated mice (Figure 20n). C3d+/S100a10+/GFP+ astrocytes rarely appeared over demyelination (blue bars; Figure 20h, 20n). Saline treated mice only showed low levels of this phenotype, whereas medrysone treatment led to a strong increase of C3d+/S100a10+/GFP+ astrocytes at the a-CC at both time points (Figure 20k, 20l, 20n; blue bars).

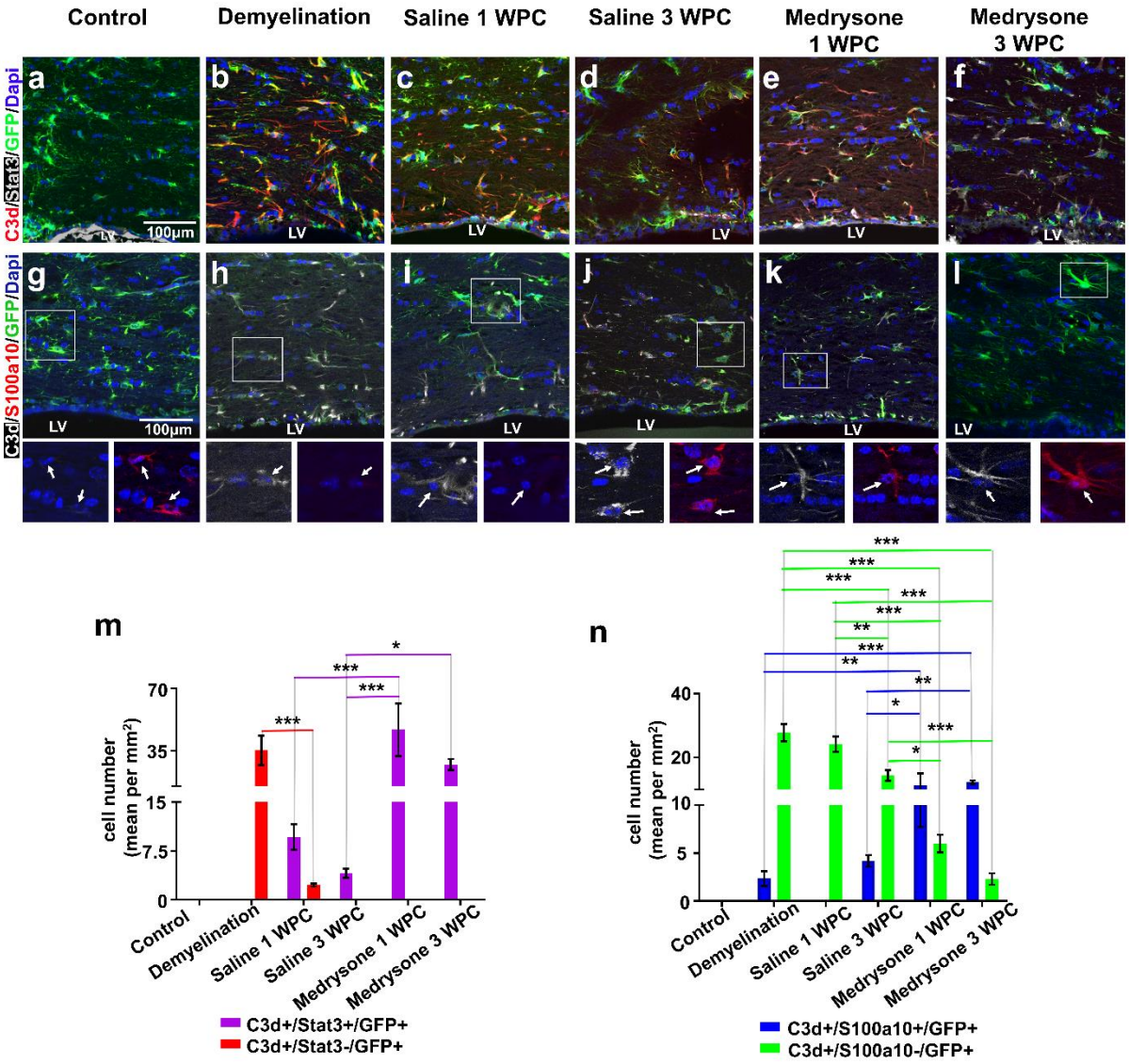

Figure 20. Numbers of hybrid astrocytes were enhanced in the a-CC after medrysone treatment. Representative pictures of a-CC tissues sections stained for C3d, Stat3 and GFP (a-f) and stained for C3d, S100a10 and GFP (g-l). (M) Graphic representation of C3d and Stat3 co-expressing cells in the a-CC. (n) Graphic representation of the number of C3d+/S100a10+/GFP+ and C3d+/S100a10- astrocytes in the a-CC indicating temporal dynamics and changes induced upon medrysone treatment (red bars: C3d+/Stat3-/GFP+; purple bars C3d+/Stat3+/GFP+; blue bars: C3d+/S100a10+/GFP+ cells; green bars: C3d+/S100a10-/GFP+ cells). White arrows point to cell nuclei. Bars correspond to mean cell numbers per mm^2 ± standard error of the mean (SEM). Statistical significance was calculated using a two-way ANOVA with multiple comparisons Bonferroni post-test (*p < 0.05, **p < 0.01, and ***p < 0.001). Number of animals n=5 (m, n). This figure corresponds to the figure 5 of Oliveira-Junior and colleagues (2022). With permission from the publisher (The Lancet).

6.4.5 Demyelination at a-CC was accompanied by DRA or RRA throughout the recovery phase

Chronic demyelination can also decrease levels of PLP and of active myelinating OLs (Sox10+/Bcas1+) in the a-CC, with a weak recovery over saline-treatment (Figure 21e, 21j) and an enhanced recovery upon medrysone treatment (Figure 21d, 21e, 21i, 21j). Lcn2 it is known for its detrimental activities upon myelin disruption (Allnoch et al., 2019) which acts by controlling iNOS expression in glial cells (Al Nimer et al., 2016; Qiang et al., 2020; Zhao et al., 2020). We found astrocytes co-expressing Lcn2 and iNOS, identified as demyelination related astrocytes (DRA), which were only found in the a-CC (Figure 9c'). DRA (Lcn2+/iNOS+/GFP+) numbers were significantly increased upon demyelination (Figure 21l, 21m, 21o) with medrysone neutralizing this effect leading to a decreased DRA numbers at both investigated time points (Figure 21n, 21o). Timp1 is a MMP inhibitor that has been reported as one of the critical factors released by astrocytes able to promote white matter recovery after demyelination (Ogier et al., 2005; Moore et al., 2011; Houben et al., 2020). We therefore investigated whether reactive astrocytes expressed Timp1 during recovery phases. By means of Timp1/C3d/GFP triple staining, we identified C3d-negative control astrocytes expressing Timp1 in healthy tissue. These astrocytes were exclusively found in the a-CC whereas no Timp1+ cells were observed in the d-SVZ and its micro-domains as well as the CCJ. However, C3d+ reactive astrocytes expressing Timp1 that were absent in healthy and demyelinated tissues appeared in saline treated animals at both recovery phases and were found to be increased in numbers in medrysone treated mice (Figure 21s, 21t). As this phenotype was exclusively observed over the recovery phase, these cells were hence designated as remyelination related astrocytes (RRA).

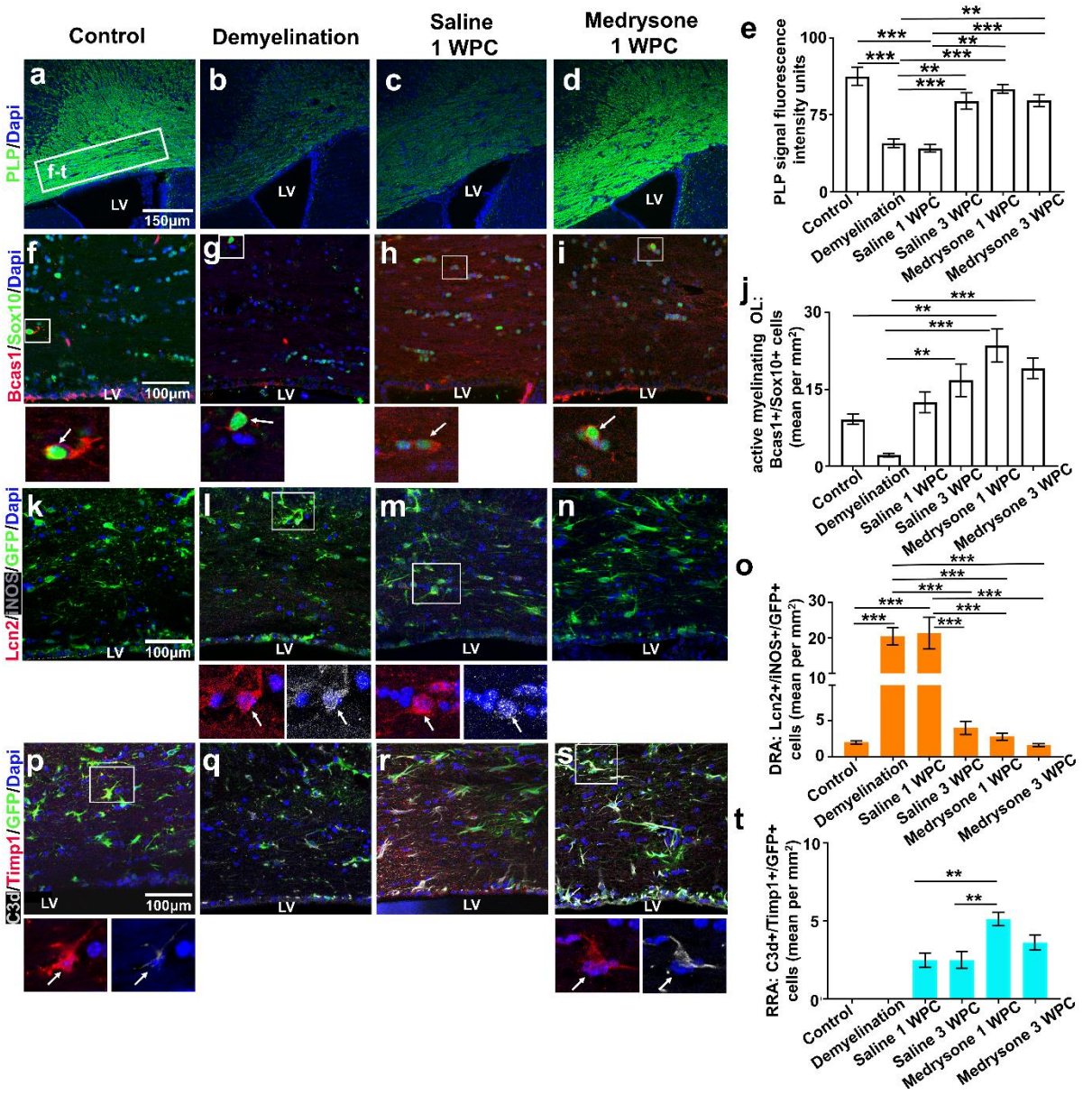

Figure 21. PLP recovery and remyelination related gliosis is fostered by medrysone at the a-CC. (a-d) Representative pictures showing PLP expression at the a-CC. (e) Quantification of PLP fluorescence intensity units revealed a demyelination induced decrease of PLP expression and a medrysone enhanced recovery of PLP levels. Representative photomicrographs of active myelinating OLs at the a-CC (Sox10+/Bcas1+). Quantification of active myelinating OLs at the a-CC (j) revealed a decrease of these cells during demyelination and medrysone to strongly counteract this effect. (k-n) Representative photomicrographs of DRAs (Lcn2+/iNOS+/GFP+) at the a-CC. (o) Quantification of DRA shows enhancement of this phenotype over demyelination and saline 1 WPC. (p-s) Representative photomicrographs of RRAs (C3d+/Timp1+/GFP+). (t) Quantification of RRA revealed that medrysone increased this phenotype at the early recovery phase. Abbreviations: Lateral ventricle (LV), demyelination related astrocytes (DRA), remyelination related astrocytes (RRA). Bars (e) correspond to PLP mean signal fluorescence intensity ± standard error of the mean (SEM), bars in (g, o, t) correspond to mean cell numbers per mm^2 ± standard error of the mean (SEM). Statistical significance was calculated using a two-way ANOVA with multiple comparisons Bonferroni post-test (*p < 0.05, **p < 0.01, and ***p < 0.001). Number of animals n=5 (e, j, o), n=4 (t). This figure corresponds to the figure 6 of Oliveira-Junior and colleagues (2022). With permission from the publisher (The Lancet).

6.4.6 Genes related to Myelination, oligodendrogenesis and astrocyte heterogeneity at the d-SVZ and a-CC.

The gene skeleton behind the reactive astrogliosis on both d-SVZ and a-CC was investigated by evaluating Gfap, Serpina3n (for the pan-reactive status of astrocytes; Figure 22a), Lcn2, Serping1 (A1/inflammation/demyelination, Figure 22b), S100a10 and Ptx3 (for A2/non-neurotoxic related genes, Figure 22c). No changes were observed in Gfap and Serpina3n gene levels. However, Lcn2 decreased in relation to demyelination in both saline and medrysone-treated groups (Figure 22b). Gene levels of Serping1, S100a10 and Ptx3 did not change between the groups. Myelination, oligodendrogenesis and neurogenesis related genes were also investigated. Saline 1 WPC mice did not present significant changes in Plp1 gene levels versus medrysone and demyelination but expressed less Mbp than medrysone-treated mice. Medrysone 1 WPC upregulate Plp1 and Mbp (Figure 22d). Gene levels of Myrf, Pdgfrα, Mash1, and Nkx2.2 did not change between groups (Figure 22e, 22f).

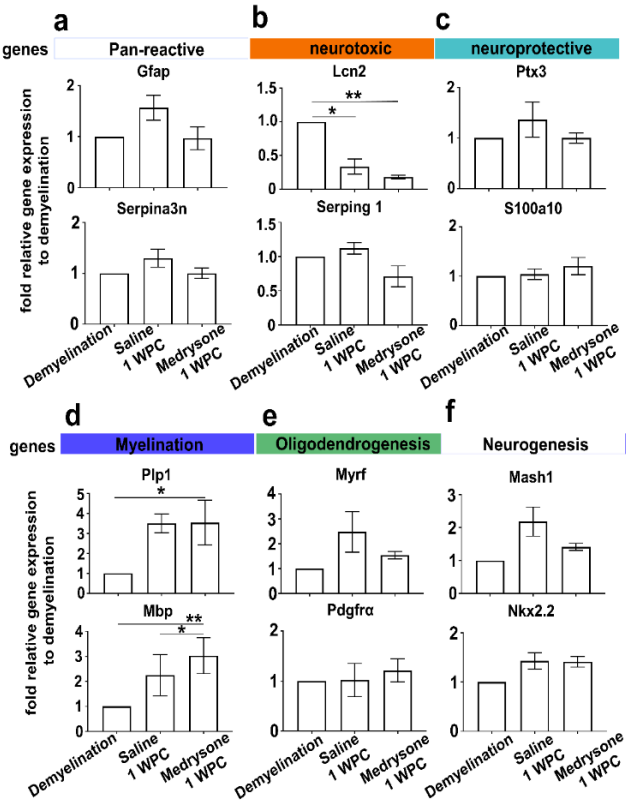

Figure 22. Expression of astrocyte heterogeneity-, myelination-, oligodendrogenesis- and neurogenesis-correlated genes in the d-SVZ and a-CC. (a-c) Graphic representation of relative gene expression of astrocyte heterogeneity showing levels of Lcn2 decreasing during the 1 WPC phase in both saline- and medrysone-treated groups. (*d*) Graphic layout and colour-tagging diagram of pan-reactive, A1 and A2 genes in reactive astrocytes (e-g) Histogram representation of relative gene expression of genes related to myelination (Plp1, Mbp), oligodendrogenesis (Myrf, Pdgfrα) and neurogenesis (Mash1, Nkx2.2). Levels of Plp1 and Mbp were upregulated by medrysone. Data are shown as mean values ± SEM. Statistical significance was calculated using a two-way ANOVA with multiple comparisons Bonferroni post-test (*p < 0.05, **p < 0.01). Number of animals n=3 Data within the figure is unpublished and will be included in a future publication.

6.4.7 The impact of medrysone on gene levels of IL-6 and C210rf91 suggests other different mechanisms undertaken by this drug in the demyelinated brain.

Gene levels of Timp1, IL-6, C21orf91 and GDNF were also evaluated in the jointly dissected a-CC-d-SVZ. We observed that Timp1 gene levels remain the same in and after demyelination (Figure 23a). On the contrary, levels of IL-6, a bias molecule that can contribute to both de- and remyelination (Leibinger et al., 2013; Petkovic et al., 2016; 2017), were upregulated in medrysone treated animals (Figure 23b). Gene levels of C21orf91, the key promoter of hypomyelination in Down syndrome and found to be expressed in aberrant glial cells (Reiche et al., 2021), were downregulated by medrysone (Figure 23c). Gene levels of GDNF remain similar in both saline and medrysone treated animals (Figure 23d).

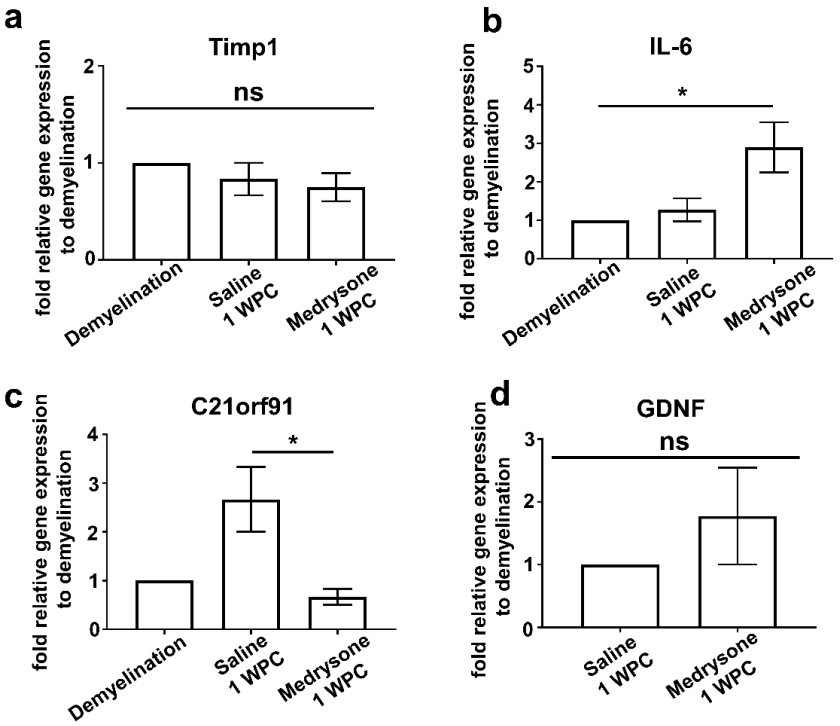

Figure 23. Gene levels of IL-6 and C21orf91 change after medrysone treatment. a-d) Graphic representation of relative gene expression of Timp1, IL-6, C21orf91 and GDNF. Levels of Timp1 (a) and GDNF (d) are similar in both groups investigated. Gene levels of IL-6 were enhanced in medrysone treated mice (b). Gene levels of C21orf91 were decreased after medrysone treatment. Abbreviation: none significant (NS). Data are shown as mean values ± SEM. Statistical significance was calculated using a two-way ANOVA with multiple comparisons Bonferroni post-test (*p < 0.05, **p < 0.01). Number of animals n=3. Data within the figure is unpublished and will be included in a future publication.

6.4.8 Levels of reactive astrogliosis-related genes change after medrysone treatment in astrocyte primary cultures

Gene levels for the reactive astrogliosis-related genes Serpina 3n, Lcn2, Gfap, S100β, Emp1, Ugta1, Clcf1, Cd14, and S100a10 (Zamanian et al., 2012; Liddelow et al., 2017) were also evaluated in primary astrocyte cultures. We observed that gene levels of Serpina 3n, Lcn2 and Ugta1 were enhanced by medrysone in both single treatment and following TNF-stimulation (Figure 24a, 24b, 24f). Levels of S100a10 only decreased in co-treated astrocytes (Figure 24i). Levels of Gfap, S100β, Emp1, Clcf1 and Cd14 remained similar in both groups (Figure 24c, 24d, 24e, 24g, 24h).

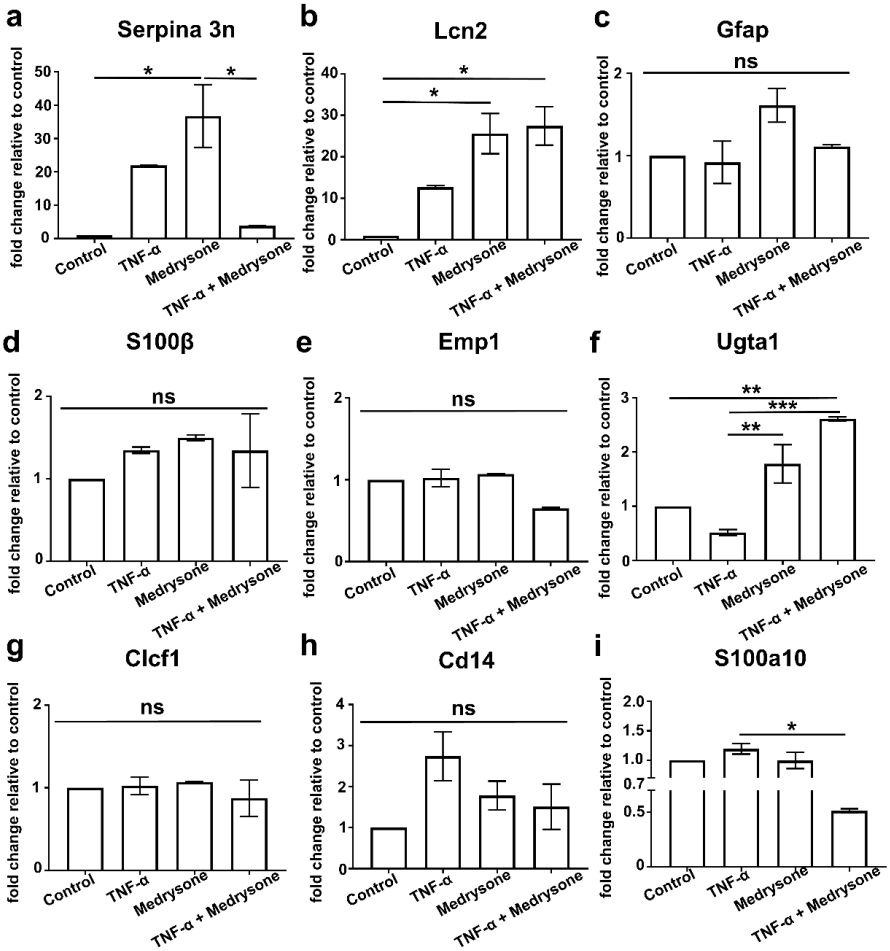

Figure 24. **Medrysone alters levels of reactive astrogliosis related genes on TNF-α treated primary astrocyte cultures.** (a-i) Graphic representation of relative gene expression of Serpina 3n, Lcn2, Gfap, S100β, Emp1, Ugta1, Clcf1, Cd14 and, S100a10. Levels of Serpina 3n (a), Lcn2 (b) and Ugta1 (f) were upregulated in both medrysone and TNF-α + Medrysone treated cells. (i) Levels of S100a10 decreased in TNF-α + Medrysone treated cells. Gene levels of Gfap (c), S100β (d), Emp1 (e), Clcf1 (g) and Cd14 (h) are similar in both groups. Data are shown as mean values ± SEM. Statistical significance was calculated using a two-way ANOVA with multiple comparisons Bonferroni post-test (*$p < 0.05$, **$p < 0.01$). Number of animals n=3. Data within the figure is unpublished and will be included in a future publication.

7. Discussion

Medrysone is an FDA-approved corticosteroid designated as a topical anti-inflammatory agent for ophthalmic use (Spaeth, 1966; Bedrossian and Eriksen, 1969). Details on its activity in a neurological context are scarce and limited to MBP upregulation in Oli-neuM cells (Porcu et al., 2015). Azim and colleagues (2017) reported medrysone as a prominent oligodendrogenesis molecule on an *in silico* investigation for drugs with an oligodendrogenesis potential in lateral-SVZ cells.

Here we describe that medrysone application promotes remyelination in a chronic myelin loss set-up, more efficiently restoring myelin content, early mature- and mature OLs numbers (Figure 11) and body weight (Figure 10). Validating the remyelination onset, we observed that medrysone was able to enhance the numbers of active myelinating OLs in the CCJ (and a-CC; see Figure 21), identified by co-expression of Sox10/Bcas1. Sox10 identified OLs that are in the early phase of generating myelin, and that populate new remyelinated regions in both chronic-CPZ and –MS (Fard et al., 2017; Lohrberg et al., 2020). In addition, the corticosteroid recovered the number of nodes of Ranvier identified by co-expression of Caspr+/MBP+ (see Figure 11). Caspr labels the terminal structure of the intact/formed myelin sheaths (Coman et al. 2006). During demyelination, a decrease in the co-expression of Caspr+/MBP+ structures highlights chronification (Wolswijk and Balesar, 2003; Susuki, 2013). Although anti-inflammatory corticosteroids were reported to not ameliorate acute demyelination outcomes in CPZ-models (Chari et al., 2006; Clarner et al., 2011), our evaluations counteract these findings, validating medrysone as a potential candidate against chronic myelin lesions.

In most cases, such regenerative activity is linked to direct effects on resident OPCs (Bond et al., 2015; Bergles and Richardson, 2016); however, our investigations using primary OPCs failed to demonstrate any promotion of oligodendroglial maturation at different levels (morphology, gene expression, myelin protein production; see Figure 6); which contradicts earlier findings using the Oli-neuM cell line (Porcu et al., 2015). Intriguingly, medrysone enhanced mature NG2-glia cells (NG2+/Gfap-; Polito and Reynolds, 2005; Sanchez-Gonzalez et al., 2020; Zuo et al., 2018) and astroglial lineage cells (Gfap+/Ng2-) in d-SVZ primary cell cultures (Figure 7). Investigations on cerebellar organotypic cultures showed that the corticosteroid enhanced the number

of myelinated axons and MBP+ cells without alterations in the number of astrocytes (Figure 8). We concluded that medrysone's activities are more directed towards mature stage OLs, and support the notion that tissue and primary cells derived from different species are better suited for a translational outcome as recently shown by our group (Manousi et al., 2021; Manousi and Küry, 2021).

Thereafter, we observed astrocytes and SVZ-dependent astrogenic progeny at distinct sites within and adjacent to the corpus callosum. We also observed the active regulation of different cellular subpopulations that potentially contribute to myelin repair. Our investigations unveiled that the numbers of hGFAP-GFP+ cells (astrocytes) did not change over time in CCJ, while in the a-CC and d-SVZ cell numbers were more variable (Figure 12) suggesting an apparent contribution from the niche. In order to more deeply identify modifications in the astrocyte population in the CCJ, we performed co-staining for S100β and Glast. We found that the number of S100β+ cells is variable between groups in the CCJ after the CPZ diet, counteracting the findings of the number of hGFAP-GFP+ cells in this niche (Figure 13). Glutamate excitotoxicity can be identified by the upregulation of Glast in astrocytes, which contributes to the demyelination onset in both CPZ (Azami-Tameh et al., 2013) and EAE (Mitosek-Szewczyk et al., 2008). We found that Glast expression per S100β+ cell decreased in saline 3 WPC and medrysone-treated mice, indicating that late-remyelination follows Glast downregulation in astrocytes (Figure 13). Complementing these findings, we evaluated the morphology complexity of astrocytes (GFP+) within the CCJ (Figure 14). We observed that the number of branches/end-feet projection per astrocyte is higher in the recovery phase, and astrocytes in the demyelinated CCJ will show a decrease in branches/end-feet projections. Interestingly, even with the branches size (length in μm) being similar in all evaluated groups, astrocytes in the demyelinated CCJ are wider, covering more tissue than those in the recovery groups which showed a radius number similar to control (Figure 14i). Indeed, astrocytes alter their morphology in response to damage, as seen in stroke (Wan et al., 2022), spinal cord injury (Vismara et al., 2020), and neuroinflammation (Zamanian et al., 2012), and our findings highlight this feature.

We also investigated the direct effect of medrysone on polarization and activation of rat cortex astrocytes. Our findings clearly revealed that astrocytes can sense medrysone by upregulating pan-reactive genes such as Serpina3n and Lcn2 (Figure

15), however there is no reaction in terms of Gfap+ cell numbers, yet the corticosteroid effectively decreased the number of neurotoxic astrocytes (Gfap+/C3d+) and neurotoxic correlated genes (C3 and IL-6) in response to TNF-α stimulation (Figure 15). TNF-α is well established in the literature as to foster the neurotoxic fate of astrocytes (Wang et al., 2017; Trindade et al., 2019; Rodgers et al., 2020), therefore indicating that *in vivo* astrocytes are also a key target for medrysone anti-inflammatory activities. Liddelow and colleagues (2017) established the effectiveness of the microglial-dependent release of TNF-α, IL-1α and C1q to trigger a neurotoxic fate of astrocytes. However, as shown by Rodgers and colleagues (2020), single stimulation with TNF-α does not discontinue astrocyte reactivity and still upregulates inflammation co-related genes such as complement factors and interleukins.

During demyelination, the d-SVZ is activated and contributes by generating OLs and astrocytes progenitors (Xing et al., 2014; Pous et al., 2020). Butti and colleagues (2019) identified that SVZ-NSCs are the main source of OPCs during CPZ and that OLs generation occurs alongside astrogliosis in the demyelinated SVZ. Of note, SVZ-astrocytes are key to inducing progenitors towards an oligodendroglial fate improving remyelination after LPC treatment (Menn et al., 2006) complementing the fact that glial progenitors with an oligodendroglial- and astroglial-fate, were observed in the SVZ of MS patients (Nait-Oumesmar et al., 2007). GFP/EGFR co-expression in hGFAP-GFP reporter mice identifies type B NSCs, those are the main glial progenitors within the SVZ (Platel and Bordey, 2016). These cells give birth to astrocytes (Platel et al., 2008; Pastrana et al., 2009; Giachino et al., 2014) and/or OLs throughout development and in response to demyelination (Zerlin et al., 2004; Menn et al., 2006). We observed that chronic-demyelinated mice are absent of type B cells (Egfr+/GFP+) at d-SVZ (see Figure 17). Moreover, medrysone seems to be able to recover these cells earlier at the 1 WPC stage, while saline-treated mice lagged during recovery. However, none statistical significance was found. Due to the spontaneous reduction of NSCs observed at SVZ of ageing mice at a minimum age of 4 months (Conover and Shook, 2011; Daynac et al., 2016), more time is necessary for non-drug treated mice to respond with a proper recovery of OLs to subsequently promote remyelination. In fact, this late response in saline-treated mice can be connected to an insufficient generation of type B cells in the d-SVZ during demyelination.

After damage, the SVZ can generate reactive astrocytes that migrate throughout the corpus callosum into damaged regions (Faiz et al., 2015). Understanding the genetic outcome within both d-SVZ and corpus callosum is crucial for unveiling the response of astrocytes in repair. Based on the gene score of reactive astrocytes of Liddelow and colleagues (2017), we selected a few genes to define the environmental gene expression of the jointly dissected d-SVZ and a-CC in mice exposed to chronic demyelination (Figure 22). Levels of Serpina 3n and Gfap did not change between the investigated groups (demyelination, saline 1 WPC, medrysone 1 WPC). Indeed, Serpina3n participates in repair in EAE models (Haile et al., 2015), while Gfap expression in astrocytes is connected to myelin clearance and remyelination improvement (Hibbits et al., 2012; Skripuletz et al., 2013). These genes remaining at levels similar to the demyelination group highlight a necessary reactive state of astrocytes in the d-SVZ to overcome an effect (Figure 22a). In contrast, Lcn2 decreases after CPZ-feeding (Figure 22b) highlighting this molecule as complementary for remyelination in the a-CC (more details about Lcn2 will be discussed next). In addition, we observed that gene levels of Timp1, a pro-myelinogenic molecule (Moore et al., 2011), and GDNF, a key neurotrophin for axonal regeneration (Zhang et al., 2009), were similar in both evaluated groups (see Figure 23). However, levels of IL-6, known for promoting either damage or repair depending on the stage of disease (Leibinger et al., 2013; Petkovic et al., 2016; 2017), were upregulated in medrysone treated animals (Figure 23). Gene levels of C21orf91, which, when overexpressed in glial cells, induced hypomyelination in Down syndrome (Reiche et al., 2021), is upregulated in saline 1 WPC groups. Thus indicating another possible mechanism of protection displayed by medrysone.

Regarding the myelination-related genes, Plp1 and Mbp, both were effectively upregulated on the 1 WPC phase in both saline- and medrysone-treated mice. However, no changes were observed in Myrf, Pdfgrα, Mash1 and Nkx2.2 expression (Figure 22). Plp1 is mainly regulated by Olig1, which drives the expression and regulation of Plp and Mbp on immature OLs, disrupting the astroglial fate, inducing the immature cells into a myelinating profile (Xin et al., 2005; Michalski et al., 2011; Lourenço et al., 2016). In addition, Plp1 guides OLs to correctly deposit myelin on the axons (Klugmann et al., 1997; Rosenbluth et al., 2006). This null effect in levels of Myrf, Pdgfrα, Mash1 and Nkx.2.2 contributes to the fact that medrysone effects are

more likely connected to mature stage OLs, cells that will essentially express high levels of PLP and MBP, and low levels of oligodendroglial progenitors genes such as Myrf (Hornig et al., 2013; Aprato et al., 2020) and Pdgfrα (Zhu et al., 2014; Emery and Lu, 2015) and neurogenesis related genes as Mash1 (Parras et al., 2004; Voronova et al., 2011) and Nkx2.2 (Lek et al., 2010; Panman et al., 2011).

During acute demyelination, reactive astrogliosis and myelin damage coincide (Steelman et al., 2012; Hibbits et al., 2012; Orthmann-Murphy et al., 2020). However, while depletion of astrogliosis can be favourable for remyelination (via reduction of astrocytic-NfκB; Brück et al., 2012; Madadi et al., 2019), chronic reactivity in astrocytes was observed to be essential for myelin clearance and reposition, as well as OLs replacement (Miyamoto et al., 2015; Wheeler et al., 2019; Tognatta et al., 2020). We identified that such reactive astrocytes showed a distinct protein expression signature, varying in numbers and localization within the de- or remyelinated corpus callosum. Lcn2 improves neurotoxic fate in MS astrocytes (Bi et al., 2013: Itoh et al., 2017) and has been reported to be enriched in the cerebral spinal fluid of MS patients and also expressed in reactive astrocytes in EAE exposed mice (Marques et al., 2012). The demyelination related astrocyte (DRA; Lcn2+/iNOS+/GFP+) was identified as a potential demyelination contributor. In addition, Lcn2 depletion in EAE animals reduced demyelination by declining MMPs production (Nam et al., 2014). Lcn2 expression naturally enhanced iNOS production in both CPZ and MS, impairing copper and iron metabolism in OLs (Al Nimer et al., 2016; Qiang et al., 2020). We found that CPZ also induced demyelination at the a-CC (Figure 21), which is restored by medrysone. Concomitantly, we observed that DRA would exclusively populate the demyelinated a-CC (Figure 21G, 21J), matching with the high Lcn2 gene levels reported in figure 22. Furthermore, Lcn2 gene levels (Figure 22) and DRA were strongly reduced upon medrysone treatment, and this feature was accompanied by PLP restoration (Figure 21). During the recovery phase, astrocytes with a neurotoxic signature (Lcn2+/iNOS+; C3d+/S100a10-; C3d+/Stat3-) were decreased in numbers and replaced by a hybrid phenotype that simultaneously expresses proteins that are known as neurotoxic (C3d), and neuroprotective (Timp1 or S100a10 or Stat3; Monteiro de Castro et al., 2015; Liddelow et al., 2017). On the one hand, medrysone application reduced numbers of neurotoxic phenotypes while synchronously enhancing cell numbers with hybrid characters. More information on this topic is described below.

Astrocytic Stat3 signalling seems mandatory for reactivity in multiple neurodegenerative diseases (Haim et al., 2015). More specifically during demyelination, Stat3 reduces inflammation and lesion spreading (Herrmann et al., 2008; Monteiro de Castro et al., 2015). In accordance, we observed medrysone enhancing numbers of C3d+/Stat3+ astrocytes at the dorsal horn SVZ (Figure 18), CCJ (Figure 16) and a-CC (Figure 20) during the early recovery phase. S100a10 distinguish pro-remyelinating astrocytes in MS (Harnisch et al., 2019). However, co expression with C3d is absent in astrocytes within the MS lesion (Liddelow et al., 2017) and healed regions of the spinal cord (Haindl et al., 2019), which contrasts with our findings of C3d+/S100a10+ astrocytes in the CCJ, a-CC and middle d-SVZ in response to medrysone (Figure 16, 18, 20). These results indicate a necessary hybrid state in astrocytes to overcome CPZ-detrimental features in chronic demyelination. Nrf2 and Mafg expression were recently identified in a large population of astrocytes in EAE. These markers characterize an anti- and pro-inflammatory state, respectively (Wheeler et al., 2020). Nonetheless, we observed a limited number of such subtypes in our investigations. Two populations, Mafg-/Nrf2+ and Mafg+/Nrf2- cells, were only observed in the a-CC of control and saline 1 WPC groups, respectively (Figure 19). Of note, this does not exclude the possibility that such reactive astrocytes might also emerge from other brain areas and might appear in a more significant number in those regions.

In conclusion, we observed that active myelinating OLs (Bcas1+/Sox10+) were enhanced by medrysone in the a-CC (in combination with an increase in PLP expression; Figure 21). In addition, a hybrid phenotype characterized by the expression of Timp1 [remyelination related astrocyte (RRA; C3d+/Timp1+/GFP+)] was identified to be upregulated in response to medrysone, particularly in the a-CC (Figure 21o). Timp1 is expressed by reactive astrocytes throughout normal ageing (Clarke et al., 2018; Hasel et al., 2021). In disease, Timp1 impairs inflammation (Ogier et al., 2009; Knight et al., 2019), contributes to neuronal protection (Saha et al., 2020), remyelination (Moore et al., 2011; Houben et al., 2020) and induces OPC/NSCs into a pro-myelinating profile (Moore et al., 2011; Samper-Agrelo et al., 2020; Schira-Heinen et al., 2021). Timp1 is commonly down-regulated in astrocytes during demyelination yet is again expressed throughout remyelination processes (Houben et al., 2020). Both Moore and colleagues (2011) and Houben and colleagues (2020)

blocked Timp1 expression in astrocytes and observed a severe reduction in the spontaneous remyelination in CPZ-treated mice, thus highlighting its importance for remyelination to occur. In fact, C3d+/Timp1+ astrocytes in our evaluations, although in minor numbers (if compared to other subtypes such as C3d+/S100a10+ and C3d+/Stat3+) localized only to the white matter above the lateral ventricle, can be still substantially modify an entire environment in the CNS under demyelination/inflammation, inducing repair towards up-regulation of myelinogenesis and anti-inflammatory-related molecules as observed and emphasized by Houben and colleagues (2020) and Hasel and colleagues (2021). Hence, it is understandable that the RRA, can still be contributing to myelin repair as provoked by medrysone.

8. Conclusion

In a chronic demyelination model, we demonstrated that the corticosteroid medrysone stimulates strong remyelination, highlighted by a pro-remyelination signature in astrocytes within the regenerated areas. This work also implies that this corticosteroid could be a conceivable treatment for late-stage MS, where regenerative approaches often do not succeed. Further analyses will be essential to describe other trophic entities associated with here-presented astrocyte subpopulations entangled in the overall repair process.

9. Funding

This work was supported by the Jürgen Manchot Stiftung, the Research Commission of the medical faculty of the Heinrich-Heine-University of Düsseldorf, the Christiane and Claudia Hempel Foundation for clinical stem cell research and the James and Elisabeth Cloppenburg, Peek and Cloppenburg Düsseldorf Stiftung.

10. References

Akkermann, R., Jadasz, J. J., Azim, K., & Küry, P. (2016). Taking advantage of nature's gift: Can endogenous neural stem cells improve myelin regeneration? *International Journal of Molecular Sciences*. https://doi.org/10.3390/ijms17111895

Al Nimer, F., Elliott, C., Bergman, J., Khademi, M., Dring, A. M., Aeinehband, S., Piehl, F. (2016). Lipocalin-2 is increased in progressive multiple sclerosis and inhibits remyelination. *Neurology - Neuroimmunology Neuroinflammation*, *3*(1), e191. https://doi.org/10.1212/nxi.0000000000000191

Al-Dalahmah, Osama. Soares, Luana Campos. Nicholson, James. Draijer, Swip. Mundim, Mayara. Lu, Victor M. Sun, Bin. Tyler, Teadora. Adorjan, Istvan. O'Neil, Eric. Szele, F. G. (2019). Galectin-3 modulates postnatal subventricular zone gliogenesis Osama. Glia, 68(2), 434–450.

Aldinucci, A., Bonechi, E., Biagioli, T., Repice, A. M., D'Elios, M. M., Emmi, L., Ballerini, C. (2018). CSF/serum matrix metallopeptidase-9 ratio discriminates neuro Behçet from multiple sclerosis. *Annals of Clinical and Translational Neurology*, *5*(4), 493–498. https://doi.org/10.1002/acn3.538

Alghamdi, B., & Fern, R. (2015). Phenotype overlap in glial cell populations: Astroglia, oligodendroglia and NG-2(+) cells. *Frontiers in Neuroanatomy*, *9*(MAY), 1–13. https://doi.org/10.3389/fnana.2015.00049

Allnoch, L., Baumgärtner, W., & Hansmann, F. (2019). Impact of astrocyte depletion upon inflammation and demyelination in a murine animal model of multiple sclerosis. *International Journal of Molecular Sciences*, *20*(16). https://doi.org/10.3390/ijms20163922

Almitairi, J. O. M., Girija, U. V., Furze, C. M., Simpson-Gray, X., Badakshi, F., Marshall, J. E., Wallis, R. (2018). Structure of the C1r–C1s interaction of the C1 complex of complement activation. *Proceedings of the National Academy of Sciences of the United States of America*, *115*(4), 768–773. https://doi.org/10.1073/pnas.1718709115

An, J., Yin, J.-J., He, Y., Sui, R.-X., Miao, Q., Wang, Q., Xiao, B.-G. (2020). Temporal and Spatial Dynamics of Astroglial Reaction and Immune Response in Curpizone-Induced Demyelination. *Neurotoxicity Research*, 587–601. https://doi.org/10.1007/s12640-019-00129-4

Aprato, J., Sock, E., Weider, M., Elsesser, O., Fröb, F., & Wegner, M. (2020). Myrf guides target gene selection of transcription factor Sox10 during oligodendroglial development. *Nucleic Acids Research*, *48*(3), 1254–1270. https://doi.org/10.1093/NAR/GKZ1158

Auwardt, R. B., Mudge, S. J., Chen, C. G., & Power, D. A. (1998). Regulation of nuclear factor κB by corticosteroids in rat mesangial cells. *Journal of the American Society of Nephrology*, *9*(9), 1620–1628. https://doi.org/10.1681/asn.v991620

Azami-Tameh, A., Clarner, T., Beyer, C., Atlasi, M. A., Hassanzadeh, G., & Naderian, H. (2013). Regional regulation of glutamate signaling during cuprizone-induced demyelination in the brain. *Annals of Anatomy*, *195*(5), 415–423. https://doi.org/10.1016/j.aanat.2013.03.004

Azevedo, Fredrico A C. Carvalho, Ludmila R B. griberg, Lea T. Farfel, Jose Marcelo, Ferretti, Renata E L. Leite, Renata E P. Filho, Wilson Jacob. Lente, Roberto. Herculano-Houzel, S. (2009). Equal numbers of neuronal and nonneuronal cells make the human brain an isometrically scaled-up primate brain. Journal of COmparative Neurology, 513(5), 532–541. https://doi.org/10.1002/9781119631729.ch5

Azim, K., Akkermann, R., Cantone, M., Vera, J., Jadasz, J. J., & Küry, P. (2018). Transcriptional profiling of ligand expression in cell specific populations of the adult mouse forebrain that regulates neurogenesis. *Frontiers in Neuroscience*, *12*, 1–15. https://doi.org/10.3389/fnins.2018.00220

Azim, K., Angonin, D., Marcy, G., Pieropan, F., Rivera, A., Donega, V., Raineteau, O. (2017). Pharmacogenomic identification of small molecules for lineage specific manipulation of subventricular zone germinal activity. *PLoS Biology*, *15*(3), 1–27. https://doi.org/10.1371/journal.pbio.2000698

Azim, K., Calzolari, F., Cantone, M., Akkermann, R., Vera, J., Hartung, H.-P., Küry, P. (2020). Resolving the transcriptional transitions associated with oligodendrocyte generation from adult neural stem cells by single cell sequencing. *BioRxiv*. https://doi.org/10.1101/2020.12.18.423285

Azim, K., Fiorelli, R., Zweifel, S., Hurtado-Chong, A., Yoshikawa, K., Slomianka, L., & Raineteau, O. (2012). 3-Dimensional Examination of the Adult Mouse Subventricular Zone Reveals Lineage-Specific Microdomains. *PLoS ONE*, *7*(11). https://doi.org/10.1371/journal.pone.0049087

Azim, K., Hurtado-Chong, A., Fischer, B., Kumar, N., Zweifel, S., Taylor, V., & Raineteau, O. (2016). Transcriptional hallmarks of heterogeneous neural stem cell niches of the subventricular zone. *Stem Cells*. https://doi.org/10.1002/stem.2017

Baaklini, C. S., Rawji, K. S., Duncan, G. J., Ho, M. F. S., & Plemel, J. R. (2019). Central Nervous System Remyelination: Roles of Glia and Innate Immune Cells. *Frontiers in Molecular Neuroscience*, *12*(September), 1–18. https://doi.org/10.3389/fnmol.2019.00225

Bacmeister, C. M., Barr, H. J., McClain, C. R., Thornton, M. A., Nettles, D., Welle, C. G., & Hughes, E. G. (2020). Motor learning promotes remyelination via new and surviving oligodendrocytes. *Nature Neuroscience*, *23*(7), 819–831. https://doi.org/10.1038/s41593-020-0637-3

Baecher-Allan, C., Kaskow, B. J., & Weiner, H. L. (2018). Multiple Sclerosis: Mechanisms and Immunotherapy. *Neuron*, *97*(4), 742–768. https://doi.org/10.1016/j.neuron.2018.01.021

Baxi, E. G., Debruin, J., Jin, J., Strasburger, H. J., Smith, M. D., Orthmann-murphy, J. L., Calabresi, P. A. (2017). Lineage tracing reveals dynamic changes in oligodendrocyte precursor cells following cuprizone-induced demyelination. *Glia*, *65*(12), 2087–2098. https://doi.org/10.1002/glia.23229.Lineage

Bedrossian, R. H., & Eriksen, S. P. (1969). The Treatment of Ocular Inflammation With Medrysone. *Archives of Ophthalmology*, *81*(2), 184–191. https://doi.org/10.1001/archopht.1969.00990010186008

Benner, E. J., Luciano, D., Jo, R., Abdi, K., Paez-Gonzalez, P., Sheng, H., Kuo, C. T. (2013). Protective astrogenesis from the SVZ niche after injury is controlled by Notch modulator Thbs4. *Nature*, *497*(7449), 369–373. https://doi.org/10.1038/nature12069

Bergles, D. E., & Richardson, W. D. (2016). Oligodendrocyte development and plasticity. Cold Spring Harbor Perspectives in Biology, 8(2), 1–27. https://doi.org/10.1101/cshperspect.a020453

Bernaus, A., Blanco, S., & Sevilla, A. (2020). Glia Crosstalk in Neuroinflammatory Diseases. *Frontiers in Cellular Neuroscience*, *14*(July), 1–17. https://doi.org/10.3389/fncel.2020.00209

Bhargava, P., Nogueras-ortiz, C., Delgado-, F., Calabresi, P. A., & Kapogiannis, D. (2021). Synaptic and Complement Markers in Extracellular Vesicles in Multiple Sclerosis. *Multiple Sclerosis*, *27*(4), 509–518. https://doi.org/10.1177/1352458520924590.Synaptic

Bi, F., Huang, C., Tong, J., Qiu, G., Huang, B., Wu, Q., Zhou, H. (2013). Reactive astrocytes secrete lcn2 to promote neuron death. *Proceedings of the National Academy of Sciences of the United States of America*, *110*(10), 4069–4074. https://doi.org/10.1073/pnas.1218497110

Bond, A., Ming, G.-L., & Song, H. (2015). Adult Mammalian Neural Stem Cells and Neurogenesis: Five Decades Later. Cell Stem Cell, 17(4), 385–395. https://doi.org/10.1016/j.stem.2015.09.003.Adult

Boos, L. A., Szalai, A. J., & Barnum, S. R. (2005). Murine complement C4 is not required for experimental autoimmune encephalomyelitis. *Glia*, *49*(1), 158–160. https://doi.org/10.1002/glia.20093

Bradl, M., & Lassmann, H. (2010). Oligodendrocytes: Biology and pathology. *Acta Neuropathologica*, *119*(1), 37–53. https://doi.org/10.1007/s00401-009-0601-5

Brambilla, R. (2019). The contribution of astrocytes to the neuroinflammatory response in multiple sclerosis and experimental autoimmune encephalomyelitis. *Acta Neuropathologica*, *137*(5), 757–783. https://doi.org/10.1007/s00401-019-01980-7

Brousse, B., Magalon, K., Durbec, P., & Cayre, M. (2015). Region and dynamic specificities of adult neural stem cells and oligodendrocyte precursors in myelin

regeneration in the mouse brain. Biology Open, 4(8), 980–992. https://doi.org/10.1242/bio.012773

Brück, W., Pförtner, R., Pham, T., Zhang, J., Hayardeny, L., Piryatinsky, V., Wegner, C. (2012). Reduced astrocytic NF-κB activation by laquinimod protects from cuprizone-induced demyelination. *Acta Neuropathologica*, *124*(3), 411–424. https://doi.org/10.1007/s00401-012-1009-1

Brune, S., Høgestøl, E. A., Cengija, V., Berg-hansen, P., & Sowa, P. (2020). LesionQuant for Assessment of MRI in Multiple Sclerosis — A Promising Supplement to the Visual Scan Inspection. 11(December), 1–10. https://doi.org/10.3389/fneur.2020.546744

Butovsky, O., Landa, G., Kunis, G., Ziv, Y., Avidan, H., Greenberg, N., Schwartz, M. (2006). Induction and blockage of oligodendrogenesis by differently activated microglia in an animal model of multiple sclerosis. Journal of Clinical Investigation, 116(4), 905–915. https://doi.org/10.1172/JCI26836

Butti, E., Bacigaluppi, M., Chaabane, L., Ruffini, F., Brambilla, E., Berera, G., Martino, G. (2019). Neural stem cells of the subventricular zone contribute to neuroprotection of the corpus callosum after cuprizone-induced demyelination. *Journal of Neuroscience*, *39*(28), 5481–5492. https://doi.org/10.1523/JNEUROSCI.0227-18.2019

Carlström, K. E., Zhu, K., Ewing, E., Krabbendam, I. E., Harris, R. A., Falcão, A. M., Piehl, F. (2020). Gsta4 controls apoptosis of differentiating adult oligodendrocytes during homeostasis and remyelination via the mitochondria-associated Fas-Casp8-Bid-axis. *Nature Communications*, *11*(1). https://doi.org/10.1038/s41467-020-17871-5

Carpanini, S. M., Torvell, M., & Morgan, B. P. (2019). Therapeutic inhibition of the complement system in diseases of the central nervous system. *Frontiers in Immunology*, *10*(MAR), 1–17. https://doi.org/10.3389/fimmu.2019.00362

Castellazzi, M., Ligi, D., Contaldi, E., Quartana, D., Fonderico, M., Borgatti, L., Pugliatti, M. (2018). Multiplex matrix metalloproteinases analysis in the cerebrospinal fluid reveals potential specific patterns in multiple sclerosis patients. *Frontiers in Neurology*, *9*(December), 1–7. https://doi.org/10.3389/fneur.2018.01080

Cayre, M., Falque, M., Mercier, O., Magalon, K., & Durbec, P. (2021). Myelin Repair: From Animal Models to Humans. *Frontiers in Cellular Neuroscience*, *15*(April), 1–20. https://doi.org/10.3389/fncel.2021.604865

Chang, A., Tourtellotte, W. W., Rudick, R., & Trapp, B. D. (2002). Premyelinating Oligodendrocytes in Chronic Lesions of Multiple Sclerosis. *New England Journal of Medicine*, *346*(3), 165–173. https://doi.org/10.1056/nejmoa010994

Chari M. Divya, Chao, Z., R.Kotter, M., Bloakemore, W. F., & Franklin, R. J. M. (2006). Corticosteroid delay remyelination of experimental demyelination in the rodent

central nervous system. *Journal of Neuroscience Research*. https://doi.org/10.1002/jnr.20763

Chari, D. M. (2007). Remyelination In Multiple Sclerosis. *International Review of Neurobiology*, *79*(January), 589–620. https://doi.org/10.1016/S0074-7742(07)79026-8

Chastain, E. M. L., Duncan, D. S., Rodgers, J. M., & Miller, S. D. (2011). The role of antigen presenting cells in multiple sclerosis. *Biochimica et Biophysica Acta - Molecular Basis of Disease*, *1812*(2), 265–274. https://doi.org/10.1016/j.bbadis.2010.07.008

Chen, T., Lennon, V. A., Liu, Y. U., Bosco, D. B., Li, Y., Yi, M. H., Wu, L. J. (2020). Astrocyte-microglia interaction drives evolving neuromyelitis optica lesion. *Journal of Clinical Investigation*, *140*(8), 4025–4038. https://doi.org/10.1172/JCI134816

Chen, Y., Qin, C., Huang, J., Tang, X., Liu, C., Huang, K., Zhou, L. (2019). The role of astrocytes in oxidative stress of central nervous system: A mixed blessing. *Cell Proliferation*, *53*(3), 1–13. https://doi.org/10.1111/cpr.12781

Chung, W., Allen, N. J., & Eroglu, C. (2015). Astrocyte & synapse. *Cold Spring Harbor Laboratory Press*, *7*(a020370), 1–19.

Clarke, L. E., Liddelow, S. A., Chakraborty, C., Münch, A. E., Heiman, M., & Barres, B. A. (2018). Normal aging induces A1-like astrocyte reactivity. *Proceedings of the National Academy of Sciences of the United States of America*, *115*(8), E1896–E1905. https://doi.org/10.1073/pnas.1800165115

Clarner, T. A., Parabuck, C., & Kipp, M. (2011). Corticosteroids impair Remyelination in the Corpus Callosum of Curpizone-Treated Mice. *Journal of Neuroendocrinology*, *23*(7), 601–611. https://doi.org/j.1365-2868.2011.20140.x

Coman, I., Aigrot, M. S., Seilhean, D., Reynolds, R., Girault, J. A., Zalc, B., & Lubetzki, C. (2006). Nodal, paranodal and juxtaparanodal axonal proteins during demyelination and remyelination in multiple sclerosis. *Brain*, *129*(12), 3186–3195. https://doi.org/10.1093/brain/awl144

Compston, Alastair. Coles, A. (2008). Multiple Sclerosis. The Lancet, 372(9648), 1502–1517. https://doi.org/https://doi.org/10.1016/S0140-6736(08)61620-7

Conover, J. C., & Shook, B. A. (2011). Aging of the subventricular zone neural stem cell niche. Aging and Disease, 2(1), 49–63.

Constantinescu, C. S., Farooqi, N., O'Brien, K., & Gran, B. (2011). Experimental autoimmune encephalomyelitis (EAE) as a model for multiple sclerosis (MS). *British Journal of Pharmacology*, *164*(4), 1079–1106. https://doi.org/10.1111/j.1476-5381.2011.01302.x

Crocker, S. J., Whitmire, J. K., Frausto, R. F., Chertboonmuang, P., Soloway, P. D., Whitton, J. L., & Campbell, I. L. (2006). Persistent macrophage/microglial activation and myelin disruption after experimental autoimmune encephalomyelitis in tissue inhibitor of metalloproteinase-1-deficient mice. *American Journal of Pathology*, *169*(6), 2104–2116. https://doi.org/10.2353/ajpath.2006.060626

Da-Cunha, I. W., de Almeida Coudry, R., de Macedo, M. P., de Assis, E. A. C. P., Stefani, S., & Soares, F. A. (2021). Correction to: A call to action: molecular pathology in Brazil. Surgical and Experimental Pathology, 4(1), 1–27. https://doi.org/10.1186/s42047-021-00101-7

Dalakas, M. C., Alexopoulos, H., & Spaeth, P. J. (2020). Complement in neurological disorders and emerging complement-targeted therapeutics. *Nature Reviews Neurology*, *16*(11), 601–617. https://doi.org/10.1038/s41582-020-0400-0

Daliot, Yisrael. "Jacqueline du Pre." Shalvi/Hyman Encyclopedia of Jewish Women. 31 December 1999. Jewish Women's Archive. (Viewed on February 8, 2022) <https://jwa.org/encyclopedia/article/du-pre-jacqueline>.

Das, S., Li, Z., Noori, A., Hyman, B. T., & Serrano-Pozo, A. (2020). Meta-analysis of mouse transcriptomic studies supports a context-dependent astrocyte reaction in acute CNS injury versus neurodegeneration. *Journal of Neuroinflammation*, *17*(1). https://doi.org/10.1186/s12974-020-01898-y

Daynac, M., Morizur, L., Chicheportiche, A., Mouthon, M. A., & Boussin, F. D. (2016). Age-related neurogenesis decline in the subventricular zone is associated with specific cell cycle regulation changes in activated neural stem cells. *Scientific Reports*, *6*(January), 1–10. https://doi.org/10.1038/srep21505

Dimou, L., Simon, C., Kirchhoff, F., Takebayashi, H., & Götz, M. (2008). Progeny of Olig2-expressing progenitors in the gray and white matter of the adult mouse cerebral cortex. Journal of Neuroscience, 28(41), 10434–10442. https://doi.org/10.1523/JNEUROSCI.2831-08.2008

Doetsch, F., Caille, I., Lim, D. A., Garcı, J. M., & Alvarez-buylla, A. (1999). Subventricular Zone Astrocytes Are Neural Stem Cells in the Adult Mammalian Brain. *Cell*, *97*, 703–716. Retrieved from internal-pdf://171.18.31.238/008693427208823Doetsch 1999.pdf

Dutta, D. J., Woo, D. H., Lee, P. R., Pajevic, S., Bukalo, O., Huffman, W. C., Fields, R. D. (2018). Regulation of myelin structure and conduction velocity by perinodal astrocytes. *Proceedings of the National Academy of Sciences of the United States of America*, *115*(46), 11832–11837. https://doi.org/10.1073/pnas.1811013115

Dutta, Ranjan. Chang, Asi. Doud, Mary K. Kidd, Grahame J. Ribuado, Michael V. Young, Elizabeth A. Fox, Robert J. Staugatis, Susan M. Trapp, B. D. (2011). Demyelination Causes Synaptic Alterations in Hippocampi from Multiple Sclerosis Patients. Annals Neurology, 69(3), 445–454. https://doi.org/10.1002/ana.22337.Demyelination

Dyer, J. K., Bourque, J. A., & Steeves, J. D. (2005). The role of complement in immunological demyelination of the mammalian spinal cord. *Spinal Cord*, *43*(7), 417–425. https://doi.org/10.1038/sj.sc.3101737

Elovaara, I., Lalla, M., Spare, E., Lehtimaki, T., Dastidar, P. (1998) 'Methylprednisolone reduces adhesion molecules in blood and cerebrospinal fluid in patients with MS', Neurology, 51(6), pp. 1703–1708. Available at: https://doi.org/10.1212/wnl.51.6.1703.

El-Waly, B. Macchi, M., Cayre, M., & Durbec, P. (2014). Oligodendrogenesis in the normal and pathological central nervous system. Frontiers in Neuroscience, 8(8 JUN), 1–22. https://doi.org/10.3389/fnins.2014.00145

Emery, B. (2013). Playing the Field: Sox10 Recruits Different Partners to Drive Central and Peripheral Myelination. *PLoS Genetics*, *9*(10), 9–11. https://doi.org/10.1371/journal.pgen.1003918

Emery, B., & Lu, Q. R. (2015). Transcriptional and epigenetic regulation of oligodendrocyte development and myelination in the central nervous system. *Cold Spring Harbor Perspectives in Biology*, *7*(9). https://doi.org/10.1101/cshperspect.a020461

Escartin, C., Galea, E., Lakatos, A., O'Callaghan, J. P., Petzold, G. C., Serrano-Pozo, A., Verkhratsky, A. (2021). Reactive astrocyte nomenclature, definitions, and future directions. *Nature Neuroscience*, *24*(3), 312–325. https://doi.org/10.1038/s41593-020-00783-4

Faiz, M., Sachewsky, N., Gascón, S., Bang, K. W. A., Morshead, C. M., & Nagy, A. (2015). Adult Neural Stem Cells from the Subventricular Zone Give Rise to Reactive Astrocytes in the Cortex after Stroke. *Cell Stem Cell*, *17*(5), 624–634. https://doi.org/10.1016/j.stem.2015.08.002

Fard, M. K., Van der Meer, F., Sánchez, P., Cantuti-Castelvetri, L., Mandad, S., Jäkel, S., Simons, M. (2017). BCAS1 expression defines a population of early myelinating oligodendrocytes in multiple sclerosis lesions. *Science Translational Medicine*, *9*(419), 1–13. https://doi.org/10.1126/scitranslmed.aam7816

Filipovic, R., & Zecevic, N. (2008). The effect of CXCL1 on human fetal oligodendrocyte progenitor cells. Glia, 56(1), 1–15. https://doi.org/10.1002/glia.20582

Filippi, M., Brück, W., Chard, D., Fazekas, F., Geurts, J. J. G., Enzinger, C., Rocca, M. A. (2019). Association between pathological and MRI findings in multiple sclerosis. The Lancet Neurology, 18(2), 198–210. https://doi.org/10.1016/S1474-4422(18)30451-4

Fiorelli, R., Azim, K., Fischer, B., & Raineteau, O. (2015). Adding a spatial dimension to postnatal ventricular-subventricular zone neurogenesis. Development (Cambridge), 142(12), 2109–2120. https://doi.org/10.1242/dev.119966

Fonseca, M. I., Chu, S. H., Hernandez, M. X., Fang, M. J., Modarresi, L., Selvan, P., Tenner, A. J. (2017). Cell-specific deletion of C1qa identifies microglia as the dominant source of C1q in mouse brain. *Journal of Neuroinflammation*, *14*(1), 1–15. https://doi.org/10.1186/s12974-017-0814-9

Frazão, Dilva. "Santos Dumont' biography 2021.eBiografia. (Viewed on February 8, 2022) https://www.ebiografia.com/santos_dumont/

French, Heather Morein. Reid, Mary. Mamontov, Polina. Simmons, Rebecca A. Grinspan, J. B. (2009). Oxidative Stress Disrupts Oligodendrocyte Maturation Heather. Journal Neuroscience Research, 14(87), 3076–3087. https://doi.org/10.1002/jnr.22139.Oxidative

Fuentealba, L. C., Rompani, S. B., Parraguez, J. I., Obernier, K., Romero, R., Cepko, C. L., & Alvarez-Buylla, A. (2015). Embryonic Origin of Postnatal Neural Stem Cells. Cell, 161(7), 1644–1655. https://doi.org/10.1016/j.cell.2015.05.041

García-Marqués, J., & López-Mascaraque, L. (2013). Clonal identity determines astrocyte cortical heterogeneity. *Cerebral Cortex*, *23*(6), 1463–1472. https://doi.org/10.1093/cercor/bhs134

García-Moreno, F., & Molnár, Z. (2015). Subset of early radial glial progenitors that contribute to the development of callosal neurons is absent from avian brain. *Proceedings of the National Academy of Sciences of the United States of America*, *112*(36), E5058–E5067. https://doi.org/10.1073/pnas.1506377112

Garcia-Verdugo, Jose Manuel. Doetsch, Fiona. Wichterle, Hynek. Lim, Daniel A. Alvarez-Buylla, A. (1998). Architecture and cell types of the adult subventricular zone: In search of the stem cells. *Developmental Neurobiology*, 27–29.

Gehr, S., Kaiser, T., Kreutz, R., Ludwig, W. D., & Paul, F. (2019). Suggestions for improving the design of clinical trials in multiple sclerosis—results of a systematic analysis of completed phase III trials. *EPMA Journal*, *10*(4), 425–436. https://doi.org/10.1007/s13167-019-00192-z

Giachino, C., Basak, O., Lugert, S., Knuckles, P., Obernier, K., Fiorelli, R., Taylor, V. (2014). Molecular diversity subdivides the adult forebrain neural stem cell population. *Stem Cells*, *32*(1), 70–84. https://doi.org/10.1002/stem.1520

Gingele, S., Henkel, F., Heckers, S., Moellenkamp, T. M., Hümmert, M. W., Skripuletz, T., Gudi, V. (2020). Delayed Demyelination and Impaired Remyelination in Aged Mice in the Cuprizone Model. *Cells*, *9*(4). https://doi.org/10.3390/cells9040945

Goetzl, E. J., Schwartz, J. B., Abner, E. L., Jicha, G. A., Kapogiannis, D., Francisco, S., Francisco, S. (2019). Alzheimer ' s disease. *Annals Neurology*, *83*(3), 544–552. https://doi.org/10.1002/ana.25172.High

Goldschmidt, T., Antel, J., König, F. B., Brück, W., & Kuhlmann, T. (2009). Remyelination capacity of the MS brain decreases with disease chronicity. *Neurology*, *72*(22), 1914–1921. https://doi.org/10.1212/WNL.0b013e3181a8260a

Gonzalez-Perez, O., & Alvarez-Buylla, A. (2011). Oligodendrogenesis in the subventricular zone and the role of epidermal growth factor. Brain Research Reviews, 67(1–2), 147–156. https://doi.org/10.1016/j.brainresrev.2011.01.001

Gorter, R. P., & Baron, W. (2020). Matrix metalloproteinases shape the oligodendrocyte (niche) during development and upon demyelination. *Neuroscience Letters*, *729*(April), 134980. https://doi.org/10.1016/j.neulet.2020.134980

Göttle, P., Manousi, A., Kremer, D., Reiche, L., Hartung, H. P., & Küry, P. (2018). Teriflunomide promotes oligodendroglial differentiation and myelination. *Journal of Neuroinflammation*, *15*(1), 1–12. https://doi.org/10.1186/s12974-018-1110-z

Greiner, T., & Kipp, M. (2021). What guides peripheral immune cells into the central nervous system? *Cells*, *10*(8). https://doi.org/10.3390/cells10082041

Gresle, M.M. et al. (2020) 'Multiple sclerosis risk variants regulate gene expression in innate and adaptive immune cells', Life Science Alliance, 3(7), pp. 1–11. Available at: https://doi.org/10.26508/LSA.202000650.

Gruchot, J., Weyers, V., Göttle, P., Förster, M., Hartung, H.-P., Küry, P., & Kremer, D. (2019). The Molecular Basis for Remyelination Failure in Multiple Sclerosis. *Cells*, *8*(8), 825. https://doi.org/10.3390/cells8080825

Gudi, V., Gingele, S., Skripuletz, T., & Stangel, M. (2014). Glial response during cuprizone-induced de- and remyelination in the CNS: Lessons learned. *Frontiers in Cellular Neuroscience*, Vol. 8. https://doi.org/10.3389/fncel.2014.00073

Guzman-Martinez, L., Maccioni, R. B., Andrade, V., Navarrete, L. P., Pastor, M. G., & Ramos-Escobar, N. (2019). Neuroinflammation as a common feature of neurodegenerative disorders. *Frontiers in Pharmacology*, *10*(SEP), 1–17. https://doi.org/10.3389/fphar.2019.01008

Haile, Y., Carmine-Simmen, K., Olechowski, C., Kerr, B., Bleackley, R. C., & Giuliani, F. (2015). Granzyme B-inhibitor serpina3n induces neuroprotection in vitro and in vivo. Journal of Neuroinflammation, 12(1), 1–10. https://doi.org/10.1186/s12974-015-0376-7

Haim, L. Ben, Ceyzériat, K., Sauvage, M. A. C. de, Aubry, F., Auregan, G., Guillermier, M., Escartin, C. (2015). The JAK/STAT3 pathway is a common inducer of astrocyte reactivity in Alzheimer's and Huntington's diseases. *Journal of Neuroscience*, *35*(6), 2817–2829. https://doi.org/10.1523/JNEUROSCI.3516-14.2015

Haindl, M. T., Köck, U., Zeitelhofer-Adzemovic, M., Fazekas, F., & Hochmeister, S. (2019). The formation of a glial scar does not prohibit remyelination in an animal model of multiple sclerosis. *Glia*, *67*(3), 467–481. https://doi.org/10.1002/glia.23556

Hammad, A., Westacott, L., & Zaben, M. (2018). The role of the complement system in traumatic brain injury: A review. *Journal of Neuroinflammation*, *15*(1), 1–13. https://doi.org/10.1186/s12974-018-1066-z

Harnisch, K., Teuber-Hanselmann, S., Macha, N., Mairinger, F., Fritsche, L., Soub, D., Junker, A. (2019). Myelination in multiple sclerosis lesions is associated with regulation of bone morphogenetic protein 4 and its Antagonist Noggin. *International Journal of Molecular Sciences*, *20*(1), 0–13. https://doi.org/10.3390/ijms20010154

Hasel, P., Rose, I. V. L., Sadick, J. S., Kim, R. D., & Liddelow, S. A. (2021). Neuroinflammatory astrocyte subtypes in the mouse brain. *Nature Neuroscience*, *24*(10), 1475–1487. https://doi.org/10.1038/s41593-021-00905-6

Hernandez-Pedro, N. Y., Magana-Maldonado, R., Ramiro, A. S., Perez-De La Cruz, V., Rangel-Lopez, E., Sotelo, J., & Pineda, B. (2016). PAMP-DAMPS interactions mediates development and progression of multiple sclerosis. *Frontiers in Bioscience - Scholar*, *8*(1), 13–28. https://doi.org/10.2741/S443

Herrmann, J. E., Imura, T., Song, B., Qi, J., Ao, Y., Nguyen, T. K., Sofroniew, M. V. (2008). STAT3 is a critical regulator of astrogliosis and scar formation after spinal cord injury. *Journal of Neuroscience*, *28*(28), 7231–7243. https://doi.org/10.1523/JNEUROSCI.1709-08.2008

Hesse, A., Wagner, M., Held, J., Brück, W., Salinas-Riester, G., Hao, Z., Kuhlmann, T. (2010). In toxic demyelination oligodendroglial cell death occurs early and is FAS independent. Neurobiology of Disease, 37(2), 362–369. https://doi.org/10.1016/j.nbd.2009.10.016

Hibbits, N., Yoshino, J., Le, T. Q., & Armstrong, R. C. (2012). Astrogliosis during acute and chronic cuprizone demyelination and implications for remyelination. *ASN Neuro*, *4*(6), 393–408. https://doi.org/10.1042/an20120062

Hillis, J. M., Davies, J., Mundim, M. V., Al-Dalahmah, O., & Szele, F. G. (2016). Cuprizone demyelination induces a unique inflammatory response in the subventricular zone. *Journal of Neuroinflammation*, *13*(1). https://doi.org/10.1186/s12974-016-0651-2

Hiremath, M. M., Chen, V. S., Suzuki, K., Ting, J. P. Y., & Matsushima, G. K. (2008). MHC class II exacerbates demyelination in vivo independently of T cells. *Journal of Neuroimmunology*, *203*(1), 23–32. https://doi.org/10.1016/j.jneuroim.2008.06.034

Hirotsu, Y., Katsuoka, F., Funayama, R., Nagashima, T., Nishida, Y., Nakayama, K., Yamamoto, M. (2012). Nrf2-MafG heterodimers contribute globally to antioxidant and metabolic networks. *Nucleic Acids Research*, *40*(20), 10228–10239. https://doi.org/10.1093/nar/gks827

Hornig, J., Fröb, F., Vogl, M. R., Hermans-Borgmeyer, I., Tamm, E. R., & Wegner, M. (2013). The Transcription Factors Sox10 and Myrf Define an Essential Regulatory

Network Module in Differentiating Oligodendrocytes. *PLoS Genetics*, *9*(10). https://doi.org/10.1371/journal.pgen.1003907

Hou, B., Zhang, Y., Liang, P., He, Y., Peng, B., Liu, W., He, X. (2020). Inhibition of the NLRP3-inflammasome prevents cognitive deficits in experimental autoimmune encephalomyelitis mice via the alteration of astrocyte phenotype. *Cell Death and Disease*, *11*(5). https://doi.org/10.1038/s41419-020-2565-2

Houben, E., Janssens, K., Hermans, D., Vandooren, J., van den Haute, C., Schepers, M., Hellings, N. (2020). Oncostatin M-induced astrocytic tissue inhibitor of metalloproteinases-1 drives remyelination. *Proceedings of the National Academy of Sciences of the United States of America*, *117*(9), 5028–5038. https://doi.org/10.1073/pnas.1912910117

Hu, C. L., Nydes, M., Shanley, K. L., Morales Pantoja, I. E., Howard, T. A., & Bizzozero, O. A. (2019). Reduced expression of the ferroptosis inhibitor glutathione peroxidase-4 in multiple sclerosis and experimental autoimmune encephalomyelitis. *Journal of Neurochemistry*, *148*(3), 426–439. https://doi.org/10.1111/jnc.14604

Hu, X., Holers, V. M., Thurman, J. M., Schoeb, T. R., Ramos, T. N., & Barnum, S. R. (2013). Therapeutic inhibition of the alternative complement pathway attenuates chronic EAE. Molecular Immunology, 54(3–4), 302–308. https://doi.org/10.1016/j.molimm.2012.12.018

Hughes, E. G., & Stockton, M. E. (2021). Premyelinating Oligodendrocytes: Mechanisms Underlying Cell Survival and Integration. *Frontiers in Cell and Developmental Biology*, *9*(July), 1–17. https://doi.org/10.3389/fcell.2021.714169

Hughes, J. P., Rees, S. S., Kalindjian, S. B., & Philpott, K. L. (2011). Principles of early drug discovery. *British Journal of Pharmacology*, *162*(6), 1239–1249. https://doi.org/10.1111/j.1476-5381.2010.01127.x

Hui-Ming, Gao. Jau-Shyong, H. (2008). Why neurodegenerative diseases are progressive: uncontrolled inflammation drives disease progression. Physiology & Behavior, 29(8), 357–365. https://doi.org/10.1016/j.it.2008.05.002.Why

ICERS. (2017). ICER's Final Report on Disease-Modifying Therapies for Multiple Sclerosis Finds Most Drugs are Over-Priced in Relation to Benefits for Patients; Highlights Need for Stakeholder Collaboration to Address System Issues - ICER. *Institute for Clinical and Economic Review*. Retrieved from https://icer.org/news-insights/press-releases/final-ms-report/

Ishibashi, T., Dakin, K. A., Stevens, B., Lee, P. R., Kozlov, S. V., Stewart, C. L., & Fields, R. D. (2006). Astrocytes promote myelination in response to electrical impulses. *Neuron*, *49*(6), 823–832. https://doi.org/10.1016/j.neuron.2006.02.006

Ishimoto, T., Ninomiya, K., Inoue, R., Koike, M., Uchiyama, Y., & Mori, H. (2017). Mice lacking BCAS1, a novel myelin-associated protein, display hypomyelination,

schizophrenia-like abnormal behaviors, and upregulation of inflammatory genes in the brain. *Glia*, *65*(5), 727–739. https://doi.org/10.1002/glia.23129

Itoh, N., Itoh, Y., Tassoni, A., Ren, E., Kaito, M., Ohno, A., Voskuhl, R. R. (2018). Cell-specific and region-specific transcriptomics in the multiple sclerosis model: Focus on astrocytes. *Proceedings of the National Academy of Sciences of the United States of America*, *115*(2), E302–E309. https://doi.org/10.1073/pnas.1716032115

Jäkel, S., & Dimou, L. (2017). Glial cells and their function in the adult brain: A journey through the history of their ablation. *Frontiers in Cellular Neuroscience*, *11*(February), 1–17. https://doi.org/10.3389/fncel.2017.00024

Jakovcevski, I., Filipovic, R., Mo, Z., Rakic, S., & Zecevic, N. (2009). Oligodendrocyte development and the onset of myelination in the human fetal brain. Frontiers in Neuroanatomy, 3(JUN), 1–15. https://doi.org/10.3389/neuro.05.005.2009

Jégou, J.-F., Chan, P., Schouft, M.-T., Griffiths, M. R., Neal, J. W., Gasque, P., Fontaine, M. (2007). C3d Binding to the Myelin Oligodendrocyte Glycoprotein Results in an Exacerbated Experimental Autoimmune Encephalomyelitis. *The Journal of Immunology*, *178*(5), 3323–3331. https://doi.org/10.4049/jimmunol.178.5.3323

Jing, X., Yao, Y., Wu, D., Hong, H., Feng, X., Xu, N., Liang, H. (2021). IFP35 family proteins promote neuroinflammation and multiple sclerosis. *Proceedings of the National Academy of Sciences of the United States of America*, *118*(32). https://doi.org/10.1073/pnas.2102642118

Juarez, Alejandro Lopez. He, Dabyeang. Lu, Q. R. (2016). Oligodendrocyte Progenitor Programming and Reprogramming: Toward Myelin Regeneration. *Brain Research*, *1638*(1), 209–220. https://doi.org/10.1016/j.brainres.2015.10.051.Oligodendrocyte

Jurga, A. M., Paleczna, M., Kadluczka, J., & Kuter, K. Z. (2021). Beyond the GFAP-astrocyte protein markers in the brain. *Biomolecules*, *11*(9). https://doi.org/10.3390/biom11091361

Kaddatz, H., Joost, S., Nedelcu, J., Chrzanowski, U., Schmitz, C., Gingele, S., Kipp, M. (2021). Cuprizone-induced demyelination triggers a CD8-pronounced T cell recruitment. *Glia*, *69*(4), 925–942. https://doi.org/10.1002/glia.23937

Kang, S. H., Fukaya, M., Yang, J. K., Rothstein, J. D., & Bergles, D. E. (2010). NG2+ CNS glial progenitors remain committed to the oligodendrocyte lineage in postnatal life and following neurodegeneration. *Neuron*, *68*(4), 668–681. https://doi.org/10.1016/j.neuron.2010.09.009

Kirby, L., Jin, J., Cardona, J. G., Smith, M. D., Martin, K. A., Wang, J., Calabresi, P. A. (2019). Oligodendrocyte precursor cells present antigen and are cytotoxic targets in inflammatory demyelination. *Nature Communications*, *10*(1). https://doi.org/10.1038/s41467-019-11638-3

Klugmann, M., & Schwab, M. H. (1997). Assembly of CNS Myelin in the Absence of Proteolipid Protein. In *Neuron* (Vol. 18).

Kremer, D., Akkermann, R., Küry, P., & Dutta, R. (2019). Current advancements in promoting remyelination in multiple sclerosis. *Multiple Sclerosis Journal*, *25*(1), 7–14. https://doi.org/10.1177/1352458518800827

Kremer, D., Heinen, A., Jadasz, J., Göttle, P., Zimmermann, K., Zickler, P., Küry, P. (2009). P57Kip2 Is Dynamically Regulated in Experimental Autoimmune Encephalomyelitis and Interferes With Oligodendroglial Maturation. *Proceedings of the National Academy of Sciences of the United States of America*, *106*(22), 9087–9092. https://doi.org/10.1073/pnas.0900204106

Kriegstein, A., & Alvarez-Buylla, A. (2009, June). The glial nature of embryonic and adult neural stem cells. *Annual Review of Neuroscience*, Vol. 32, pp. 149–184. https://doi.org/10.1146/annurev.neuro.051508.135600

Kuhlmann, T., Miron, V., Cuo, Q., Wegner, C., Antel, J., & Brück, W. (2008). Differentiation block of oligodendroglial progenitor cells as a cause for remyelination failure in chronic multiple sclerosis. *Brain*, *131*(7), 1749–1758. https://doi.org/10.1093/brain/awn096

Kuhn, S., Gritti, L., Crooks, D., & Dombrowski, Y. (2019). Oligodendrocytes in Development, Myelin Generation and Beyond. *Cells*, Vol. 8. https://doi.org/10.3390/cells8111424

Küry, P., Kremer, D., & Göttle, P. (2018). Drug repurposing for neuroregeneration in multiple sclerosis. *Neural Regeneration Research*, *13*(8), 1366–1367. https://doi.org/10.4103/1673-5374.235242

Lampron, A., Larochelle, A., Laflamme, N., Préfontaine, P., Plante, M. M., Sánchez, M. G., Rivest, S. (2015). Inefficient clearance of myelin debris by microglia impairs remyelinating processes. Journal of Experimental Medicine, 212(4), 481–495. https://doi.org/10.1084/jem.20141656

Larsen, P. H., Wells, J. E., Stallcup, W. B., Opdenakker, G., & Yong, V. W. (2003). Matrix Metalloproteinase-9 Facilitates Remyelination in Part by Processing the Inhibitory NG2 Proteoglycan. *Journal of Neuroscience*, *23*(35), 11127–11135. https://doi.org/10.1523/jneurosci.23-35-11127.2003

Lassmann, H. (2019). Pathogenic mechanisms associated with different clinical courses of multiple sclerosis. Frontiers in Immunology, 10(JAN), 1–14. https://doi.org/10.3389/fimmu.2018.03116

Lassmann, H., & van Horssen, J. (2016). Oxidative stress and its impact on neurons and glia in multiple sclerosis lesions. *Biochimica et Biophysica Acta - Molecular Basis of Disease*, *1862*(3), 506–510. https://doi.org/10.1016/j.bbadis.2015.09.018

Lee, E., & Chung, W. S. (2019). Glial control of synapse number in healthy and diseased brain. *Frontiers in Cellular Neuroscience*, *13*(February), 1–8. https://doi.org/10.3389/fncel.2019.00042

Lee, M. A., Palace, J., Stabler, G., Ford, J., Gearing, A., & Miller, K. (1999). Serum gelatinase B, TIMP-1 and TIMP-2 levels in multiple sclerosis. A longitudinal clinical and MRI study. *Brain*, *122*(2), 191–197. https://doi.org/10.1093/brain/122.2.191

Lee, S., Park, J. Y., Lee, W. H., Kim, H., Park, H. C., Mori, K., & Suk, K. (2009). Lipocalin-2 is an autocrine mediator of reactive astrocytosis. *Journal of Neuroscience*, *29*(1), 234–249. https://doi.org/10.1523/JNEUROSCI.5273-08.2009

Leibinger, M., Müller, A., Gobrecht, P., Diekmann, H., Andreadaki, A., & Fischer, D. (2013). Interleukin-6 contributes to CNS axon regeneration upon inflammatory stimulation. Cell Death and Disease, 4(4), 1–13. https://doi.org/10.1038/cddis.2013.126

Lek, M., Dias, J. M., Marklund, U., Uhde, C. W., Kurdija, S., Lei, Q., Ericson, J. (2010). A homeodomain feedback circuit underlies step-function interpretation of a Shh morphogen gradient during ventral neural patterning. *Development*, *137*(23), 4051–4060. https://doi.org/10.1242/dev.054288

Li, J., Zhang, L., Chu, Y., Namaka, M., Deng, B., Kong, J., & Bi, X. (2016). Astrocytes in oligodendrocyte lineage development and white matter pathology. *Frontiers in Cellular Neuroscience*, *10*(MAY), 1–13. https://doi.org/10.3389/fncel.2016.00119

Li, Y., Dittmann, N. L., Eve, A., Watson, S., de Almeida, M. M. A., Footz, T., & Voronova, A. (2022). Hepatoma Derived Growth Factor Enhances Oligodendrocyte Genesis from Subventricular Zone Precursor Cells. *ASN Neuro*, *14*, 175909142210863. https://doi.org/10.1177/17590914221086340

Liberman, A. C., Budziñski, M. L., Sokn, C., Gobbini, R. P., Steininger, A., & Arzt, E. (2018). Regulatory and mechanistic actions of glucocorticoids on T and inflammatory cells. *Frontiers in Endocrinology*, *9*(MAY), 1–14. https://doi.org/10.3389/fendo.2018.00235

Liddelow, S. A., Guttenplan, K. A., Clarke, L. E., Bennett, F. C., Bohlen, C. J., Schirmer, L., Barres, B. A. (2017). Neurotoxic reactive astrocytes are induced by activated microglia. *Nature*, *541*(7638), 481–487. https://doi.org/10.1038/nature21029

Liu, Q., Sanai, N., Jin, W. N., La Cava, A., Van Kaer, L., & Shi, F. D. (2016). Neural stem cells sustain natural killer cells that dictate recovery from brain inflammation. *Nature Neuroscience*, *19*(2), 243–252. https://doi.org/10.1038/nn.4211

Lohrberg, M., Winkler, A., Franz, J., van der Meer, F., Ruhwedel, T., Sirmpilatze, N., Barrantes-Freer, A. (2020). Lack of astrocytes hinders parenchymal oligodendrocyte precursor cells from reaching a myelinating state in osmolyte-

induced demyelination. *Acta Neuropathologica Communications*, *8*(1). https://doi.org/10.1186/s40478-020-01105-2

Lourenço, T., Paes De Faria, J., Bippes, C. A., Maia, J., Lopes-Da-Silva, J. A., Relvas, J. B., & Graõs, M. (2016). Modulation of oligodendrocyte differentiation and maturation by combined biochemical and mechanical cues. *Scientific Reports*, *6*. https://doi.org/10.1038/srep21563

Lublin, F. D., Reingold, S. C., Cohen, J. A., Cutter, G. R., Thompson, A. J., Wolinsky, J. S., Sormani, M. P. (2014). Defining the clinical course of multiple sclerosis. Neurology.Retrievedfromhttps://www.ncbi.nlm.nih.gov/pmc/articles/PMC4117366/pdf/NEUROLOGY2013555623.pdf

Ludwin, S. K. (2006). The pathogenesis of multiple sclerosis: Relating human pathology to experimental studies. *Journal of Neuropathology and Experimental Neurology*, *65*(4), 305–318. https://doi.org/10.1097/01.jnen.0000225024.12074.80

Lunde, H. M. B., Assmus, J., Myhr, K. M., Bø, L., & Grytten, N. (2017). Survival and cause of death in multiple sclerosis: A 60-year longitudinal population study. *Journal of Neurology, Neurosurgery and Psychiatry*, *88*(8), 621–625. https://doi.org/10.1136/jnnp-2016-315238

Madadi, S., Pasbakhsh, P., Tahmasebi, F., Mortezaee, K., Khanehzad, M., Boroujeni, F. B., Kashani, I. R. (2019). Astrocyte ablation induced by La-aminoadipate (L-AAA) potentiates remyelination in a cuprizone demyelinating mouse model. *Metabolic Brain Disease*, *34*, 593–603. https://doi.org/10.1007/s11011-019-0385-9

Manousi, A., & Küry, P. (2021). Small molecule screening as an approach to encounter inefficient myelin repair. *Current Opinion in Pharmacology*, *61*, 127–135. https://doi.org/10.1016/j.coph.2021.09.008

Manousi, A., Göttle, P., Reiche, L., Cui, Q. L., Healy, L. M., Akkermann, R., Küry, P. (2021). Identification of novel myelin repair drugs by modulation of oligodendroglial differentiation competence. *EBioMedicine*, *65*. https://doi.org/10.1016/j.ebiom.2021.103276

Marques, F., Mesquita, S. D., Sousa, J. C., Coppola, G., Gao, F., Geschwind, D. H., Palha, J. A. (2012). Lipocalin 2 is present in the EAE brain and is modulated by natalizumab. *Frontiers in Cellular Neuroscience*, *6*(AUG). https://doi.org/10.3389/fncel.2012.00033

Matias, I., Morgado, J., & Gomes, F. C. A. (2019). Astrocyte Heterogeneity: Impact to Brain Aging and Disease. *Frontiers in Aging Neuroscience*, *11*(March), 1–18. https://doi.org/10.3389/fnagi.2019.00059

Mccarthy, Ken, D., deVellis, J. (1980). Preparation of separate astroglial and oligodendro. *J. Cell Biology*, *85*(June), 890–902. https://doi.org/10.1083/jcb.85.3.890.

McKenzie, B. A., Mamik, M. K., Saito, L. B., Boghozian, R., Monaco, M. C., Major, E. O., Power, C. (2018). Caspase-1 inhibition prevents glial inflammasome activation and pyroptosis in models of multiple sclerosis. *Proceedings of the National Academy of Sciences of the United States of America*, *115*(26), E6065–E6074. https://doi.org/10.1073/pnas.1722041115

Melamed, E., & Lee, M. W. (2020). Multiple Sclerosis and Cancer: The Ying-Yang Effect of Disease Modifying Therapies. Frontiers in Immunology, 10(January), 1–16. https://doi.org/10.3389/fimmu.2019.02954

Menn, B., Garcia-Verdugo, J. M., Yaschine, C., Gonzalez-Perez, O., Rowitch, D., & Alvarez-Buylla, A. (2006). Origin of oligodendrocytes in the subventricular zone of the adult brain. *Journal of Neuroscience*, *26*(30), 7907–7918. https://doi.org/10.1523/JNEUROSCI.1299-06.2006

Michailidou, I., Naessens, D. M. P., Hametner, S., Guldenaar, W., Kooi, E. J., Geurts, J. J. G., Ramaglia, V. (2017). Complement C3 on microglial clusters in multiple sclerosis occur in chronic but not acute disease: Implication for disease pathogenesis. *Glia*, *65*(2), 264–277. https://doi.org/10.1002/glia.23090

Michalski, J. P., Anderson, C., Beauvais, A., de Repentigny, Y., & Kothary, R. (2011). The proteolipid protein promoter drives expression outside of the oligodendrocyte lineage during embryonic and early postnatal development. *PLoS ONE*, *6*(5). https://doi.org/10.1371/journal.pone.0019772

Miljković, D., & Spasojević, I. (2013). Multiple Sclerosis: Molecular Mechanisms and Therapeutic Opportunities. Antioxidants and Redox Signaling, 19(18), 2286–2334. https://doi.org/10.1089/ars.2012.5068

Minagar, A., & Alexander, J. S. (2003). Blood-brain barrier disruption in multiple sclerosis. Multiple Sclerosis, 9(6), 540–549. https://doi.org/10.1191/1352458503ms965oa

Mirshafiey, A., Asghari, B., Ghalamfarsa, G., Jadidi-Niaragh, F., & Azizi, G. (2014). The significance of matrix metalloproteinases in the immunopathogenesis and treatment of multiple sclerosis. *Sultan Qaboos University Medical Journal*, *14*(1), 13–25. https://doi.org/10.12816/0003332

Miyamoto, N., Maki, T., Shindo, A., Liang, A. C., Maeda, M., Egawa, N., Arai, K. (2015). Astrocytes promote oligodendrogenesis after white matter damage via brain-derived neurotrophic factor. *Journal of Neuroscience*, *35*(41), 14002–14008. https://doi.org/10.1523/JNEUROSCI.1592-15.2015

Mizrak, Dogukan. Levitin, Hanna Mendes. Delgado, Ana C. Crotet, Valerie. Yuan, Jinzhou. Chaker, Zayna. Silva-Vargas, Violeta. Sims, Peter A. Doetsch, F. (2019). Single-Cell Analysis of Regional Differences in Adult V-SVZ Neural Stem Cell Lineages. Cell Reports, 26(2), 394–406. https://doi.org/10.1016/j.celrep.2018.12.044.Single-Cell

Mohammadhosayni, M., Khosrojerdi, A., Lorian, K., Aslani, S., Imani, D., Razi, B., Torkamandi, S. (2020). Matrix metalloproteinases (MMPs) family gene polymorphisms and the risk of multiple sclerosis: Systematic review and meta-analysis. *BMC Neurology*, *20*(1), 1–10. https://doi.org/10.1186/s12883-020-01804-2

Monteiro De Castro, G., Deja, N. A., Ma, D., Zhao, C., & Franklin, R. J. M. (2015). Astrocyte Activation via Stat3 Signaling Determines the Balance of Oligodendrocyte versus Schwann Cell Remyelination. *American Journal of Pathology*, *185*(9), 2431–2440. https://doi.org/10.1016/j.ajpath.2015.05.011

Moore, C. S., Milner, R., Nishiyama, A., Frausto, R. F., Serwanski, D. R., Pagarigan, R. R., Crocker, S. J. (2011). Astrocytic tissue inhibitor of metalloproteinase-1 (TIMP-1) promotes oligodendrocyte differentiation and enhances CNS myelination. *Journal of Neuroscience*, *31*(16), 6247–6254. https://doi.org/10.1523/JNEUROSCI.5474-10.2011

Moraga, A., Pradillo, J. M., García-Culebras, A., Palma-Tortosa, S., Ballesteros, I., Hernández-Jiménez, M., … Lizasoain, I. (2015). Aging increases microglial proliferation, delays cell migration, and decreases cortical neurogenesis after focal cerebral ischemia. *Journal of Neuroinflammation*, *12*(1), 1. https://doi.org/10.1186/s12974-015-0314-8

Moreno-García, Á., Bernal-Chico, A., Colomer, T., Rodríguez-Antigüedad, A., Matute, C., & Mato, S. (2020). Gene expression analysis of astrocyte and microglia endocannabinoid signaling during autoimmune demyelination. *Biomolecules*, *10*(9), 1–19. https://doi.org/10.3390/biom10091228

Morgan, B. P., Gommerman, J. L., & Ramaglia, V. (2021). An “Outside-In” and “Inside-Out” Consideration of Complement in the Multiple Sclerosis Brain: Lessons From Development and Neurodegenerative Diseases. *Frontiers in Cellular Neuroscience*, *14*(January), 1–22. https://doi.org/10.3389/fncel.2020.600656

Moulson, A. J., Squair, J. W., Franklin, R. J. M., Tetzlaff, W., & Assinck, P. (2021). Diversity of Reactive Astrogliosis in CNS Pathology: Heterogeneity or Plasticity? *Frontiers in Cellular Neuroscience*, *15*(July). https://doi.org/10.3389/fncel.2021.703810

MSIF. (2020). Atlas of MS 3rd edition. *The Multiple Sclerosis International Federation (MSIF), 2020*, (09), 1–37.

Nait-Oumesmar, B., Picard-Riera, N., Kerninon, C., Decker, L., Seilhean, D., nter Hö glinger, G. U., Baron-Van Evercooren, A. (2007). Activation of the subventricular zone in multiple sclerosis: Evidence for early glial progenitors. *Proceedings of the National Academy of Sciences of the United States of America*, *104*(11), 4694–4699. Retrieved from www.pnas.orgcgidoi10.1073pnas.0606835104

Nait-Oumesmar, Brahim. Decker, Laurence. Lachapelle, Francois. Avellana-Adalid, Virginia. Bcahelin, Corinne. Baron, Baron-Van Evercooren, A. (1999). Progenitor cells of the adult mouse subventricular zone proliferate, migrate and di?erentiate

into oligodendrocytes after demyelination. European Journal of Neuroscience, 11(12), 4357–4366. https://doi.org/10.1002/9781119631729.ch5

Nakatani, H., Martin, E., Hassani, H., Clavairoly, A., Maire, C. L., Viadieu, A., Parras, C. (2013). Ascl1/Mash1 promotes brain oligodendrogenesis during myelination and remyelination. Journal of Neuroscience, 33(23), 9752–9768. https://doi.org/10.1523/JNEUROSCI.0805-13.2013

Nam, Y., Kim, J. H., Seo, M., Kim, J. H., Jin, M., Jeon, S., Suk, K. (2014). Lipocalin-2 protein deficiency ameliorates experimental autoimmune encephalomyelitis: The pathogenic role of lipocalin-2 in the central nervous system and peripheral lymphoid tissues. *Journal of Biological Chemistry*, *289*(24), 16773–16789. https://doi.org/10.1074/jbc.M113.542282

Naray-Fejes-Tóth, A., Rosenkranz, B., Frölich, J. C., & Fejes-Tóth, G. (1988). Glucocorticoid effect on arachidonic acid metabolism in vivo. Journal of Steroid Biochemistry, 30(1–6), 155–159. https://doi.org/10.1016/0022-4731(88)90088-X

Nash, B., Ioannidou, K., & Barnett, S. C. (2011). Astrocyte phenotypes and their relationship to myelination. *Journal of Anatomy*, *219*(1), 44–52. https://doi.org/10.1111/j.1469-7580.2010.01330.x

Nash, B., Thomson, C. E., Linington, C., Arthur, A. T., McClure, J. D., Mcbride, M. W., & Barnett, S. C. (2010). Functional duality of astrocytes in myelination. *Journal of Neuroscience*, *31*(37), 13028–13038. https://doi.org/10.1523/JNEUROSCI.1449-11.2011

Nave, K. A. (2010, November 11). Myelination and support of axonal integrity by glia. *Nature*, Vol. 468, pp. 244–252. https://doi.org/10.1038/nature09614

Neumann, B., Segel, M., Chalut, K. J., & Franklin, R. J. M. (2019). Remyelination and ageing: Reversing the ravages of time. *Multiple Sclerosis Journal*, Vol. 25, pp. 1835–1841. https://doi.org/10.1177/1352458519884006

Nomura, T., Bando, Y., Nakazawa, H., Kanemoto, S., & Yoshida, S. (2019). Pathological changes in mice with long term cuprizone administration. *Neurochemistry International*, *126*(June), 229–238. https://doi.org/10.1016/j.neuint.2019.03.018

Ofengeim, D., Ito, Y., Trapp, B., Yuan, J., Najafov, A., Zhang, Y., Amin, P. (2016). Activation of Necroptosis in Multiple Sclerosis Article Activation of Necroptosis in Multiple Sclerosis. CellReports, 10(11), 1836–1849. https://doi.org/10.1016/j.celrep.2015.02.051.Activation

Ogier, C., Creidy, R., Boucraut, J., Soloway, P. D., Khrestchatisky, M., & Rivera, S. (2005). Astrocyte reactivity to Fas activation is attenuated in TIMP-1 deficient mice. An in vitro study. *BMC Neuroscience*, *6*, 1–12. https://doi.org/10.1186/1471-2202-6-68

Okazaki, R., Doi, T., Hayakawa, K., Morioka, K., Imamura, O., Takishima, K., Ogata, T. (2016). The crucial role of Erk2 in demyelinating inflammation in the central nervous system. Journal of Neuroinflammation, 13(1), 1–15. https://doi.org/10.1186/s12974-016-0690-8

Oliveira-Junior, M. S., Schira-Heinen, J., Reiche, J., Han, S., de Amorim, V. C. M., Lewen, I., Gruchot, J., Göttle, P., Akkermann, R., Azim, K., Küry, P. (2022). Myelin repair is fostered by the corticosteroid medrysone specifically acting on astroglial subpopulations. *EBioMedicine*, (accepted for publication on July 22, 2022)

Onwuha-Ekpete, L. C., Tokmina-Roszyk, D., & Fields, G. B. (2017). Selective inhibition of matrix metalloproteinase-9 in CD4+ T-cells reduces clinical severity in a murine model of Multiple Sclerosis. *The Journal of Immunology*, *198*(1 Supplement), 219.8-219.8. Retrieved from https://www.jimmunol.org/content/198/1_Supplement/219.8

Ortega, F., Berninger, B., & Costa, M. R. (2013.1). Primary culture and live imaging of adult neural stem cells and their progeny. *Methods in Molecular Biology*, *1052*, 1–11. https://doi.org/10.1007/7651-2013-22

Ortega, F., Gascón, S., Masserdotti, G., Deshpande, A., Simon, C., Fischer, J., Berninger, B. (2013.2). Oligodendrogliogenic and neurogenic adult subependymal zone neural stem cells constitute distinct lineages and exhibit differential responsiveness to Wnt signalling. *Nature Cell Biology*, *15*(6), 602–613. https://doi.org/10.1038/ncb2736

Orthmann-Murphy, J. L., Abrams, C. K., & Scherer, S. S. (2008). Gap junctions couple astrocytes and oligodendrocytes. *Journal of Molecular Neuroscience*, *35*(1), 101–116. https://doi.org/10.1007/s12031-007-9027-5

Orthmann-Murphy, J., Call, C. L., Molina-Castro, G. C., Hsieh, Y. C., Rasband, M. N., Calabresi, P. A., & Bergles, D. E. (2020). Remyelination alters the pattern of myelin in the cerebral cortex. *ELife*, *9*, 1–61. https://doi.org/10.7554/eLife.56621

Oveland, E., Ahmad, I., Lereim, R. R., Kroksveen, A. C., Barsnes, H., Guldbrandsen, A., Wergeland, S. (2021). Cuprizone and EAE mouse frontal cortex proteomics revealed proteins altered in multiple sclerosis. *Scientific Reports*, *11*(1), 1–16. https://doi.org/10.1038/s41598-021-86191-5

Palumbo, S., Toscano, C. D., Parente, L., Weigert, R., & Bosetti, F. (2011). Time-dependent changes in the brain arachidonic acid cascade during cuprizone-induced demyelination and remyelination. Prostaglandins Leukotrienes and Essential Fatty Acids, 85(1), 29–35. https://doi.org/10.1016/j.plefa.2011.04.001

Pandur, E., Pap, R., Varga, E., Jánosa, G., Komoly, S., Fórizs, J., & Sipos, K. (2019). Relationship of iron metabolism and short-term cuprizone treatment of c57bl/6 mice. *International Journal of Molecular Sciences*, *20*(9). https://doi.org/10.3390/ijms20092257

Panman, L., Andersson, E., Alekseenko, Z., Hedlund, E., Kee, N., Mong, J., Perlmann, T. (2011). Transcription factor-induced lineage selection of stem-cell-derived neural progenitor cells. *Cell Stem Cell*, *8*(6), 663–675. https://doi.org/10.1016/j.stem.2011.04.001

Parks, W. C., Wilson, C. L., & López-Boado, Y. S. (2004). Matrix metalloproteinases as modulators of inflammation and innate immunity. *Nature Reviews Immunology*, *4*(8), 617–629. https://doi.org/10.1038/nri1418

Parras, C. M., Galli, R., Britz, O., Soares, S., Galichet, C., Battiste, J., Guillemot, F. (2004). Mash1 specifies neurons and oligodendrocytes in the postnatal brain. *EMBO Journal*, *23*(22), 4495–4505. https://doi.org/10.1038/sj.emboj.7600447

Parras, C. M., Hunt, C., Sugimori, M., Nakafuku, M., Rowitch, D., & Guillemot, F. (2007). The proneural gene Mash1 specifies an early population of telencephalic oligodendrocytes. Journal of Neuroscience, 27(16), 4233–4242. https://doi.org/10.1523/JNEUROSCI.0126-07.2007

Pastrana, E., Cheng, L.-C., & Doetsch, F. (2009). Simultaneous prospective purification of adult subventricular zone neural stem cells and their progeny. *Proceedings of the National Academy of Sciences of the United States of America*, *106*(15), 6387–6392. https://doi.org/10.173/pnas.0810407106

Petkovic, F., Campbel, I. L., Gonzalez, B., & Castellano, B. (2017). Reduced curpizone-induced cerebellar demyelination in mice with astrocyte-tarfeted production of IL-6 is associated with chronically activated, but less responsive microglia. *Journal of Neuroimmunology*, *15*, 310–397. https://doi.org/10.1016/j.neuroim.2017.07.003

Petkovic, F., Campbell, L. L., Gonzalez, B., & Castellano, B. (2016). Astrocyte-targeted production of interleukin-6 reduces astroglial and microglial activation in the cuprizone demyelination model: implications for myelin clearance and oligodendrocyte maturation. *Glia*, *64*(12), 2101–2119. https://doi.org/10.1002/glia.23043

Petryniak, Magdalena A. Potter, Gregory B. Rowitch, David H. Rubenstein, J. L. R. (2007). Dlx1 and Dlx2 control neuronal versus oligodendroglial cell fate acquisition in the developing forebrain. Neuron, 55(3), 417–433.

Piraino, P. S., Yednock, T. A., Messersmith, E. K., Pleiss, M. A., Freedman, S. B., Hammond, R. R., & Karlik, S. J. (2005). Spontaneous remyelination following prolonged inhibition of α4 integrin in chronic EAE. *Journal of Neuroimmunology*, *167*(1–2), 53–63. https://doi.org/10.1016/j.jneuroim.2005.06.018

Platel, J. C., & Bordey, A. (2016). The multifaceted subventricular zone astrocyte: From a metabolic and pro-neurogenic role to acting as a neural stem cell. *Neuroscience*, Vol. 323, pp. 20–28. https://doi.org/10.1016/j.neuroscience.2015.10.053

Platel, J. C., Angelova, A., Bugeon, S., Wallace, J., Ganay, T., Chudotvorova, I., Cremer, H. (2019). Neuronal integration in the adult mouse olfactory bulb is a non-selective addition process. *ELife*, *8*, 1–21. https://doi.org/10.7554/eLife.44830

Platel, J.-C., Gordon, V., Heintz, T., & Bordey, A. (2008). GFAP-GFP neural progenitors are antigenically homogeneous and anchored in their enclosed mosaic niche. *Glia*, *57*(1), 66–78. https://doi.org/10.1002/glia.20735

Pluchino, S., Muzio, L., Imitola, J., Deleidi, M., Alfaro-Cervello, C., Salani, G., Martino, G. (2008). Persistent inflammation alters the function of the endogenous brain stem cell compartment. Brain, 131(10), 2564–2578. https://doi.org/10.1093/brain/awn198

Pluchino, S., Quattrini, A., Brambilla, E., Gritti, A., Salani, G., Dina, G., Martino, G. (2003). Injection of adult neurospheres induces recovery in a chronic model of multiple sclerosis. Nature, 422(6933), 688–694. https://doi.org/10.1038/nature01552

Polito, A., & Reynolds, R. (2005). NG2-expressing cells as oligodendrocyte progenitors in the normal and demyelinated adult central nervous system. *Journal of Anatomy*, *207*, 707–716.

Porcu, G., Serone, E., De Nardis, V., Di Giandomenico, D., Lucisano, G., Scardapane, M., Ragnini-Wilson, A. (2015). Clobetasol and halcinonide act as smoothened agonists to promote myelin gene expression and RxRγ receptor activation. PLoS ONE, 10(12), 1–22. https://doi.org/10.1371/journal.pone.0144550

Pous, L., Deshpande, S. S., Nath, S., Mezey, S., Malik, S. C., Schildge, S., Schachtrup, C. (2020). Fibrinogen induces neural stem cell differentiation into astrocytes in the subventricular zone via BMP signaling. *Nature Communications*, *11*(1). https://doi.org/10.1038/s41467-020-14466-y

Praet, J., Guglielmetti, C., Berneman, Z., Van der Linden, A., & Ponsaerts, P. (2014). Cellular and molecular neuropathology of the cuprizone mouse model: Clinical relevance for multiple sclerosis. Neuroscience and Biobehavioral Reviews, 47(November), 485–505. https://doi.org/10.1016/j.neubiorev.2014.10.004

Pushpakom, S., Iorio, F., Eyers, P. A., Escott, K. J., Hopper, S., Wells, A., Pirmohamed, M. (2018). Drug repurposing: Progress, challenges and recommendations. *Nature Reviews Drug Discovery*, *18*(1), 41–58. https://doi.org/10.1038/nrd.2018.168

Qiang, Li. Xufang, Ru. Yang, Yang. Hengli, Zhao. Jie, Qu. Weixiang, Chen. Pengyu, Pan. Huaizhen, Ruan. Chaojun, Li3. Hua, Feng. Yujie, C. (2020). Inactivation of LCN2/EGR1 Promotes Oligodendrocyte Progenitor Cell Differentiation and Remyelination after White Matter Injury Running. *BioRxiv*, 275. https://doi.org/10.35393/1730-006-002-014

Rakic, S., & Zecevic, N. (2003). Early oligodendrocyte progenitor cells in the human fetal telencephalon. Glia, 41(2), 117–127. https://doi.org/10.1002/glia.10140

Ramon y Cajal, S. (1909). *Histologie du Systeme Nerveux De L'Homme et Des Vertebres*. *563*, 1–2092.

Rash, B. G., Duque, A., Morozov, Y. M., Arellano, J. I., Micali, N., & Rakic, P. (2019). Gliogenesis in the outer subventricular zone promotes enlargement and gyrification of the primate cerebrum. *Proceedings of the National Academy of Sciences of the United States of America*, *116*(14), 7089–7094. https://doi.org/10.1073/pnas.1822169116

Rawji, K. S., Gonzalez Martinez, G. A., Sharma, A., & Franklin, R. J. M. (2020). The Role of Astrocytes in Remyelination. *Trends in Neurosciences*, *43*(8), 596–607. https://doi.org/10.1016/j.tins.2020.05.006

Reiche, L., Göttle, P., Lane, L., Duek, P., Park, M., Azim, K., Küry, P. (2021). C21orf91 Regulates Oligodendroglial Precursor Cell Fate—A Switch in the Glial Lineage? *Frontiers in Cellular Neuroscience*, *15*(March), 1–18. https://doi.org/10.3389/fncel.2021.653075

Rempe, R. G., Hartz, A. M. S., & Bauer, B. (2016). Matrix metalloproteinases in the brain and blood-brain barrier: Versatile breakers and makers. *Journal of Cerebral Blood Flow and Metabolism*, *36*(9), 1481–1507. https://doi.org/10.1177/0271678X16655551

Resztak, J.A. et al. (2022) 'Genetic control of the dynamic transcriptional response to immune stimuli and glucocorticoids at single cell resolution', bioRxiv, p. 2021.09.30.462672..

Rodgers, K. R., Lin, Y., Langan, T. J., Iwakura, Y., & Chou, R. C. (2020). Innate Immune Functions of Astrocytes are Dependent Upon Tumor Necrosis Factor-Alpha. *Scientific Reports*, *10*(1). https://doi.org/10.1038/s41598-020-63766-2

Rosenbluth, J., Nave, K.-A., Mierzwa, A., & Schiff, R. (2006). Subtle myelin defects in PLP-null mice. *Glia*, *15*(3), 172–182. https://doi.org/10.1002/glia.20370

Rus, H., Cudrici, C., David, S., & Niculescu, F. (2006). The complement system in central nervous system diseases. *Autoimmunity*, *39*(5), 395–402. https://doi.org/10.1080/08916930600739605

Sadeghian, M., Mastrolia, V., Rezaei Haddad, A., Mosley, A., Mullali, G., Schiza, D., Smith, K. J. (2016). Mitochondrial dysfunction is an important cause of neurological deficits in an inflammatory model of multiple sclerosis. Scientific Reports, 6(August), 1–14. https://doi.org/10.1038/srep33249

Safaeinejad, F., Bahrami, S., Redl, H., & Niknejad, H. (2018). Inhibition of inflammation, suppression of matrix metalloproteinases, induction of neurogenesis, and antioxidant property make Bryostatin-1 a Therapeutic choice for multiple sclerosis. *Frontiers in Pharmacology*, *9*(JUN), 1–6. https://doi.org/10.3389/fphar.2018.00625

Saha, P., Sarkar, S., Paidi, R. K., & Biswas, S. C. (2020). TIMP-1: A key cytokine released from activated astrocytes protects neurons and ameliorates cognitive behaviours in a rodent model of Alzheimer's disease. Brain, Behavior, and Immunity, 87(July), 804–819. https://doi.org/10.1016/j.bbi.2020.03.014

Salas, I. H., Burgado, J., & Allen, N. J. (2020). Glia: victims or villains of the aging brain?. Neurobiology of Disease, 143, 105008. https://doi.org/10.1016/j.nbd.2020.105008

Salic, A., and Mitchison, T. J. (2008). A chemical method for fast and sensitive detection ofDNA synthesis in vivo. Proc. Natl. Acad. Sci. US A. 105, 2415–2420. doi:10.1073/pnas.072168105

Samper-Agrelo, I., Schira-Heinen, J., Beyer, F., Groh, J., Bütermann, C., Estrada, V., Küry, P. (2020). Secretome analysis of mesenchymal stem cell factors fostering oligodendroglial differentiation of neural stem cells in vivo. International Journal of Molecular Sciences, 21(12), 1–25. https://doi.org/10.3390/ijms21124350

Sánchez-González, R., Bribián, A., & López-Mascaraque, L. (2020). Cell Fate Potential of NG2 Progenitors. *Scientific Reports*, *10*(1). https://doi.org/10.1038/s41598-020-66753-9

Sanmarco, L. M., Wheeler, M. A., Gutiérrez-Vázquez, C., Polonio, C. M., Linnerbauer, M., Pinho-Ribeiro, F. A., Quintana, F. J. (2021). Gut-licensed IFNγ+ NK cells drive LAMP1+TRAIL+ anti-inflammatory astrocytes. *Nature*, *590*(7846), 473–479. https://doi.org/10.1038/s41586-020-03116-4

Schartz, N. D., & Tenner, A. J. (2020). The good, the bad, and the opportunities of the complement system in neurodegenerative disease. *Journal of Neuroinflammation*, *17*(1), 1–25. https://doi.org/10.1186/s12974-020-02024-8

Schindelin, J., Arganda-Carreras, I., Frise, E., Kaynig, V., Longair, M., Pietzsch, T., Cardona, A. (2012). Fiji: An open-source platform for biological-image analysis. *Nature Methods*, *9*(7), 676–682. https://doi.org/10.1038/nmeth.2019

Schira-Heinen, Jessica.Samper Agrelo, Iria. Estrada, Veronica. Küry, P. (2021). Functional in vivo assessment of stem cell-secreted pro- oligodendroglial factors. *Neural Regeneration Research*, *17*(x), 1–3.

Schirmer, L., Schafer, D. P., Bartels, T., Rowitch, D. H., & Calabresi, P. A. (2021). Diversity and Function of Glial Cell Types in Multiple Sclerosis. *Trends in Immunology*, *42*(3), 228–247. https://doi.org/10.1016/j.it.2021.01.005

Schiweck, J., Eickholt, B. J., & Murk, K. (2018). Important shapeshifter: Mechanisms allowing astrocytes to respond to the changing nervous system during development, injury and disease. *Frontiers in Cellular Neuroscience*, Vol. 12. https://doi.org/10.3389/fncel.2018.00261

Siotto, M., Filippi, M. M., Simonelli, I., Landi, D., Ghazaryan, A., Vollaro, S., Vernieri, F. (2019). Oxidative stress related to iron metabolism in relapsing remitting

multiple sclerosis patients with low disability. *Frontiers in Neuroscience*, *13*(FEB), 1–9. https://doi.org/10.3389/fnins.2019.00086

Skripuletz, T., Hackstette, D., Bauer, K., Gudi, V., Pul, R., Voss, E., Stangel, M. (2013). Astrocytes regulate myelin clearance through recruitment of microglia during cuprizone-induced demyelination. *Brain*, *136*(1), 147–167. https://doi.org/10.1093/brain/aws262

Sofroniew, M. V. (2020). Astrocyte Reactivity: Subtypes, States, and Functions in CNS Innate Immunity. *Trends in Immunology*, *41*(9), 758–770. https://doi.org/10.1016/j.it.2020.07.004

Sofroniew, M. V., & Vinters, H. V. (2010). Astrocytes: Biology and pathology. *Acta Neuropathologica*, *119*(1), 7–35. https://doi.org/10.1007/s00401-009-0619-8

Song, J., Wu, C., Korpos, E., Zhang, X., Agrawal, S. M., Wang, Y., Sorokin, L. (2015). Focal MMP-2 and MMP-9 Activity at the Blood-Brain Barrier Promotes Chemokine-Induced Leukocyte Migration. *Cell Reports*, *10*(7), 1040–1054. https://doi.org/10.1016/j.celrep.2015.01.037

Spaeth, G. L. (1966). Hydroxymethylprogesterone: An Anti-Inflammatory Steroid without Apparent Effect on Intraocular Pressure. *Archives of Ophthalmology*, *75*(6), 783–787. https://doi.org/10.1001/archopht.1966.00970050785014

Stadelmann, C., Timmler, S., Barrantes-Freer, A., & Simons, M. (2018). Myelin in the central nervous system: Structure, function, and pathology. *Physiological Reviews*, *99*(3), 1381–1431. https://doi.org/10.1152/physrev.00031.2018

Steelman, A. J., Thompson, J. P., & Li, J. (2012). Demyelination and remyelination in anatomically distinct regions of the corpus callosum following cuprizone intoxication. *Neuroscience Research*, *72*(1), 32–42. https://doi.org/10.1016/j.neures.2011.10.002

Steelman, A. J., Zhou, Y., Koito, H., Kim, S. J., Payne, H. R., Lu, Q. R., & Li, J. (2016). Activation of oligodendroglial Stat3 is required for efficient remyelination. *Neurobiology of Disease*, *91*, 336–346. https://doi.org/10.1016/j.nbd.2016.03.023

Stidworthy, M. F., Genoud, S., Suter, U., Mantei, N., & Frankiln, R. J. M. (2006). Quantifying the Early Stages of Remyelination Following Curpizone-induced Demyelination. *Brain Pathology*, *13*(3), 329–338. https://doi.org/j.1750-3639.2003.tb00032.x

Susuki, K. (2013). Node of ranvier disruption as a cause of neurological diseases. *ASN Neuro*, *5*(3), 209–219. https://doi.org/10.1042/AN20130025

Tabata, H. (2015). Diverse subtypes of astrocytes and their development during corticogenesis. *Frontiers in Neuroscience*, *9*(APR), 1–7. https://doi.org/10.3389/fnins.2015.00114

Tanner, D. C., Cherry, J. D., & Mayer-Proschel, M. (2011). Oligodendrocyte Progenitors Reversibly Exit The Cell Cycle And Give Rise To Astrocytes In Response To Interferon-γ. *Journal of Neuroscience*, *31*(16), 6235–6246. https://doi.org/10.1523/JNEUROSCI.5905-10.2011

Taraboletti, A., Walker, T., Avila, R., Huang, H., Caporoso, J., Leeper, T. C., States, U. (2017). Cuprizone Intoxication Induces Intrinsic Alterations in Oligodendrocyte Metabolism Independent of Copper Chelation. *Biochemistry*, *56*(10), 1518–1528. https://doi.org/10.1021/acs.biochem.6b01072.Further

Tassoni, A., Farkhondeh, V., Itoh, Y., Itoh, N., Sofroniew, M. V., & Voskuhl, R. R. (2019). The astrocyte transcriptome in EAE optic neuritis shows complement activation and reveals a sex difference in astrocytic C3 expression. *Scientific Reports*, *9*(1). https://doi.org/10.1038/s41598-019-46232-6

Tatomir, A., Talpos-caia, A., Anselmo, F., Kruszewski, A. M., Boodhoo, D., Rus, V., & Rus, H. (2019). The complement system as a biomarker of disease activity and response to treatment in multiple sclerosis. *Immunology Research*, *65*(6), 1103–1109. https://doi.org/10.1007/s12026-017-8961-8.The

Tegla, C. A. (2009). Neuroprotective effects of the complement terminal pathway. *Journal of Neuroimmunology*, *213*(1), 1–28.

Ten-Bosch, G. J. A., Bolk, J., 't Hart, B. A., & Laman, J. D. (2021). Multiple sclerosis is linked to MAPKERK overactivity in microglia. Journal of Molecular Medicine, 99(8), 1033–1042. https://doi.org/10.1007/s00109-021-02080-4

Tognatta, R., Karl, M. T., Fyffe-Maricich, S. L., Popratiloff, A., Garrison, E. D., Schenck, J. K., Miller, R. H. (2020). Astrocytes Are Required for Oligodendrocyte Survival and Maintenance of Myelin Compaction and Integrity. *Frontiers in Cellular Neuroscience*, *14*. https://doi.org/10.3389/fncel.2020.00074

Toomey, L. M., Papini, M., Lins, B., Wright, A. J., Warnock, A., McGonigle, T., Fitzgerald, M. (2021). Cuprizone feed formulation influences the extent of demyelinating disease pathology. *Scientific Reports*, *11*(1), 1–16. https://doi.org/10.1038/s41598-021-01963-3

Trentini, A., Manfrinato, M. C., Castellazzi, M., Tamborino, C., Roversi, G., Volta, C. A., Monaldini, C. (2015). TIMP-1 resistant matrix metalloproteinase-9 is the predominant serum active isoform associated with MRI activity in patients with multiple sclerosis. *Multiple Sclerosis Journal*, *21*(9), 1121–1130. https://doi.org/10.1177/1352458514560925

Trindade, P., Loiola, E. C., Gasparotto, J., Ribeiro, C. T., Cardozo, P. L., Devalle, S., Rehen, S. K. (2019). Short and long TNF-alpha exposure recapitulates canonical astrogliosis events in human induced pluripotent stem cell-derived astrocytes. *BioRxiv Preprint*.

Tripathi, R. B., Rivers, L. E., Young, K. M., Jamen, F., & Richardson, W. D. (2010). NG2 glia generate new oligodendrocytes but few astrocytes in a murine

experimental autoimmune encephalomyelitis model of demyelinating disease. *Journal of Neuroscience*, *30*(48), 16383–16390. https://doi.org/10.1523/JNEUROSCI.3411-10.2010

Valério-Gomes, B., Guimarães, D. M., Szczupak, D., & Lent, R. (2018). The absolute number of oligodendrocytes in the adult mouse brain. *Frontiers in Neuroanatomy*, *12*. https://doi.org/10.3389/fnana.2018.00090

Vancamp, P., Gothié, J. D., Luongo, C., Sébillot, A., Le Blay, K., Butruille, L., Remaud, S. (2019). Gender-specific effects of transthyretin on neural stem cell fate in the subventricular zone of the adult mouse. Scientific Reports, 9(1), 1–14. https://doi.org/10.1038/s41598-019-56156-w

Vasile, F., Dossi, E., & Rouach, N. (2017). Human astrocytes: structure and functions in the healthy brain. *Brain Structure and Function*, *222*(5), 2017–2029. https://doi.org/10.1007/s00429-017-1383-5

Vega-Riquer, J. M., Mendez-Victoriano, G., Morales-Luckie, R. A., & Gonzalez-Perez, O. (2019). Five Decades of Cuprizone, an Updated Model to Replicate Demyelinating Diseases. *Current Neuropharmacology*, *17*(2), 129–141. https://doi.org/10.2174/1570159x15666170717120343

Vernerey, J., Macchi, M., Magalon, K., Cayre, M., & Durbec, P. (2013). Ciliary neurotrophic factor controls progenitor migration during remyelination in the adult rodent brain. *Journal of Neuroscience*, *33*(7), 3240–3250. https://doi.org/10.1523/JNEUROSCI.2579-12.2013

Vismara, I., Papa, S., Veneruso, V., Mauri, E., & Mariani, A. (2020). Selective Modulation of A1 Astrocytes by Drug-Loaded Nano-. *ACS Nano*, (1), 1–9.

von Bartheld, Chrstopher S. Bahney, Jami. Herculano-Houzel, S. (2016). The Search for True Numbers of Neurons and Glial Cells in the Human Brain: A Review of 150 Years of Cell Counting. *Journal of Computational Neurology*, *524*(198), 3865–3895. https://doi.org/10.1002/cne.24040.The

Voronova, A., Fischer, A., Ryan, T., Al Madhoun, A., & Skerjanc, I. S. (2011). Ascl1/Mash1 is a novel target of Gli2 during Gli2-induced neurogenesis in P19 EC cells. *PLoS ONE*, *6*(4). https://doi.org/10.1371/journal.pone.0019174

Vukojicic, A., Delestrée, N., Fletcher, E. V., Pagiazitis, J. G., Sankaranarayanan, S., Yednock, T. A., … Mentis, G. Z. (2019). The Classical Complement Pathway Mediates Microglia-Dependent Remodeling of Spinal Motor Circuits during Development and in SMA. *Cell Reports*, *29*(10), 3087-3100.e7. https://doi.org/10.1016/j.celrep.2019.11.013

Wan, T., Zhu, W., Zhao, Y., Zhang, X., Ye, R., Zuo, M., Liu, X. (2022). Astrocytic phagocytosis contributes to demyelination after focal cortical ischemia in mice. *Nature Communications*, *13*(1). https://doi.org/10.1038/s41467-022-28777-9

Wang, B., Wu, L., Chen, J., Dong, L., Chen, C., Wen, Z., Wang, D. W. (2021). Metabolism pathways of arachidonic acids: mechanisms and potential therapeutic targets. *Signal Transduction and Targeted Therapy*, *6*(1). https://doi.org/10.1038/s41392-020-00443-w

Wang, C., Barnett, M. H., Yiannikas, C., Barton, J., Parratt, J., You, Y.,Klistorner, A. (2019). Lesion activity and chronic demyelination are the major determinants of brain atrophy in MS. *Neurology: Neuroimmunology and NeuroInflammation*, *6*(5), 1–10. https://doi.org/10.1212/NXI.0000000000000593

Wang, K., Ye, L., Lu, H., Chen, H., Zhang, Y., Huang, Y., & Zheng, J. C. (2017). TNF-α promotes extracellular vesicle release in mouse astrocytes through glutaminase. *Journal of Neuroinflammation*, *14*(1). https://doi.org/10.1186/s12974-017-0853-2

Wang, M., Liu, F., Fang, B., Huo, Q., & Yang, Y. (2021). Proteome-scale profiling reveals MAFF and MAFG as two novel key transcription factors involved in palmitic acid-induced umbilical vein endothelial cell apoptosis. *BMC Cardiovascular Disorders*, *21*(1), 1–13. https://doi.org/10.1186/s12872-021-02246-5

Wang, X., Huang, S., Jiang, Y., Liu, Y., Song, T., Li, D., & Yang, L. (2018). Reactive astrocytes increase the expression of P-gp and Mrpl via TNF-α and NF-κB signaling. *Molecular Medicine Reports*, *17*(1), 1198–1204. https://doi.org/10.3892/mmr.2017.7939

Waubant, E., Goodkin, D. E., Gee, L., Bacchetti, P., Sloan, R., Stewart, T., Miller, K. (1999). Serum MMP-9 and TIMP-1 levels are related to MRI activity in relapsing multiple sclerosis. *Neurology*, *53*(7), 1397–1401. https://doi.org/10.1212/wnl.53.7.1397

Wei, W., Ma, D., Li, L., & Zhang, L. (2021). Progress in the Application of Drugs for the Treatment of Multiple Sclerosis. *Frontiers in Pharmacology*, *12*(July), 1–13. https://doi.org/10.3389/fphar.2021.724718

Wheeler, M. A., Jaronen, M., Covacu, R., Zandee, S. E. J., Scalisi, G., Rothhammer, V., Quintana, F. J. (2019). Environmental Control of Astrocyte Pathogenic Activities in CNS Inflammation. *Cell*, *176*(3), 581-596.e18. https://doi.org/10.1016/j.cell.2018.12.012

Wheeler, Michael A. Clark, Iain C. Tjon, Emily C. Zhaorong Li., Stephanie E. J. Zandee., Charles P. Couturier., Brianna R. Watson., Giulia Scalisi., Srah Alkwai., Veit Rothhammet., Assaf Rotem., John A. Heyman., Shraven Thaploo., Lilian M. Sanmarco., J, F. J. Q. (2020). MAFG-driven astrocytes promote CNS inflammation. *Nature*, *176*(3), 139–148. https://doi.org/10.1038/s41586-020-1999-0.MAFG-driven

Williams, D. M. (2018). Clinical pharmacology of corticosteroids. *Respiratory Care*, *63*(6), 655–670. https://doi.org/10.4187/respcare.06314

Wolswijk, G., & Balesar, R. (2003). Changes in the ’expression and localization of the paranodal protein Caspr on axons in chronic multiple sclerosis. *Brain*, *126*(7), 1638–1649. https://doi.org/10.1093/brain/awg151

Wu, G. F., & Alvarez, E. (2011). The Immunopathophysiology of Multiple Sclerosis. *Neurologic Clinics*, *29*(2), 257–278. https://doi.org/10.1016/j.ncl.2010.12.009

Xin, M., Yue, T., Ma, Z., Wu, F. F., Gow, A., & Lu, Q. R. (2005). Myelinogenesis and axonal recognition by oligodendrocytes in brain are uncoupled in Olig1-null mice. *Journal of Neuroscience*, *25*(6), 1354–1365. https://doi.org/10.1523/JNEUROSCI.3034-04.2005

Xin, W., & Chan, J. R. (2020). That Wasn’t a Complement—Too Much C3 in Demyelinating Disease. *Immunity*, *52*(1), 11–13. https://doi.org/10.1016/j.immuni.2019.12.014

Xing, Y. L., Röth, P. T., Stratton, J. A. S., Chuang, B. H. A., Danne, J., Ellis, S. L., Merson, T. D. (2014). Adult neural precursor cells from the subventricular zone contribute significantly to oligodendrocyte regeneration and remyelination. *Journal of Neuroscience*, *34*(42), 14128–14146. https://doi.org/10.1523/JNEUROSCI.3491-13.2014

Xu, J. (2018). New insights into GFAP negative astrocytes in Calbindin D28k immunoreactive astrocytes. *Brain Sciences*, *8*(8). https://doi.org/10.3390/brainsci8080143

Yakovlev P. I., Lecourse A. R. (1967). The myelinogenetic cycles in regional maturation of the brain. In Regional Development of the Brain in Early Life, Minkowsky A., ed (Oxford, Blackwell;), pp. 3–70

Yang, Yongjie. Jackson, R. (2019). Astrocyte identity: Evolutionary perspectives on astrocyte functions and heterogeneity. *Current Opinion in Neurobiology*, *56*(10), 40–46. https://doi.org/10.1016/j.conb.2018.11.006.Astrocyte

Yong, V. W. (2005). Metalloproteinases: Mediators of pathology and regeneration in the CNS. *Nature Reviews Neuroscience*, *6*(12), 931–944. https://doi.org/10.1038/nrn1807

You, Y., Barnett, M. H., Yiannikas, C., Parratt, J., Matthews, J., Graham, S. L., & Klistorner, A. (2020). Chronic demyelination exacerbates neuroaxonal loss in patients with MS with unilateral optic neuritis. *Neurology(R) Neuroimmunology & Neuroinflammation*, *7*(3). https://doi.org/10.1212/NXI.0000000000000700

Yuasa, S. (2001). Development of astrocytes in the mouse embryonic cerebrum tracked by tenascin-C gene expression. *Archives of Histology and Cytology*, Vol. 64, pp. 119–126. https://doi.org/10.1679/aohc.64.119

Zamanian, J. L., Xu, L., Foo, L. C., Nouri, N., Zhou, L., Giffard, R. G., & Barres, B. A. (2012). Genomic analysis of reactive astrogliosis. *Journal of Neuroscience*, *32*(18), 6391–6410. https://doi.org/10.1523/JNEUROSCI.6221-11.2012

Zarruk, J. G., Berard, J. L., Passos dos Santos, R., Kroner, A., Lee, J., Arosio, P., & David, S. (2015). Expression of iron homeostasis proteins in the spinal cord in experimental autoimmune encephalomyelitis and their implications for iron accumulation. *Neurobiology of Disease*, *81*, 93–107. https://doi.org/10.1016/j.nbd.2015.02.001

Zelic, M., Pontarelli, F., Woodworth, L., Zhu, C., Mahan, A., Ren, Y., Ofengeim, D. (2021). RIPK1 activation mediates neuroinflammation and disease progression in multiple sclerosis. Cell Reports, 35(6). https://doi.org/10.1016/j.celrep.2021.109112

Zerlin, M., Milosevic, A., & Goldman, J. E. (2004). Glial progenitors of the neonatal subventricular zone differentiate asynchronously, leading to spatial dispersion of glial clones and to the persistence of immature glia in the adult mammalian CNS. *Developmental Biology*, *270*(1), 200–213. https://doi.org/10.1016/j.ydbio.2004.02.024

Zhan, J., Mann, T., Joost, S., Behrangi, N., Frank, M., & Kipp, M. (2020). The Cuprizone Model: Dos and Do Nots. *Cells*, *9*(4). https://doi.org/10.3390/cells9040843

Zhang, K., Chen, S., Yang, Q., Guo, S., Chen, Q., Liu, Z., Mo, W. (2022). The Oligodendrocyte Transcription Factor 2 OLIG2 regulates transcriptional repression during myelinogenesis in rodents. *Nature Communications*, *13*(1), 1–13. https://doi.org/10.1038/s41467-022-29068-z

Zhang, Liqun. Zhengwen, Ma. Smith, George M. Wen, Xuejun. Pressman, Yelena, Wood, Patrick M. Xu, X.-M. (2009). GDNF-Enhanced Axonal Regeneration and Myelination Following Spinal Cord Injury is Mediated by Primary Effects on Neurons. *Glia*, *57*(11), 1178–1191. https://doi.org/10.1002/glia.20840.GDNF-Enhanced

Zhao, N., Xu, X., Jiang, Y., Gao, J., Wang, F., Xu, X., Xu, G. (2020). Lipocalin-2 may produce damaging effect after cerebral ischemia by inducing astrocytes classical activation. *Journal of Neuroinflammation*, *16*(1), 1–15. https://doi.org/10.1186/s12974-019-1556-7

Zhen, W., Liu, A., Lu, J., Zhang, W., Tattersall, D., & Wang, J. (2017). An Alternative Cuprizone-Induced Demyelination and Remyelination Mouse Model. *ASN Neuro*, *9*(4). https://doi.org/10.1177/1759091417725174

Zhu, Q., Zhao, X., Zheng, K., Li, H., Huang, H., Zhang, Z., Qiu, M. (2014). Genetic Evidence that Nkx2.2 and Pdgfralfa are major determinants of the timing of oligodendrocyte differentiation in the developing CNS. *The Company of Biologists*, *1*(14), 548–555. https://doi.org/10.1242/dev.095323

Zhuo, L., Sun, B., Zhang, C. L., Fine, A., Chiu, S. Y., & Messing, A. (1997). Live astrocytes visualized by green fluorescent protein in transgenic mice. *Developmental Biology*, *187*(1), 36–42. https://doi.org/10.1006/dbio.1997.8601

Zuo, H., Wood, W. M., Sherafat, A., Hill, R. A., Richard Lu, Q., & Nishiyama, A. (2018). Age-dependent decline in fate switch from NG2 cells to astrocytes after Olig2 deletion. *Journal of Neuroscience*, *38*(9), 2359–2371. https://doi.org/10.1523/JNEUROSCI.0712-17.2018

11. Materials and methods

11.1 Ethics statement for animal experiment

Transgenic hGFAP-GFP promoter mice (34) [FVB/N-Tg (GFAPGFP) 14mes/J; Jax stock number: Cat#003257, female and male] provided by Prof. Dr. Nikolaj Klöcker (Medicine Faculty, Heinrich-Heine-University, Düsseldorf, Germany) mice were housed in a pathogen-free facility with 12 hours light/dark cycle and supplied with nutrition and hydration ad libitum. In vivo experiments were performed in adult mice of either sex (from 24 weeks until 36 weeks of age). For primary astrocyte and OPC monocultures 0 or 1 day old neonatal Wistar rats of either sex were utilized. The Review Board for the Care of Animal Subjects of the district Government (LANUV, North-Rhine Westphalia, Germany) approved all research procedures under the following ethic approval numbers: Az.:8102.04.2019.A20 for in vivo experiments, O69/11 and V54/09 for in vitro.

11.2 Primary OPC monoculture

Primary OPC cultures were prepared from P0-1 Wistar rats according to McCarthy and de Vellis (1980) with modifications by our group (Kremer et al., 2009; Göttle et al., 2018; Manousi et al., 2021). Primary OPCs (>97 % pure) were either seeded onto 0.25 mg/ml PDL coated glass coverslips (13 mm) in 24-well plates (for immunocytochemistry; 2.5×104 cells/well) or 0.25 mg/ml PDL coated 24-well plates for qRT-PCR (5×104 cells/well) in high-glucose DMEM-based Sato medium [(5 µg/ml bovine insulin; 50 µg/ml human transferrin; 100 µg/ml bovine serum albumin fraction V (BSA; Thermo Fisher Scientific); 6.2 ng/ml progesterone; 16 µg/ml putrescine, 5 ng/ml, sodium selenite; 400 ng/ml T3 (tri-iodo-thyronine); 400 ng/ml T4 (thyroxin; all Sigma-Aldrich unless stated otherwise); 4 mM L-glutamine; 100 U/ml penicillin/0.1 mg/l streptomycin (both Thermo Fisher Scientific)]. After 1.5 hours, cell differentiation was induced by changing to differentiation medium (Sato medium supplemented with 0.5 % FBS). The medium was exchanged every 3 days. OPCs were supplemented with 0.1 % DMSO or 5 µM medrysone for 72 hours without medium exchange.

11.3 Dorsal SVZ primary culture

Eleven days old postnatal mice brains (FVB-hGFAP GFP reporter) were sectioned in 500 µm slices, using a neonatal brain slicer matrix (Zivic, BSMNS005-1). To localize the d-SVZ, a GFP/RFP fluorescence-dissecting microscope (Tritech research, SMT1-FL-QC) was used. The micro-dissected d-SVZ were disposed in a 24 well plate coated with DMEM was first centrifuged at 300g for 3 minutes in room temperature. The supernatant once removed give place to a 10 % papain solution (P4762, Sigma Aldrich) diluted in DMEM (at 37°C), the tissue was then triturated with a Pasteur glass pipette and incubated for 7 minutes in slow continuous rotation at centrifuged at at 37°C. Pipette the tissue for a few times, and incubate the same cell solution for another 7 minutes at at 37°C. In the same cell solution dilute the DNase (EN0521, Thermo Fisher Scientific) in order to obtain a 2.5 % solution, incubate for 7 minutes at 37°C. Subsequently, pipette the cell pool for a few times and incubate for another 7 minutes at 37°C. Spin the cell solution for 5 minutes at 500g. Remove the supernatant and wash the cell pellet with HBSS and centrifuge the cells for 10 minutes at 500g. The supernatant was discarded and cells were resuspended in DMEM (25 %, Gibco) supplemented with Ham-F12 (25 %, Gibco), 2% B27 (Gibco), HEPES (1 M, Gibco), GlutaMAX high glucose (1 M, Gibco), sodium pyruvate (1 M, Gibco), penicilin/streptomicin 10.000 units (1.25 M, Life Technologies). Cells were diluted in the medium containing either DMSO 0.1% or medrysone 5 µM (6α-methyl-11β-hydroxy-Progesterone; Cayman Chemical, 19533). Subsequently, 25.000 cells/cm2 were plated onto coverslips previously coated with poly-L-ornithine/Laminin (100 µg/mL and 12 µg/mL, respectively; Sigma Aldrich). An additional treatment either with DMSO or medrysone were performed once after seeding. Cells were incubated for five days at 37°C and 5% CO2. This culture model is a modified protocol based on Ortega and colleagues (2013).

11.4 Primary astrocyte monoculture

Primary astrocyte cultures were generated from postnatal rats (Wistar, 0-1 day old) according to McCarthy and de Vellis (1980). Brains were collected from the rat's skull and rinsed on MEM-Hepes medium (Life Technologies; Cat#12360038). The hemispheres were separated and cut off, meninges were removed, and the remaining cortices were cut into small pieces. The tissue was collected in centrifuge tubes

containing 50 ml MEM-Hepes medium and spun down for 1 minute (min) at 2000 rpm. The tissue pellet was then triturated 10 times with a flame-polished Pasteur pipette and passed through a 40 µm cell strainer. Afterwards, the cell suspension was split onto 2 T-75 flasks and 20 ml of astrocyte medium [DMEM-low glucose (Life Technologies, Cat#D6046), 10% fetal calf serum (FCS; Gibco, Cat#10500-064), 2 ml of L-Glutamine (Life Technologies, Cat#G7513), 50 units per ml of penicillin/streptomycin (Life Technologies, Cat#P4333)], each. The medium was changed 3 times a week, and after 10 days, flasks were placed onto a shaker (Excella E24 incubator, 4 h, 180 rpm, 37°C) to remove all microglial and dead cells. Afterwards, remaining astroglia were washed with Dulbecco's phosphate buffer solution (DPBS; Life Technologies, Cat#14190144), and subsequently 5 ml of trypsin was added for 5 min at 37°C and 5% CO2. The reaction was stopped by adding astrocyte medium and the cell suspension collected into a 50 ml Falcon tube. Cells were centrifuged at 1200 rpm for 5 min, and the supernatant was completely aspirated afterwards. Afterwards, magnetic activated cell sorting (MACS; Miltenyi Biotec, Cat#130707677) was performed according to the manufacturer's protocol to purify the culture. Briefly, the cell pellet was resuspended in 80 uL of PB buffer (0.5% Bovine Serum Albumine, Capricorn, Cat#FBS-16A in DPBS) and 20 uL of anti-Glast (ACSA-1; Miltenyi Biotec, Cat#130095822; RRID:AB_10829302) Biotin antibodies were added, well mixed and incubated for 10 min at 2-8°C. 2 ml of cold PB buffer were added and the cells centrifuged at 1200 rpm for 5 min. The supernatant was removed, and cells were resuspended again in 80 µL of the cold PB buffer. 20 µL of anti-Biotin microbeads were added, mixed, and incubated for another 15 min at 2-8°C. The cells were washed with 2 ml cold PB buffer and centrifuged at 1200 rpm for 5 min, the supernatant was removed, and cells were resuspended in 500 µL of buffer. For magnetic separation, the columns were placed in the magnetic field within 500 µL buffer per column. The cell suspension was disposed in it, and the columns were washed 3x with 500 µL of buffer; the magnetically labelled cells were flushed out by pressing the plunger within the column. The cell suspension was centrifuged for 5 min at 1200 rpm, and the supernatant was fully removed; the cells were resuspended in astrocyte medium. Purified astrocytes were cultured for 3 days onto 0.25 mg/ml poly-D-lysine coated (PDL, Sigma-Aldrich; N/A) glass coverslips (13 mm) in 24-well plates (for immunocytochemistry; 6.0×104 cells/well) or 0.25 mg/ml PDL coated 24-well plates for quantitative reverse transcription-polymerase chain reaction (qRT-PCR; 5×104

cells/well). Astrocytes were subjected to 0.1 % Dymethilsulfoxide (DMSO, Sigma Aldrich, Cat#D2650), 30ng/ml tumour necrosis factor-alpha (TNF-α, R&D System, Cat#510RT) or 2.5 µM medrysone (6α-methyl-11β-hydroxy-Progesterone; Cayman Chemical, Cat#19533) for 48 hours.

11.5 Immunocytochemistry

PFA 4% fixed astrocytes, OPCs and d-SVZ cells were incubated with 0.5 % Triton X-100 (Sigma Aldrich) in DPBS for 30 minutes (min), followed by a 60 min incubation with blocking solution containing 10 % normal goat serum (NGS, Gibco, Cat#PCN5000) in DPBS supplemented with 0.5 % Triton X-100 (Sigma Aldrich, Cat#85111) and 10 % BSA. Primary antibodies for astrocytes were diluted in blocking buffer with following concentrations: Chicken anti-glial fibrillary acid protein (GFAP; 1:500, Aves labs, Cat#SKU: GFAP; RRID: AB_2307313); Rabbit anti-complement component 3d (C3d; 1:300, Dako, Cat#A0063; RRID: AB_578478). OPCs were blocked with 10% NGS in DPBS containing 0.1% Triton X-100 at RT for 45 min. Primary antibodies for OPCs were diluted in 10% NGS in DPBS containing 0.01% Triton X-100 with following concentrations: Rat anti-myelin basic protein (MBP; 1:250, Biorad, Cat#aa8287, RRID:AB_32500). D-SVZ cells were blocked with 10% NGS in DPBS containing 0.1% Triton X-100 at RT for 45 min. Primary antibodies for d-SVZ cells were diluted in 10% NGS in DPBS containing 0.01% Triton X-100 with following concentrations: Neural/Glial Antigen 2 (NG2;1:800, Anti-rabbit, NG2, Merck Millipore, RRID:AB11213678), GFAP (1:1000, Anti-mouse, Merck Millipore, Cat#: MAB3402, RRID:AB_94844). Primary antibody incubations were performed overnight. Secondary antibodies were all used at 1:500 [anti-rabbit AlexaFluor 594 (Cat#A32740; RRID: AB_2762824); anti-chicken AlexaFluor 488 (Cat#A32931; RRID: AB_2762843); anti-rat AlexaFluor 488 (Cat#A-11006; RRID: AB_2534074); anti-mouse AlexaFluor 405 (Cat#A-48255; RRID: AB_2890536)]; all from Thermo Fisher Scientific). Nuclear dye, 4',6'-diamino-2-phenylindole (Dapi, Roche diagnostic GmbH) or Topro (TO-PRO^{tm}-3 Iodide, 642/661, Thermo Fisher, Cat#T3605) were applied at a concentration of 5 µM both. Secondary antibodies and dye incubation were performed for 120 min. Coverslips were mounted with Immu-mount (Thermo Fisher Scientific, Cat#1900331) on a glass-slide for subsequently confocal microscopy.

11.6 RNA preparation, cDNA synthesis and quantitative RT-PCR analysis *in vitro*

Total RNA purification from OPC and astrocyte monocultures was done using 350 µL of RLT lysis buffer (Qiagen, Cat#1015762) supplemented with β-mercaptoethanol (1:100, Sigma, Cat#M3148-25). The total RNA was purified by utilizing RNeasy Mini Kit according to manufacturer instructions including DNase digestion. Before quantitative real-time polymerase chain reaction (qPCR), reverse transcription with 250 ng RNA measured using a NanoDropND 1000 was done using the High-Capacity cDNA Reverse Transcription Kit (Thermo Fisher Scientific, Cat# N8080234). Gene expression levels were determined on a 7900HT sequence detection system (Applied Biosystems, Thermo Fisher Scientific), applying SybrGreen universal master mix (Thermo Fisher Scientific, Cat#4367659). Following amplification primers were used: For OPCs rat (rt) Gapdh: fwd- GAA CGG GAA GCT CAC TGG C, rev- GCA TGT CAG ATC CAC AAC GG (as reference gene); rtMyrf: fwd- CCT GTG TCC GTG GTA CTG TG, rev- TCA CAC AGG CGG TAG AAG TG; rtPdgfrα: fwd- AGC TCT CTG TTC CCA ATG CC, rev- GCC TCC ATT CTG GAG CTT GT ; rtSox10: fwd- GTC AGA TGG GAA CCC AGA GCA C, rev- CCC GTA GCC AGC TGC CGA G; rtCNPase: fwd- GCC GTT GTG GTA CTT CTC CA, rev- GCC CGA AAA AGC CAC ACA TT. For astrocytes rtHprt: fwd- CAG TCC CAG CGT CGT GAT TA, rev- ATG GCC TCC CAT CTC CTT CA (as reference gene); rtGfap: fwd- CTG GTG TGG AGT GCC TTC GT, rev- CAC CAA CCA GCT TCC GAG AG; rtSerpina3n: fwd-GGG CAG GTG CTT CGT , rev-AGC GCC TTT GTC TTT CTT TCT G ; rtLcn2: fwd-TCT CAG GCC CAC CAT GAT AGA , rev-CAG GTT GTA GTC AGC AGA GAT GGA; rtSerping1: fwd-GAC AGC CTG CCC TCT GAC A , rev-GCA CTC AAG TAG ACG GCA TTG; rtC3: fwd- CCT TCC CGG GAG CAT CA , rev- GGG CAT ACC CAG CAA TGG ; rtClcf1: fwd- TGG CCC ATT TCT GTA CCA GTC T, rev- GTA GCC AAG AGT TGC CAT GAC A; rtEmp1: fwd- TGG TGG CGG ACG GTA TAG A, rev- TGC CAC TGG TGC AGT TCT TC; rtUgt1a: fwd- CCT GTG CCA TTC CAA AAT GA, rev- CAC TCC GCC CAA GTT CCA; rtC1qa: fwd- CAG AAC CCA CCG ACG TAT GG , rev- TCC TGG TTG GTG AGG ACC TT; rtIL6: fwd- GTT GTG CAA TGG CAA TTC TGA, rev-TCT GAC AGT GCA TCA TCG CTG; rtCd14: fwd- ACA ACA GGC TGG ATA GGA AAC C , rev-TGA CAG GCT CCC CAC TTC AG; rtS100a10: fwd- GCC ATC CCA AAT GGA GCA T , rev- CCC CTG CAA ACC TGT GAA AT (all primers manufactured by Eurofins genomics, Germany).

11.7 *Ex vivo* organotypic cerebellar slice cultures

Organotypic cerebellar slice cultures were prepared from P6 Wistar rats according to Manousi et al. (2021). Briefly, the cerebellum was embedded in 2 % agarose and sectioned into 350 µm thick sections with coronal orientation by using a vibration microtome (Thermo Fisher, Microm HM 650 V). Sections were cultured on inserts (Merck Millipore, Millicell cell culture inserts, 0.4 µm, diameter 30mm) placed above 1mL culture Minimum essential medium (50 %, Gibco), Hank´s balanced salt solution (HBSS, 25 %, Gibco), heat inactivated horse serum (25 %, Gibco), penicillin/streptomycin (1 %, Life Technologies), glutamine (1%, Life Technologies), D-Glucose monohydrate (5 mg/mL, Merck). Slice cultures were incubated at 37°C, 5 % CO2. The first medium change containing either 0.1% DMSO or 5 µM medrysone (6α-methyl-11β-hydroxy Progesterone; Cayman Chemical) was done 2 hours after seeding and slices were incubated for 4 days with no medium change. Afterwards, slices were fixed with 4 % PFA for 15 minutes and stored at 4°C until further processing.

12.8 Immunofluorescence staining of cerebellar slice cultures

Fixed slices were permeabilized with a 0.5 % Triton X-100 overnight followed by blocking using 10 % NGS, 1 % BSA and 1 % Triton X-100 in DPBS overnight. Primary antibodies were diluted in blocking solution with following concentrations: rat anti-MBP (1:300, Biorad, Cat#aa8287, RRID:AB_32500); rabbit anti-Neurofilament (NF, 1:800, Antibodies.com, Cat#A85336, RRID:AB_2748920); rabbit anti-Glial fibrillary acid protein (Gfap, 1:1000, Dako, Cat#Z0334, RRID:AB_10013382). After overnight incubation at 4°C, slices were washed and incubated with secondary antibodies anti-rat AlexaFluor 488 (Cat#A-11006; RRID:AB_2534074), anti-rabbit AlexaFluor 594 (Cat#A32740; RRID:AB_2762824), each at 1:500 diluted in DPBS and DAPI overnight. Stained slices were placed on glass slides and mounted with Immu-mount and evaluated as next.

All sections were analysed using a confocal laser scanning microscope (CLSM) 510 (Zeiss, 510, Carl Zeiss AG, Oberkirchen, Germany). 2 sections per n (n=3) were evaluated per group. Each section were 350 µm thick and cell quantification, were performed in an area of observation of 150 µm in a z-stack orientation. For quantification, areas corresponding to 150 µm of the cerebellum were analysed per

section. Z-stack orientation was performed and at least 80 slices per Z-stack file were taken for each sample.

11.9 Cuprizone diet and drug-treatment procedure

To induce demyelination, 24 weeks old hGFAP-GFP reporter mice were exposed to a regular diet of 0.4 % CPZ (Sniff, Cat#V1534) for nine weeks. During the last five days of CPZ feeding, mice received daily intraperitoneal injections of 500 µL of 0.5 % saline solution or of 5 mg/kg b.w. medrysone [first diluted in DMSO (20 mg/ml stock solution), thereafter diluted using saline to a 7.25 % final concentration of DMSO]. For recovery, mice received normal food for one or three weeks after CPZ feeding (see Figure 1A). Six groups were analysed: (i) control/non-CPZ fed; (ii) 9 weeks CPZ /demyelination; (iii-iv) 9 weeks CPZ, plus saline injection and one or three weeks of normal food (saline 1/3 WPC respectively); (v-vi) 9 weeks CPZ, plus medrysone injection and one or three weeks of normal food (medrysone 1/3 WPC respectively). We measured the body weight of the animals since CPZ is known to have an impact on body weight. Immunohistochemical analysis was performed on rostrocaudal brain sections (bregma: 0.745µm to -1.25µm) analysing the corpus callosum junction (Figure 9C' area 1), adjacent corpus callosum (a-CC; Figure 9C' area 2) and the d-SVZ (Figure 9C' area 3; divided into three micro-domains: 3.1-medial dorsal-SVZ; 3.2-middle d-SVZ and 3.3-dorsal-horn SVZ).

11.10 Tissue processing and immunohistochemistry

For immunohistochemistry mice were transcardially perfused with 20 ml ice-cold DPBS and 20 ml 4 % PFA and dissected brains were post fixed with 4 % PFA 48 hours. Subsequently, brains were incubated with 30 % sucrose for 72 hours, embedded in 2 % agarose and cut into 50µm thick sections using a vibration microtome. Sections were permeabilised by incubation with 0.5 % Triton X-100 for 30 min, blocked with 10 % NGS supplemented with 5 % BSA and 1% Triton for 120 min and incubated with following antibodies overnight at 4°C: rat anti-MBP (rat; 1:300, Biorad, Cat#aa8287, RRID:AB_32500); mouse anti-adenomatous polyposis coli (CC1-APC; 1:300, anti-APC-Ab7-clone CC1, Merck millipore, Cat#OP80, RRID: AB_2057371); rabbit anti-glutathione S-transferase-pi (GSTπ; 1:500, Enzo, Cat#ADIMSA101, RRID: AB_10615079); rabbit anti-oligodendrocyte transcription factor 2 (Olig2; 1:500, Millipore, Cat#AB9610, RRID:AB_570666); mouse anti-

contactin associated protein 1 (Caspr; 1:400, anti-Caspr-paranodin, neuroxin-IV, clone k65/35, Neuromab, Cat#75-001, RRID: AB_10671175); rabbit anti-sex-determining region Y-box 1- (Sox10; 1:100, DCS immunoline, Cat#S1058C002, RRID: AB_2313583); mouse anti-breast carcinoma-amplified sequence 1 (Bcas1/NaBC1; 1:200, Santa Cruz, Cat#sc-136342, RRID:AB_10839529); chicken anti-green fluorescent protein (GFP; 1:500, Aves labs, Cat#GFP1010, RRID:AB_2307313); rabbit anti-human C3d (1:500, Dako, Cat#A0063; RRID: AB_578478); mouse anti-signal transducer and activator of transcription 3 (Stat3; 1:400, Invitrogen, Cat#MA1-13042, RRID: AB_10985240); mouse anti-human S100 calcium-binding protein A10 (S100a10; 1:500, Thermo Fisher Scientific, Cat#MA5-15326, RRID: AB_2092361); rabbit anti-myelin proteolipid protein (PLP; 1:250, kind gift from Dr. Bruce Trapp, Department of Neurosciences, Cleveland Clinic, Ohio, United States; Chen et al., 2015); goat anti-tissue metallopeptidase inhibitor 1 (Timp1; 1:100, R&D System, Cat#AF580, RRID:AB_355455); goat anti-lipocalin-2/NGAL (Lcn2; 1:180, R&D System, Cat#AF1857, RRID:AB_355022); rabbit anti-nitric oxide synthase (iNOS; Abcam, Cat#ab95441, RRID:AB_10688716); rat anti-nuclear factor-erythroid factor 2-related factor 2 (Nrf2; 1:100, Cell Signalling Technology, Cat#14596, RRID:AB_2798531); rabbit anti-transcription factor Mafg (Mafg; 1:100, Genetex, Cat#GTX114541, RRID:AB_10619599); mouse anti-epidermal growth factor receptor (Egfr; 1:500, Anti-Egfr endoplasmic domain, Millipore, Cat#8662051047, RRID: AB_2096607). Rabbit anti- S100 calcium-binding protein beta (S100β, clone EP157BY; 1:500, Abcam, Cat#ab52642, RRID: AB_882426). Mouse anti-Glast astrocyte cell surface antigen-1 (Glast-ACSA1; 1:600; Miltenyl Biotec, Cat#130095822, RRID: AB_10829302). Antigen retrieval disrupts the GFP signal, thus, it was used only for anti-MBP, anti-Olig2 (Figure 10), anti-Sox10 (Figure 10 and Figure 18) and anti-PLP (Figure 18) staining. For this purpose, sections were rinsed in 0.1 M phosphate buffer (pH 7.4) for 3 x 5 min, transferred to 10 mM sodium citrate buffer (pH 8.5) pre-heated to 80°C in a water bath for 20 min and rinsed 0.1 M phosphate buffer (pH 7.4) for 3 x 5 min before blocking and incubation with primary antibodies. After incubation with primary antibodies, sections were washed and incubated with secondary antibodies and Dapi for 120 min. All secondary antibodies were used at a concentration of 1:200 [anti-rat AlexaFluor 647 (Cat#A-11006; RRID:AB_2534074); anti-mouse AlexaFluor 594 (Cat#A32742; RRID:AB_2762825); anti-rabbit AlexaFluor 647 (Cat#A32733; RRID:AB_2633282); anti-chicken AlexaFluor

488 (Cat#A32931; RID:AB_2762843); anti-mouse AlexaFluor 647 (Cat#A32728; RRID:AB_2633277), Donkey anti-goat AlexaFluor 594 (Cat#A32758; RRID:AB_2762828), all Thermo Fisher Scientific]. Subsequently, sections were washed in DPBS and mounted onto glass slides (Superfrost Ultra Plus, Thermo Fisher Scientific).

All sections were analysed using a confocal laser scanning microscope (CLSM) 510 (Zeiss, 510, Carl Zeiss AG, Oberkirchen, Germany). Rostral, middle and coronal sections each 50 µm thick were utilized for cell quantification per n or individual, totalizing an area of observation of 150 µm in a z-stack orientation. For quantification, areas corresponding to 150 µm of the junction corpus callosum and to 100µm of the d-SVZ were analysed per section. Z-stack orientation was performed and at least 35 slices per Z-stack file were taken for each sample. For MBP and PLP fluorescence at the CCJ and a-CC respectively (see Figure 1C') photomicrographs were analysed using the software Fiji-ImageJ version 1.47 (Schindelin et al., 2012) using a virtual line traced around the region of interest (ROI) to determine fluorescence units No normalization of ROIs was performed within the histogram algorithm. By using the ImageJ software, a square of 280 µm x 220 µm (standardised by using the ImageJ dimension rule) was drawn on each picture obtained for MBP and PLP quantification. Moreover, by using the histogram algorithm the fluorescence intensity was quantified within the squared area – being aware that the corpus callosum at both CCJ and a-CC areas changes in thickness and size and that our evaluation was based on rostral, middle and caudal orientation.

11.11 Morphology and cell complexity of Astrocytes

Astrocyte morphological complexity was analyzed on an adapted protocol based on Young and Morrison (2018), using Fiji-ImageJ version 1.47 (Schindellin et al., 2012). Z-stack files over 50 µM thick tissue with a minimum resolution of 1250x1050 pixels and 1 µm range per Z-stack slide with at least 30 frames per file investigated. The following steps were performed for a 2D/X-Y-axis morphology evaluation (i) photomicrographs were converted into an 8-bit binary png. file and images were turned into grayscale, (ii) followed by a 'bandpass' filtering to better visualize the cellular structure. (iii) Contrast and brightness adjustment were applied to avoid image fragmentation through the following steps. (iv) "Unsharp" mask filter with a radius

sigma of 3.0 was applied, (v) followed by a noise reduction via “despeckle” tool, (vi) threshold was adjusted, (vii) the close function via binary tool was applied with a noise reduction via out-layers deletion. (vii) Afterwards, binary images were cropped in the areas with the cells of interest. Once compared to the colored files to observe the proper cell accurately, binary pictures were skeletonized. (viii) Utilizing the white brush tool, small fragments and artefacts that do not belong to the skeletonized astrocytes were erased to avoid inaccuracy in the analysis. (ix)The “skeleton 2D/3D” plugin was used to run the morphology analyses, and the data generated were transferred to an excel spreadsheet. The parameters for morphology evaluation were branch number per cell/endpoint voxels, which determines the number of cytoplasm prolongations or end-feet per cell, and branch length values, which represent the length in µm of those branches. To determine cell complexity (radius), the following steps were performed for a 3D/Z-X-Y axis based investigation using the Fraclac plugin. (i) The skeletonize image containing all the cells of interest was turned into a binary-outlined file. (ii) Each cell of interest was cropped in separated image files. (iii) Fractal analyses were performed by opening the BC setup in the Fraclac plugin window, grid design of 4 colored sections was established, and the metrics option was selected in the graphic options. (iv) After scanning the images generated, the data of the “Hull and circle results” window were transferred to an excel spreadsheet. “Fraclac Db potency" was evaluated to define the cell complexity into the fractal dimension range, followed by the “maximum radium from circle center” that provides data on the radius and diameter of each cell, determining how far the branches of the astrocytes are spreading from the soma. 6 cells were analyzed per group.

11.12 RNA preparation, cDNA synthesis and quantitative RT-PCR analysis of cuprizone-fed mice tissue

For qRT-PCR analysis, native brains were dissected by using an adult brain slicer matrix (Zivic, BSMAS005), a-CC and d-SVZ were jointly isolated by the guidance of a GFP/RFP fluorescence dissecting microscope (Tritech research, SMT1-FL-QC). Tissue homogenization were performed in 1 mL TRIzol reagent (Life Technologies, 15536026) on ice. Subsequently, homogenates were incubated at room temperature for 5 min. 200µL of chloroform (Merck, B25666100) was added and mixed for 5 sec. Samples were centrifuged at 15,300 g for fifteen minutes at 4°C. The aqueous phase

was proceeded for RNA isolation and 10 µL glycogen (Roche, 10901393001) was added as a carrier. About 250 µL of 100 % isopropanol was added and incubated at 80°C over night. After centrifugation at 12,000 r.p.m. for 30 minutes at 4°C, samples were incubated and supernatants were removed. Pellets were washed with 1 ml 75 % ethanol (Merck, 64175), centrifuged at 12,000 r.p.m. for 5 min at 4°C and air-dried for 20 min. RNA was resuspended in 100µL RNase-free water and incubated at 60°C for 10 min. Subsequently, RNA clean-up was performed with RNeasy Mini Kit (Qiagen, 74104) according to manufacturer's instructions including DNase digestion (RNase free DNase Kit; Qiagen, 79656) to avoid genomic DNA contaminations. Synthesis of cDNA was performed by means of the High Capacity cDNA Reverse Transcription Kit with RNase inhibitor (Applied Bioscience, N8080234) using 250 ng total RNA per reaction measured using a NanoDropND 1000 (Peqlab, Erlangen, Germany). Gene expression levels were determined on a 7900HT sequence detection system (Applied Biosystems) applying SybrGreen universal mastermix (Applied Biosystems, 4367659). Relative gene expression levels were determined using the ΔΔCt method. ODC were used as reference genes. Samples were measured in duplicates. Following primers were used: mouse (ms) msODC (as reference gene): fwd- GGT TCC AGA GGC CAA ACA TC, rev-GTT GCC ACA TTG ACC GTG AC; msSerpina3n: fwd-*ACA CAG GCA ATG CCA GCG CA*, rev-*CCT GGC CCC TGT GAT CCC TGA*; msGfap: fwd- CCA GCT TCG AGC CAA GAA, rev- GAA GCT CCG CCT GGT AGA CA; msSerping1: fwd- AGC CTC TGC CAT CTC CTT TG, rev-AAA GGT CGC TGC ACC TCA A; msS100A10: fwd-CAG TGC CGA GAT GGC AAA GT, rev-TGG TGA GCC CTG CCA CTA G; msIL-6: fwd- GTT GTG CAA TGG CAA TTC TGA, rev- TCT GAC AGT GCA TCA TCG CTG; msTimp1:fwd-,rev-; msC21orf91:fwd- CTT CAG CAA GCG TCA TCG AAT T , rev- GTA TCC TGG AAG ACG CGG ATG ; msGdnf: fwd: GGG ATT CGG GCC ACT TG , rev- CGG ATC CGG TCT CCG TAG A, (all primers manufactured by Eurofins genomics, Germany).

11.13 Statistical analysis

Data are shown as mean values ± standard error of the mean (mean ± SEM). GraphPad Prism 7.0.2 (GraphPad Prism, San Diego, CA, RRID: rid_000081) was used for statistics and graphics collection. To assess the absence of Gaussian distribution, Shapiro-Wilk normality test was used for all datasets. Student's t-test was

applied for comparing two groups and two-way analysis of variance (ANOVA) with Bonferroni post-test for multiple comparisons was applied to compare three or more groups. For data sets not passing the Shapiro-Wilk normality test, Kruskal-Wallis test with Dunn's post-test for multiple comparisons of three or more groups was applied. P values are defined as follows: * represents p≤0.05; ** represents p≤0.01; *** represents p≤0.001. Asterisks absence means no statistically significant difference was observed. Absent bars in certain groups indicate that the respective cell subtype was not found, these groups were not considered for the statistical analysis. A priori sample size calculation for the in vivo experiments was performed using the G*Power 3.1.9.2 software (40) (test family: t-tests; statistical test: means: Wilcoxon-Mann-Whitney test (two groups); tails: two; effect size d: 2.6; alpha error 0.05, power 0.95; allocation ratio N2/N1: 1; resulting max sample size: 6). This analysis was also necessary to have animal experiments legally granted by the authorities (The Review Board for the Care of Animal Subjects of the district Government (LANUV, North-Rhine Westphalia, Germany). The number of animals per analysis was at least n=10 per experiment for in vitro/cell culture analyses, given that primary cells are generally generated from 10 neonatal rats and then pooled. Nevertheless, reproduction and statistical evaluation of such experiments was then undertaken by performing 3-4 different and independent experiments. Sample sizes for our in vitro/cell culture experiments are based on our (published) experience with primary neural cell types.

12. Key Resource tables

REAGENT or RESOURCE	SOURCE	CONCENTRATION/IDENTIFIER
Antibodies utilized on *in vivo* samples		
Chicken anti-green fluorescent protein	Aves lab	Cat#GFP1010, RRID:AB_2307313
Rabbit anti-human complement component 3d C3d	Dako	Cat#A0063; RRID: AB_578478
Rat anti-myelin basic protein MBP	Biorad	Cat#aa8287, RRID:AB_32500
Mouse anti-adenomatous polyposis coli/anti-APC-Ab7-clone CC1	Merck millipore	Cat#OP80, RRID: AB_2057371

Rabbit anti-glutathione S-transferase-pi GSTpi	Enzo	Cat#ADIMSA101, RRID: AB_10615079
Mouse anti-contactin associated protein 1, anti-Caspr-paranodin, neuroxin-IV, clone k65/35 Caspr	Neuromab	Cat#75-001, RRID: AB_10671175
Mouse anti-signal transducer and activator of transcription 3 Stat3	Invitrogen	Cat#MA1-13042, RRID: AB_10985240
Mouse anti-human S100 calcium-binding protein A10 S100a10	Thermo Fisher	Cat#MA5-15326, RRID: AB_2092361
Goat anti-tissue metallopeptidase inhibitor 1 Timp1	R&D System	Cat#AF580, RRID:AB_355455
Goat anti-mouse Lipocalin-2/NGAL Ng2	R&D System	Cat#AF1857 RRID:AB_355022
Rabbit anti- inducible nitric oxide synthase iNOS	Abcam	Cat#ab95441 RRID:AB_10688716
Rabbit anti- S100 calcium-binding protein beta, S100β	Abcam	Cat#ab52642, RRID: AB_882426
Mouse anti-Glast astrocyte cell surface antigen-1/Glast-ACSA1	Miltenyl Biotec,	Cat#130095822, RRID: AB_10829302
rat anti-nuclear factor-erythroid factor 2-related factor 2, Nrf2	Cell Signalling Technology	Cat#14596, RRID:AB_2798531
rabbit anti-transcription factor Mafg	Genetex	Cat#GTX114541, RRID:AB_10619599
rabbit anti-sex-determining region Y-box 1-,Sox10	DCS immunoline	Cat#S1058C002, RRID: AB_2313583
mouse anti-breast carcinoma-amplified sequence 1, Bcas1/NaBC1	Santa Cruz	Cat#sc-136342, RRID:AB_10839529
Goat anti-rat (H+L) AlexaFluor 488	Thermo Fisher Scientific	Cat#A-11006; RRID:AB_2534074

Goat anti-rabbit (H+L) AlexaFluor 594	Thermo Fisher Scientific	Cat#A32740; RRID:AB_2762824
Goat anti-rat (H+L) AlexaFluor 647	Thermo Fisher Scientific	Cat#A-21247; RRID:AB_141778
Goat anti-mouse (H+L) AlexaFluor 594	Thermo Fisher Scientific	Cat#A32742; RRID:AB_2762825
Goat anti-rabbit (H+L) AlexaFluor 647	Thermo Fisher Scientific	Cat#A32733; RRID:AB_2633282
Goat anti-chicken (H+L) AlexaFluor 488	Thermo Fisher Scientific	Cat#A32931; RID:AB_2762843
Goat anti-mouse(H+L) AlexaFluor 647	Thermo Fisher Scientific	Cat#A32728; RRID:AB_2633277
Donkey anti-goat (H+L) AlexaFluor 594	Thermo Fisher Scientific	Cat#A32758; RRID:AB_2762828

Antibodies utilized on *ex vivo* and in-vitro samples		
rat anti-myelin basic protein MBP	Bio rad	Cat#aa8287, RRID:AB_32500
rabbit anti-Glial fibrillary acid protein, Gfap	Dako	Cat#Z0334, RRID:AB_10013382
rabbit anti-Neurofilament, NF	Antibodies.com	Cat#A85336, RRID:AB_2748920
Rabbit anti-complement component 3d, C3d	Dako	Cat#A0063; RRID: AB_578478
Chicken anti-glial fibrillary acid protein, GFAP	Aves labs	Cat#SKU:GFAP; RRID: AB_2307313
Neural/Glial Antigen 2, NG2	Merck Millipore	RRID:AB11213678
mouse anti-Glial fibrillary acid protein,GFAP	Merck Millipore	Cat#: MAB3402, RRID:AB_94844
anti-rat AlexaFluor 488	Thermo Fisher Scientific	Cat#A-11006; RRID:AB_2534074
anti-rabbit AlexaFluor 594	Thermo Fisher Scientific	Cat#A32740; RRID:AB_2762824

anti-chicken AlexaFluor 488	Thermo Fisher Scientific	Cat#A32931; RID:AB_2762843
anti-mouse AlexaFluor 405	Thermo Fisher Scientific	Cat#A-48255;RRID:AB_2890536
Chemicals, peptides, and recombinant proteins		
Sterile Saline solution (0.9%)	Braun	Cat#9511040
Phosphate buffer	PAA laboratories	N/A
Minimum essential medium (MEM) Hepes	Life Technologies	Cat#12360038
DMEM-low Glucose	Life Technologies	Cat#D6046
Fetal Calf Serum	Gibco	Cat#10500-064
Fetal Bovine Serum	Capricorn	Cat#FBS-16A
L-Glutamine	Life Technologies	Cat#G7513
penicilin/streptomicin 50 units per ml	Life Technologies	Cat#P4333
Trypsin	Thermo Fisher Scientific	N/A
PB buffer	PAA laboratories	N/A
Hepes Buffer 1M	Thermo Fisher Scientific	Cat#15630056
Triton X-100	Sigma Aldrich	Cat#85111
poly-D-Lysine coated	Sigma Aldrich	N/A
DMSO	Sigma Aldrich	Cat#D2650
Tumor Necrosis Factor alpha (rr isotype)	R&D System	Cat#510RT
Medrysone (6α-methyl-11β-hydroxy-Progesterone)	Cayman Chemical	Cat#19533
normal goat serum	Gibco	Cat#PCN5000
bovine serum albumin	PAN Biotech	Cat#P06-1391025
4',6'-diamino-2-phenylindole (Dapi)	Roche diagnostic	N/A

TO-PROtm-3 Iodide, 642/661 (Topro)	Thermo Fisher	Cat#T3605
Agarose (Ultrapure low melting point)	Thermo Fisher Scientific	Cat#16500100
MEM Hepes	Thermo Fisher Scientific	Cat#51417C
Hank´s balanced salt solution	Thermo Fisher Scientific	Cat#88284
Heat inactivated horse serum	Thermo Fisher Scientific	Cat#26050-070
Glutamine	Life Technologies	Cat#1294808
D-Glucose monohydrate	Merck	Cat#108342
Paraformaldehyde (PFA)	Sigma Aldrich	Cat#158127
Cuprizone 0.4%	Sniff	Cat#V-1534
TRIzol reagent	Life Technologies	Cat#15536026
Chloroform	Merck	Cat#B25666100
Glycogen	Roche	Cat#10901393001
Ethanol	Merck	Cat#64175
RLT lysis buffer	Qiagen	Cat#1015762
β-mercaptoethanol	Sigma Aldrich	Cat#M3148-25
Immu-mount	Thermo Fisher Scientific	Cat#1900331
Sodium citrate buffer	Merck	Cat#111037
Trypan Blue 0.4%	Sigma Aldrich	Cat#T8154
Dulbecco's phosphate buffer solution	Life Technologies	Cat#14190144
Critical commercial assays		
Magnetic activated Cell sorting (Glast ACSA-1)	Miltenyi Biotec	Cat#130707677
Glast (ACSA1) antibody	Miltenyi Biotec	Cat#130095822;RRID:AB_10829302

Rneasy Mini Kit	Qiagen	74104
RNase free DNase Kit	Qiagen	79656
High Capacity cDNA Reverse Transcription Kit with RNase inhibitor	Applied Bioscience	N8080234
SybrGreen universal mastermix	Applied Biosystems	4367659
Experimental models: Organisms/strains		
Mouse: Transgenic hGFAP-GFP promoter mice 14mes/J	Jackson Labs	Cat#Jax stock number: #003257
Rat: Wistar RjHan:WI	Janvier Labs	N/A
Oligonucleotides		
rtGAPDH:fwd- GAA CGG GAA GCT CAC TGG C	Eurofins genomics	N/A
rtGAPDH:rev- GCA TGT CAG ATC CAC AAC GG	Eurofins genomics	N/A
rtMyrf:fwd- CCT GTG TCC GTG GTA CTG TG	Eurofins genomics	N/A
rtMyrf:rev- TCA CAC AGG CGG TAG AAG TG	Eurofins genomics	N/A
rtPdgfra:fwd- AGC TCT CTG TTC CCA ATG CC	Eurofins genomics	N/A
rtPdgfra:rev- GCC TCC ATT CTG GAG CTT GT	Eurofins genomics	N/A
rtSox10:fwd- GTC AGA TGG GAA CCC AGA GCA C	Eurofins genomics	N/A
rtSox10:rev- CCC GTA GCC AGC TGC CGA G	Eurofins genomics	N/A
rtCNPase:fwd GCC GTT GTG GTA CTT CTC CA-	Eurofins genomics	N/A
rtCNPase:rev- GCC CGA AAA AGC CAC ACA TT	Eurofins genomics	N/A
rtHprt: fwd- CAG TCC CAG CGT CGT GAT TA,	Eurofins genomics	N/A
rtHprt: rev- ATG GCC TCC CAT CTC CTT CA	Eurofins genomics	N/A

rtGfap: fwd- CTG GTG TGG AGT GCC TTC GT	Eurofins genomics	N/A
rtGfap: rev- CAC CAA CCA GCT TCC GAG AG	Eurofins genomics	N/A
rtSerpina3n: fwd-GGG CAG GTG CTT CGT	Eurofins genomics	N/A
rtSerpina3n: rev-AGC GCC TTT GTC TTT CTT TCT G	Eurofins genomics	N/A
rtLcn2: fwd-TCT CAG GCC CAC CAT GAT AGA	Eurofins genomics	N/A
rtLcn2: rev-CAG GTT GTA GTC AGC AGA GAT GGA	Eurofins genomics	N/A
rtSerping1: fwd-GAC AGC CTG CCC TCT GAC A	Eurofins genomics	N/A
rtSerping1; rev-GCA CTC AAG TAG ACG GCA TTG	Eurofins genomics	N/A
rtC3: fwd- CCT TCC CGG GAG CAT CA	Eurofins genomics	N/A
rtC3: rev- GGG CAT ACC CAG CAA TGG	Eurofins genomics	N/A
rtClcf1: fwd- TGG CCC ATT TCT GTA CCA GTC T	Eurofins genomics	N/A
rtClcf1: rev- GTA GCC AAG AGT TGC CAT GAC A	Eurofins genomics	N/A
rtEmp1: fwd- TGG TGG CGG ACG GTA TAG A	Eurofins genomics	N/A
rtEmp1: rev- TGC CAC TGG TGC AGT TCT TC	Eurofins genomics	N/A
rtUgt1a: fwd- CCT GTG CCA TTC CAA AAT GA	Eurofins genomics	N/A
rtUgt1a: rev- CAC TCC GCC CAA GTT CCA	Eurofins genomics	N/A
rtC1qa: fwd- CAG AAC CCA CCG ACG TAT GG	Eurofins genomics	N/A
rtC1qa: rev- TCC TGG TTG GTG AGG ACC TT	Eurofins genomics	N/A

rtIL6: fwd- GTT GTG CAA TGG CAA TTC TGA	Eurofins genomics	N/A
rtIL6: ev-TCT GAC AGT GCA TCA TCG CTG;	Eurofins genomics	N/A
rtCd14: fwd- ACA ACA GGC TGG ATA GGA AAC C	Eurofins genomics	N/A
rtCd14: rev-TGA CAG GCT CCC CAC TTC AG	Eurofins genomics	N/A
rtS100a10: fwd- GCC ATC CCA AAT GGA GCA T	Eurofins genomics	N/A
rtS100a10: rev- CCC CTG CAA ACC TGT GAA AT	Eurofins genomics	N/A
msODC: fwd- GGT TCC AGA GGC CAA ACA TC	Eurofins genomics	N/A
msODC rev-GTT GCC ACA TTG ACC GTG AC	Eurofins genomics	N/A
msSerpina3n: fwd-ACA CAG GCA ATG CCA GCG CA	Eurofins genomics	N/A
msSerpina3n: rev-CCT GGC CCC TGT GAT CCC TGA	Eurofins genomics	N/A
msGfap: fwd- CCA GCT TCG AGC CAA GAA	Eurofins genomics	N/A
msGfap: rev- GAA GCT CCG CCT GGT AGA CA	Eurofins genomics	N/A
msSerping1: fwd- AGC CTC TGC CAT CTC CTT TG	Eurofins genomics	N/A
msSerping1: rev-AAA GGT CGC TGC ACC TCA A	Eurofins genomics	N/A
msS100A10: fwd-CAG TGC CGA GAT GGC AAA GT	Eurofins genomics	N/A
msS100A10: , rev-TGG TGA GCC CTG CCA CTA G	Eurofins genomics	N/A
msIL-6: fwd- GTT GTG CAA TGG CAA TTC TGA	Eurofins genomics	N/A
msIL-6: rev- TCT GAC AGT GCA TCA TCG CTG	Eurofins genomics	N/A

msC21orf91:fwd- CTT CAG CAA GCG TCA TCG AAT T	Eurofins genomics	N/A
msC21orf91: rev- GTA TCC TGG AAG ACG CGG ATG	Eurofins genomics	N/A
msGdnf: fwd: GGG ATT CGG GCC ACT TG	Eurofins genomics	N/A
msGdnf: rev- CGG ATC CGG TCT CCG TAG A	Eurofins genomics	N/A
Software and algorithms		
Fiji	ImageJ	RRID:SCR_003070; Version 1.47; Schindelin et al., 2012
GraphPad Prism 7.0.2	GraphPad Prism	RRID:rid_000081
Confocal Microscope image acquisition program ZEN Zen blue/black software	Carl Zeiss AG	Version 9
GIMP (GNU image manipulation program)	GIMP Startup	Version 2.10
MS Office 2007 /2016	Microsoft	N/A
Artflow	Artflow Studio	Version 2.8.105
Other		
Incubator	Excella	model E24
vibration microtome	Thermo Fisher	model Microm HM 650 V
confocal laser scanning microscope	Carl Zeiss AG	model 510
adult brain slicer matrix	Zivic	Cat#BSMAS005
GFP/RFP fluorescence dissecting microscope	Tritech research	Cat#SMT1-FL-QC
NanoDrop	Peqlab	model ND 1000

13 Annexe

13.1 Published research article

In accordance with the paragraph § 2 (4) of the doctoral regulations (15.06.2018) of the Faculty of Mathematics and Natural Sciences of Heinrich Heine University Düsseldorf, all sections (results) which are reproduced or adapted from a published manuscript (Oliveira-Junior et al., 2022) have been clearly marked within the thesis.

Accepted for publication on July 22, 2022 (letter of acceptance can be accessed at page 123)

Myelin repair is fostered by the corticosteroid medrysone specifically acting on astroglial subpopulations

Markley Silva Oliveira Junior, Jessica Schira-Heinen, Laura Reiche, Seulki Han, Vanessa Cristina Meira de Amorim, Isabel Lewen, Joel Gruchot, Peter Göttle, Rainer Akkermann, Kasum Azim, Patrick Küry

M. Phil. Markley Silva Oliveira Junior performed the majority of experiments, data analysis, data interpretation, text writing and figure design (80%). Dr Jessica Schira-Heine contributed with experimental design, data analysis, interpretation and figure design. Msc. Laura Reiche and Dr Peter Göttle conducted primary OPC experiments and provided corresponding data analysis. M. Phil. Vanessa Cristina Meira de Amorim and Msc. Seulki Han provided support in data interpretation and data presentation. Md. Isabel Lewen and Msc. Joel Gruchot executed primary astrocyte experiments and provided corresponding data analysis. Dr Rainer Akkermann established the transgenic mouse strain and the cuprizone experiments. Dr Kasum Azim developed the experimental design, funding acquisition, data analysis and interpretation. Prof. Dr Patrick Küry (PK) conceived the final project and main manuscript (Oliveira Junior et al., 2022) and confirms the information described above. PK was also involved in experimental design, funding acquisition, data analysis and interpretation, and figure composition. In addition, Birgit Blomenkamp, Brigida Ziegler and Julia Jadasz provide technical support. Dr. Nikolaj Klöcker (Heinrich-Heine-University of Düsseldorf) for providing breeding pairs of the hGFAP-GFP transgenic mouse line. The anti-PLP antibody was kindly provided by Dr Bruce Trapp (Department of Neurosciences at the Cleveland Clinic, Ohio, USA).

13.2 Main manuscript letter of acceptance

Date: Jul 22, 2022
To: "Patrick Küry" kuery@uni-duesseldorf.de
From: "Julie Stacey" jstacey@lancet.com
Subject: Your Submission EBIOM-D-22-00414R3

Manuscript reference number: EBIOM-D-22-00414R3
Title: Myelin repair is fostered by the corticosteroid medrysone specifically acting on astroglial subpopulations
Article (Original Research)

Dear Dr Patrick Küry,

I am pleased to inform you that your paper has been accepted for publication in *eBioMedicine*. Congratulations on an exciting story! We are pleased to be bringing it to the attention of our readers. My apologies for the delay.

We would like to invite you to submit a cover candidate using an image related to the work. If you have an original, visually compelling image which you would like to submit as a candidate for the issue cover, please send a high resolution file (specifications below) directly to ebiom@lancet.com. Be sure to include the manuscript number and corresponding author name in the email, along with "cover candidate" in the subject line, and please confirm that the image has not been published elsewhere. The submitted cover candidate will be discussed by in-house editors together with other authors' cover candidates, and only one cover may be chosen per journal issue.

the work or, if the article is to be published under a CC BY license or for some government employees, a non-exclusive publishing agreement. To support the costs of publishing including reviewing (first by internal review, and then external peer review), technical, copy editing, typesetting and graphics, online hosting, archiving, and promotion, authors will need to pay an article processing charge (APC), upon acceptance. The APC is payable for all full-length peer-reviewed article types. Information on the APC can be found at https://www.thelancet.com/open-access. You will in due course receive an email inviting you to complete our Rights & Access form online where you will be able to select your licence choice and pay the APC. Please ensure this form is completed within 48 hours of receipt.

WHO/IARC/PAHO AUTHORS
If you or any of your co-authors are employed directly by the World Health Organization/International Agency for Research on Cancer/Pan American Health Organisation, you have the option of either signing Elsevier's standard agreement or our WHO/Elsevier non-exclusive licence agreement. Please contact our Deputy Operations Manager, Marco Conforti (m.conforti@elsevier.com) for a copy of the WHO agreement.

Our Production team will be in touch soon regarding proofs of your manuscript. We look forward to working with you to get your work published in *eBioMedicine*. In the meantime, if you have any queries related to the galley proofs, please contact the Journal Manager, Rachel Vinitha at r.pareenargunam@elsevier.com.

Thank you for submitting your work to *eBioMedicine*.

Yours sincerely,

Dr. Julie Stacey
, *eBioMedicine*
jstacey@lancet.com

13.3 Manuscripts in preparation

The chapters 1, 2, 3 and 4 will be utilized for the preparation of a literature review article entitled as “if you don’t know, now you know, astrocytes can foster remyelination” authored by Markley Silva Oliveira Junior, Prof. Dr. Maryam Faiz and Prof. Dr. Patrick Küry. This article is not yet submitted. Figures not published at Oliveira-Junior et al., 2022, will be included in a future publication.

13.4 Further investigations

In collaboration with Prof. Dr Patrick Kury, research on the proteic, transcriptomic and epigenetic signature of reactive astrocytes in stroke, demyelination, and gut dysbiosis will be developed under a post-doctoral position at Prof. Dr Maryam Faiz's laboratory at the University of Toronto, Canada, starting in November 2022. This position will be funded by the Ontario Institute of Regenerative Medicine and Stem Cell Networks Canada.

13.5 No-reproducible staining.

A portion of the experiments performed throughout the development of this dissertation was not reproducible, thus inefficient to complement the main objective of this work. Some immunofluorescence experiments performed on *in vivo* samples were not replicable. Those samples presented no specific binding labelling blood vessels or artefacts of dissection. The antibodies and respectively concentration utilized were HOP- Homeobox protein (Hopx; 1:800, anti-mouse; Anti-HopE-1/Hopx, Santa Cruz, sc-398703, RRID: AB_2687966; Figure 25a); Neural/Glial Antigen 2 (1:800, Anti-rabbit, NG2, Merck Millipore, RRID:AB11213678; Figure 25b); Minichromosome Maintenance Complex Component 2 (Mcm2; 1:500, Anti-rabbit Mcm2, Abcam, RRID: EPR4120; Figure 25c); Achaete-scute homolog 1 (Mash1; 1:500, anti-mouse Mash1, Abcam, RRID: ab211327; Figure 25d); Platelet-derived growth factor receptor alpha (Pdgfrα; 1:1000; anti-rabbit Pdgfrα, Abcam, RRID: ab61219); A 10-formiltetrahidrofolato dehydrogenase [Aldh1l1; 1:1000, anti-mouse Aldh1l1(3E9), Abcam, RRID: ab56777); Aquaporin 4 (Aqp4; 1:500,.anti-rabbit Aqp4, Sigma, RRID: A59712ML; Figure 25f); Proliferating cell nuclear antigen (PCNA;1:500, Anti-mouse PCNA, Invitrogen, RRID:13-3900; Figure 25g). Injection of the thymidine analogue 5-Ethinyl-2'-deoxyuridine (EdU, Abcam, ab146186; 80 mg/kg diluted in saline solution) was also conducted in a few animals as a test for proliferation staining. Intraperitoneal

injections (500µL per mice) of diluted EdU were performed in parallel to saline or medrysone administration. However, the protocol utilized (Salic and Mitchison, 2008) were ineffective for identifying binding (Figure 25b). The antigen retrieval protocol detailed in the materials and methods of this document was performed before primary antibody incubation for Hopx, Mcm2 and Pcna (Figure 25a, 25c, 25g). Of note, antigen retrieval procedures were also ineffective in making those staining work.

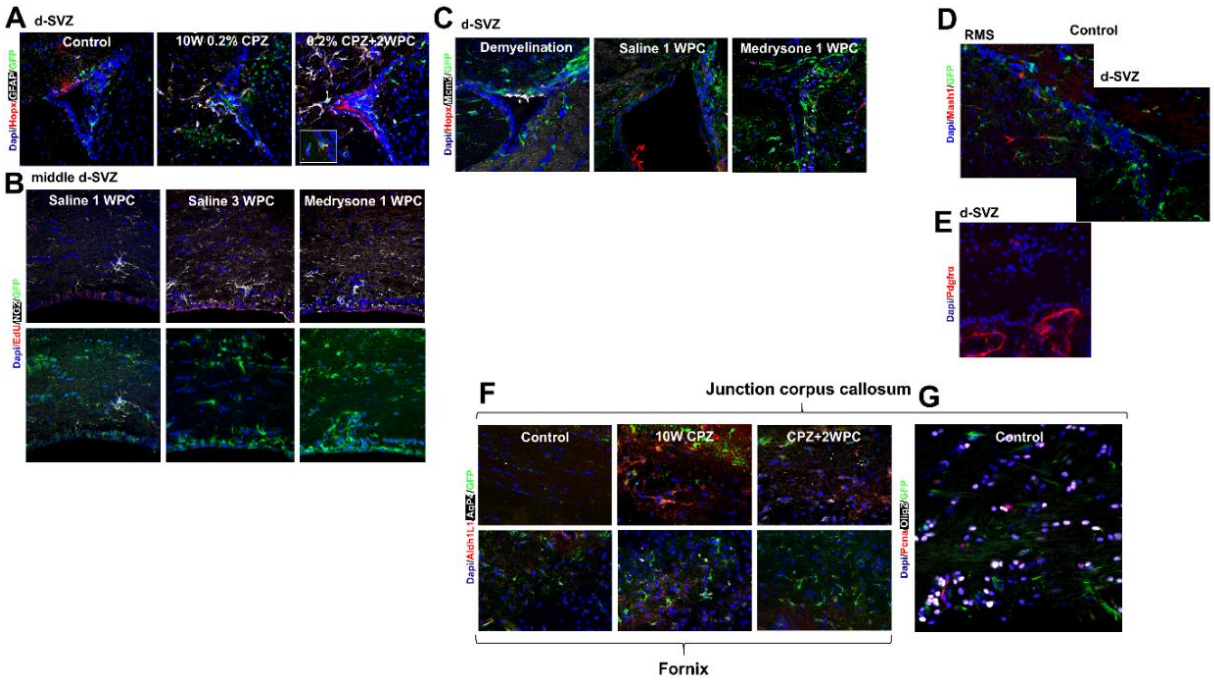

Figure 25. Non-reproducible data. The following antibodies were evaluated in tissues exposed or not to antigen retrieval procedures and do not work on *in vivo* samples: Hopx (a); NG2 (b); Mcm2 (c); Mash1 (d); Pdgfrα (e); Aldh1l1 (f); Aqp4 (f); PCNA (g). Stainings for EdU were also performed. However, it does not effectively identify binding structures (b). Samples at (a) correspond to 0.2%CPZ-fed mice. Samples at (b-g) correspond to 0.4% CPZ-fed mice.

14. Declaration of authorship

I declare under oath that I have produced my thesis independently and without any undue assistance by third parties under consideration of the ‘Principles for the Safeguarding of Good Scientific Practice at Heinrich Heine University Düsseldorf.

Markley Silva Oliveira Junior, Düsseldorf, 10.25.2022

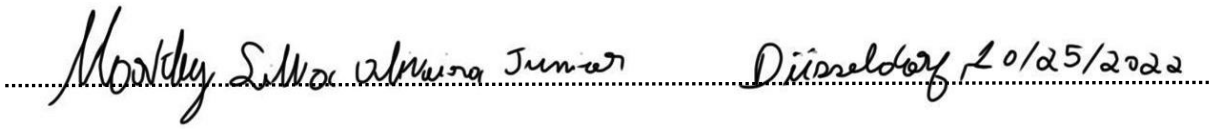

Name, Signature **Place, Date**